T-AM-Sy1

T-AM-Sy2 STRUCTURAL INTERACTIONS IN THE CYTOSKELETON. Manfred Schliwa, Dept. Molecular, Cellular, and Developmental Biology, University of Colorado, Boulder, CO 80309.

Most animal cells display ordered arrays of three major cytoskeletal fiber systems: actin filaments, intermediate filaments, and microtubules. Their distribution has been extensively studied in a variety of systems, but little is known about their possible interactions in the control of cell form and motility. We have combined detergent extraction with stereo high voltage electron microscopy of whole mount preparations to gain an insight into the arrangement and interaction of cytoskeletal components. Using an improved extraction protocol, cells of both epithelial and fibroblastic morphology have been analysed at low and high levels of resolution. Extensive structural interaction between the major fiber systems in the form of lateral and end-to-surface contacts can be demonstrated. Of particular interest is the role of actin filaments and a new subclass of filaments with a diameter of 2-3 nm. The latter seem to act as links between both like (e.g., actin-actin) and unlike (e.g., actin-microtubule) filamentous components. Actin filaments form end-to-surface contacts not only with other actin filaments, resulting in a Y-shaped branching pattern, but also with microtubules and intermediate filaments. We have analysed the importance of the interaction of actin filaments with microtubules for the course of microtubules in the cytoplasm and conclude that directional changes are imposed by such interactions. Studies on the action of the cytochalasins in this lysed cell model system revealed some insights into the mode of action of these compounds and help to explain their effect on cell morphology and motility. Taken together, these studies favor the concept that the detergent-extracted cytoskeleton is a highly crosslinked structural unit.

Supported by NIH grant GM 27324-01 to Keith R. Porter and a Heisenberg Felloswhip from the Deutsche Forschungsgemeinschaft to M. Schliwa.

T-AM-Sy3 ENDOGENOUS DETERMINATION OF DETAILED CELLULAR MORPHOLOGY. F. Solomon, Department of Biology and Center for Cancer Research, Massachusetts Institute of Technology, Cambridge, MA 02139.

The elaboration of a specific cellular morphology is an important aspect of expression of a differentiated phenotype. The conditions required for a round cell to spread to an asymmetric shape have been studied extensively in recent years. However, the information which specifies the details of that shape are more difficult to identify. There is considerable evidence that external cues, such as patterns of the substratum or chemical signals in the medium, can induce a defined cell shape. It is also possible that a particular cell, arising from a particular cell lineage, contains information which specifies its shape in detail. We have demonstrated such endogenous determination of morphology, using cultured neuroblastoma cells which can be induced to extend neurites and therefore to resemble the differentiated morphology of neurons in the animal. The detailed shapes of neuroblastoma cells vary over a wide range, as defined by number, position, and shape of the neurites themselves. We find that greater than 60 percent of neuroblastoma cells pairs which arise as mitotic sisters display neurite morphologies related in striking detail. These studies suggest that sister cells share determinants of morphology. The fundamental questions which this observation poses are how are these determinants are stored in cells, transmitted to daughter cells, and expressed. We are addressing these questions by perturbing cell morphologies, either by successive rounds of mitosis or by drugs which disrupt the underlying cytoskeleton. These experiments are directed toward understanding how cells organize their components to produce a particular morphology, regardless of the source of the specifying information.

T-AM-Sy4 ORGANIZATION OF CELL FORM BY ARRAYS OF ACTIN FILAMENTS. Lewis G. Tilney
Department of Biology, University of Pennsylvania, Philadelphia, Pennsylvania 19104.

Organized arrays of actin filaments are conspicuous features of non-muscle cells. Examples include extensions of cells such as microvilli and filopodia, the "contractile ring" in dividing cells, stress fibers, and specialized extensions of cells such as stereocilia. I will examine how actin filaments are connected to each other to form paracrystalline arrays present in non-muscle cells using, as examples, stereocilia of cochlear hair cells, the microvilli of intestinal epithelial cells, and the acrosomal processes of sperm. I will then attempt to show how these clusters form during development and derive what appear to be some of the rules which govern the assembly of actin filaments and their interactions to form bundles in vivo.

Supported by NSF grant #GB22863.

T-AM-Min-A1 TWO DIMENSIONAL ENERGY TRANSFER AND FLUORESCENCE POLARIZATION. Bruce Hudson and Paul Wolber. Department of Chemistry and Institute of Molecular Biology, University of Oregon, Eugene, OR 97403.

The theory of energy transfer for a two-dimensional array of donors and acceptors has been developed for a random distribution, a distribution which is random beyond a cutoff or exclusion distance, two displaced random distributions and binding of donors to acceptors [Wolber and Hudson, Biophys. J. 28, 197-210 (1979)]. Some additional numerical results using this analytic theory will be presented. The effect of energy transfer on both time resolved and static fluorescence polarization anisotropy measurements will be discussed including a comparison with the corresponding effect due to collisional (Stern-Volmer) quenching. Examples will be presented corresponding to realistic lipid bilayer systems.

T-AM-Min-A2 ORIENTATIONAL EFFECTS IN INTER-MOLECULAR LONG RANGE RESONANCE ENERGY TRANSFER ON SPHERICAL SURFACES. J. Eisinger, W. E. Blumberg, and R. E. Dale. *Department of Molecular Biophysics, Bell Laboratories, Murray Hill, N.J. 07974, and Paterson Laboratory and Holt Radium Institute, Manchester, M20 9BX, U.K.*

The orientational dependence of long range resonance energy transfer is examined for inter-molecular energy transfer between donors and acceptors distributed randomly over a spherical surface. It is shown that the energy transfer efficiency has an appreciable dependence on the orientations and reorientational motion of donors and acceptors in this situation, just as in the three dimensional case treated previously by us. The results of fluorescence depolarization experiments may be used to provide estimates of the magnitude of these orientational effects, and protocols for doing so are to be presented. Time-resolved fluorometry provides the best method of determining the required depolarization factors, complementing the steady state determination of the average anisotropy $\langle r \rangle$. For fluorophores on spherical surfaces, both the general case is treated and the limiting cases in which the dynamically average transition moments approach linear, planar and isotropic distributions. The dependence of the dynamically averaged transfer efficiency on sphere size and on acceptor concentration has been calcualted and is compared with that for planar distributions of fluorophores.

T-AM-Min-A3 STRUCTURAL STUDIES OF THE HUMAN ERYTHROCYTE MEMBRANE BY MEANS OF RESONANCE ENERGY TRANSFER. J. Eisinger and J. Flores. *Department of Molecular Biophysics, Bell Laboratories, Murray Hill, N.J. 07974.*

We have measured the efficiency of resonance energy transfer from tryptophans of proteins of erythrocyte membrane to a series of suitable acceptors in the lipid phase. The tryptophan emission has a quantum yield of 0.1 and has a maximum at 330nm. With *n*-anthroyloxy stearic acids (*n*-AS) as acceptors the average Förster distance was about 22Å. With $n = 2$, 6, 9, 12, and 16, the *n*-AS fluorophores have been shown to be at increasing depths in the lipid bilayer, and their steady state emission anisotropies, $\langle r \rangle$, reveal a increasing fluidity of their environment: $\langle r \rangle$ drops from 0.195 to 0.113 at 0°C and from 0.165 to 0.060 at 37°C. The efficiency of energy transfer from tryptophan increases with *n*. When the data are analyzed in terms of 2-dimensional Förster transfer theory, the average distance of closest approach for the *n*-AS probes drops from 29 to 25Å for *n* between 2 and 16.

For the band 3 protein in human erythrocytes, labelled specifically with a diisothiocyanate stilbene derivative (DIDS), the distance of closest approach a lipid carbocyanine probe (transition moment parallel to the membrane surface) is 26Å. From the measured average transfer depolarization factor, it is concluded that the virtually immobile DIDS molecule ($\langle r \rangle = 0.37$) has a transition moment which makes an angle of about 60° with the normal to the membrane surface. These and other energy transfer experiments on intact erythrocytes and their ghosts are used to extract structural information about the membrane.

T-AM-Min-A4 NA,K ATPASE SHAPE, SURFACE DENSITY AND PROXIMITY OF PROTEIN SITES TO LIPIDS STUDIED WITH FLUORESCENCE ENERGY TRANSFER. E.G. Moczydlowski and P.A.G. Fortes. Biology Department, University of California, San Diego, La Jolla, Ca. 92093.

In purified eel electroplax Na,K ATPase we measured energy transfer efficiency (E) between the following donor (D) and acceptor (A) couples: a) 4 D-A pairs of lipid probes (L) to estimate the total surface area and ATP or ouabain site density in the preparation. b) L and protein labels to estimate the distance of closest approach, R_e, between L and: 1) the ouabain site labeled with 4 D or A fluorescent cardiac glycosides; 2) the ATP site labeled with TNP-ATP; 3) D-labeled SH groups. c) D and A cardiac glycosides bound to ouabain sites to estimate R_e between proteins. The data, analyzed by 2-dimensional E theory (Biophys. J. 28:192-210), show that: 1) the areas estimated from E with the 4 L couples tested were all similar: $(3.8\text{-}5.6)\times10^{19}$ A^2/mg protein and $(1.6\text{-}2.4)\times10^4$ A^2/ATP site, although there was a 2-fold difference between estimates with the highest and lowest [A] tested. 2) R_e between L and the ouabain site was similar to R_e between L and L (≤10A). 3) No E between L and the ATP site was detected. 4) R_e between L and SH groups was 26-35A. 5) R_e between ouabain sites was 37-49A, assuming a random distribution. These results suggest that the R_e values reflect the diameter of the excluded volume occupied by the enzyme, so that it has an asymmetric shape with most of the protein mass located in the intracellular domain containing the SH groups and the ATP site, and a smaller mass in the extracellular domain containing the ouabain site, which is close to the lipids. (Supported by NIH grants HL-20262 and RR-08135).

T-AM-Min-A5 A FLUORESCENCE ENERGY TRANSFER STUDY ON THE AGGREGATION STATE OF PURIFIED RHODOPSIN RECONSTITUTED IN PHOSPHOLIPID VESICLES. H. Borochov-Neori, P.A.G. Fortes, and M. Montal. Departments of Physics and Biology, University of California, San Diego, La Jolla, CA 92093

Rod outer segments were labelled with two sets of donor-acceptor fluorescent couples: one directed towards ε-amino residues (dansylchloride and fluorescein isothiocyanate) and the other towards free -SH groups (pyrenemaleimide and monobromobimane). Rhodopsin labelled with either one of these probes at approximately 1:1 molar ratio was affinity purified on Concanavalin A - Sepharose 4B using octylglucoside as detergent. Purified rhodopsin was combined with a mixture of diphytanoyl-phosphatidylcholine and bacterial phosphatidylethanolamine (1:1, w/w) at different protein to lipid ratios. Vesicles were formed by detergent dialysis. Vesicles containing both pyrene-rhodopsin and bimane-rhodopsin (R_o=30Å) exhibited energy transfer both under dark and light conditions. The transfer efficiencies were sensitive to donor-acceptor ratio, to the presence of unlabelled rhodopsin and at different acceptor concentrations their values exceeded those expected from randomly distributed[1] monomers with a distance of closest approach ≥27Å, i.e., the estimated diameter of rhodopsin. Vesicles containing dansyl-rhodopsin and fluorescein-rhodopsin (R_o=35Å) displayed no significant energy transfer in the dark. Bleaching induced an increase in transfer efficiency to values higher than expected from random distribution.[1] The results suggest that in these vesicles rhodopsin is aggregated both in the dark and when bleached. Bleaching, however, induces conformational changes which increase either the proximity of ε-amino groups of individual rhodopsin molecules within a preformed aggregate or the aggregation number. (Supported by the Damon Runyon-Walter Winchell Cancer Fund and NIH-EY02084).

[1]Wolber, P. Y., and Hudson, B.S. (1979); Biophys. J. 28:197-210.

T-AM-Min-A6 RHODOPSIN PHOSPHORESCENCE AND FLUORESCENCE: TYROSINE⟶TRYPTOPHAN ENERGY TRANSFER UPON LIGHT-INDUCED CONFORMATIONAL CHANGE OF OPSIN. Usha P. Andley and Bireswar Chakrabarti, Eye Research Institute of Retina Foundation and Harvard Medical School, Boston, MA 02114.

Phosphorescence and fluorescence measurements of rhodopsin in bovine rod disc membrane were carried out to study changes in protein conformation on bleaching, by probing the environment of tryptophan and tyrosine residues of the protein. Bleaching decreased the tyrosine phosphorescence by about 20% and significantly affected the triplet decay curve excited at 280 nm, where both tyrosine and tryptophan absorb. Computer analysis of the decay curve at 410 nm in dark-adapted ROS showed the presence of two components — one with a lifetime of 2.5 s, the other with a lifetime of 5.8 s — which are typical of tyrosine and tryptophan, respectively. When the ROS sample was bleached, the decay curve showed only one component with a lifetime of 4.5 s. No change in phosphorescence lifetime was observed on bleaching when tryptophan or tyrosine emission alone was monitored. Both Chiba et al. (1978, Biochem. Biophys. Res. Commun. 85, 551-557) and we have observed an enhancement of tryptophan fluorescence intensity on bleaching ROS membranes. Light-induced change in phosphorescence and fluorescence can be explained by energy transfer between tyrosine and tryptophan singlet states, which results from a conformational change of the opsin moiety on bleaching.

T-AM-Min-A7 AGGREGATION OF PHOSPHOLIPID VESICLES MONITORED BY FLUORESCENCE ENERGY TRANSFER. Leslie M. Loew, Mary Bridge, and George A. Gibson, Dept. of Chemistry, SUNY at Binghamton Binghamton, N.Y. 13901.

The development of fluorescence energy transfer after mixing of 2 lipid vesicle preparations, containing a bilayer bound donor and acceptor, respectively, can signal, in principle, membrane aggregation or fusion and has been demonstrated for the fusion case (Gibson and Loew, Biochem. Biophys. Res. Comm., 88, 135, 141 (1979)). One of the major difficulties in the implementation of this methodology is the design of fluorescent probes which do not randomize by a unimolecular dissociation-reassociation process. We have prepared a new fluorescent probe from the reaction of monobromobimane and dimethylphosphatidylethanolamine which is insensitive to ionic solutes or pH, is very tightly bound to membranes, and is a good donor for several available acceptors. The aggregation of vesicles composed of phosphatidylserine, phosphatidylethanolamine, and a mixture of lecithin and glycolipid, were followed by the appearance of energy transfer and simultaneously by light scattering. Aggregation is triggered by the addition of an external reagent and can be reversed for each of these systems. Energy transfer before aggregation was insignificant on the experimental timescale for all of these experiments. Aggregation was accompanied by a large amount of energy transfer in 2 of the 3 systems investigated but only partial loss of this energy transfer accompanied subsequent breakdown of the aggregates. The energy transfer is thus composed of 2 components in the aggregated vesicles - 1) the expected intermembrane energy transfer; 2) intramembrane energy transfer resulting from enhanced randomization of the probes in the aggregated state. (Supported by USPHS Grant CA23838 and a Research Career Development Award, CA00677, to L.M.L.)

T-AM-Min-A8 QUANTITATIVE MEASUREMENT OF CALCIUM-INDUCED LIPOSOME FUSION USING ENERGY TRANSFER

Paul S. Uster and David W. Deamer; Dept. of Zoology; Univ. of California, Davis 95616

A sensitive, quantitative assay has been developed which measures the extent of liposome fusion by monitoring fluorescence resonance energy transfer (RET) between two lipid analogues originally in separate membranes. This transfer of photon energy occurs only if both probes are in the same membrane. The extent of fusion was estimated by comparing the extent of RET due to the fusion protocol with the maximum RET possible from "mock-fused" vesicles. This assay was used to investigate the effects of Ca^{2+} concentration, Ca^{2+} permeability, and lipid composition on fusion competence. The calcium ion concentration threshold and extent of fusion was a function of lipid composition. At a given molar percentage of phosphatidylserine (PS), increasing the phosphatidylcholine (PC) content raised the threshold. The extent of fusion decreased when the content of PS was decreased. The inclusion of either cholesterol or phosphatidylethanolamine (PE) facilitated fusion competence, but the latter was more effective. Increasing the Ca^{2+} permeability by adding the ionophore X-537a moderately enhanced the extent of fusion in most cases, although it never appreciably affected the threshold. X-537a did not enhance fusion in the presence of unsaturated PE. We conclude that it is possible for large unilamellar vesicles with near physiological molar percentages of PS and PE to undergo calcium-induced fusion at millimolar Ca^{2+}. This finding provides a useful model system for investigating mechanisms of membrane fusion phenomena such as exocytosis and cell-cell fusion. (This work was supported by NIH grant GM07377.)

T-AM-Min-A9 EXCITATION ENERGY TRANSFER STUDIES ON THE PROXIMITY BETWEEN THE ATPase SITE AND SH_1 IN MYOSIN SUBFRAGMENT-1. Mark Lamkin and Terence Tao (Intr. by S. Sarkar), Dept. of Muscle Research, Boston Biomedical Research Institute, 20 Staniford St., Boston, MA 02114.

Excitation energy transfer studies were carried out to determine the distance between the ATPase site and the fast reacting sulfhydryl (referred to as SH_1) in myosin subfragment-1. The fluorescent moiety of the probe N-iodoacetyl-N'-(5-sulfo-1-naphthyl) ethylene diamine (1,5-IAEDANS) was used as the donor attached at SH_1. The chromophoric nucleotide analog 2'(3')-trinitrophenyladenosine-5'-diphosphate (TNP-ADP) was used as the acceptor noncovalently bound at the ATPase site. The energy transfer efficiency was found to be 56% by measuring the decrease in donor fluorescence lifetime. The critical transfer distance, R_0(2/3), was determined to be 40.3Å. Since both donor and acceptor are likely to be rigid, a probabilistic interpretation of the data was applied (Hillel and Wu, Biochemistry 15, 2105, 1976). The method yielded the following conclusion: Most probable distance = 38.7Å; maximum possible distance = 52Å; 10% probability for the distance to be less than 20Å; 3% probability to be less than 15Å. It may be concluded that in spite of the profound influence that the two sites exert on each other, it is not likely that SH_1 interacts directly with the ATPase site in myosin subfragment-1. It should be pointed out that similar results were obtained by Perkins et al. (Fed. Proc. 39, 1937, 1980), and similar conclusions were reached by Botts et al. (Biochemistry 18, 5157, 1979) and by Wiedner et al. (J. Biol. Chem. 253, 2763, 1978). (Supported by NIH grant AM-21673.)

T-AM-Min-A10 STUDY OF THE SPATIAL ARRANGEMENT OF TROPONIN,TROPOMYOSIN,AND ACTIN IN THIN FILAMENT USING FLUORESCENCE ENERGY TRANSFER. Tsung-I Lin and Robert M. Dowben, Dept. of Physiol., UTHSCD,Dallas,TX 75235 and Dept. of Pathology,Baylor Univ. Med. Ctr.,Dallas,TX 75246

The spatial arrangement of troponin(TN), tropomyosin(TM), and actin of rabbit skeletal muscle in the reconstituted thin filaments was investigated under various conditions using fluorescence energy transfer. Fluorescent probes, N-(iodoacetylaminoethyl)-5-naphthylamine-1-sulfonic acid was labeled on TN in one set of experiments and on actin in another set of experiments as energy donor, while 5-iodoacetamido-fluorescein was labeled on TM as acceptor. The energy transfer efficiency was obtained by comparing the donor lifetimes in the presence or absence of acceptor labeled proteins using nanosecond pulse fluorimetry. The distances between the donor-acceptor pair on TN and TM and on TM and actin were calculated in various reconstituted complexes and also in the presence or absence of Ca. The results support our previous view (Fed. Proc. 39:1621a) that (1) the distance between the donor and acceptor on TM and actin was about 65 Å; and (2) upon Ca binding, the fluorophore pair on actin and TM only moved slightly apart, less than 2 Å. Furthermore, using a critical distance of 46 Å, the distance between the donor and acceptor on TN and TM , in the presence of Ca, was calculated to be about 64 to 68 Å. In the absence of Ca, TN moved further away from TM, about 6 to 10 Å. These results seem to bear some important implications on the spatial relationship of TN, TM, and actin in the thin filament and the mechanism of Ca regulation.

Supported by grants from the National Heart,Lung, and Blood Institute and Texas Affiliate, American Heart Association.

T-AM-A1 SEGMENTAL FLEXIBILITY OF MONOCLONAL IMMUNOGLOBULINS: MODE-LOCKED LASER STUDIES OF FLUORESCENCE EMISSION ANISOTROPY. J. Reidler, V.T. Oi, W.F. Carlsen, I. Pecht, L.A. Herzenberg and L. Stryer, Depts. of Structural Biology and Genetics, Stanford Univ. School of Medicine, Stanford, CA 94305.

The segmental flexibility of two monoclonal mouse IgG1 immunoglobulins differing in both their V and C regions was investigated by nanosecond fluorescence polarization spectroscopy. These antibodies (DNS1 and DNS2) have high affinity ($K > 10^7\ M^{-1}$) for the dansyl group. The time-dependence of the emission anisotropy of dansyl lysine bound to IgG and to F_{ab} was measured with a single-photon counting apparatus (response time=0.5 nsec). Picosecond excitation pulses at 325 nm (repetition rate=800 KHz) were generated by doubling the 650 nm output of a synchronously-pumped mode-locked argon-ion/rhodamine 6G laser. The emission anisotropy kinetics showed that these monoclonal mouse immunoglobulins, like heterogeneous rabbit anti-dansyl antibodies (Yguerabide, Epstein, and Stryer, 1970), exhibit segmental flexibility in the nanosecond time range. Most interesting, the segmental flexibility of DNS1 increases markedly with temperature, whereas that of DNS2 stays nearly constant between 8 and 37°C. Thus, the properties of the hinge at the junction of the F_{ab} and F_c domains are affected by amino acid sequence differences between the C regions of DNS1 and DNS2, which are specified by allelic genes. Supported by research grants from the National Institutes of Health.

T-AM-A2 CARBON-13 NMR RELAXATION STUDIES OF MYOSIN, S1 AND ROD

Thomas M. Eads and Leo Mandelkern
Department of Chemistry and Institute of Molecular Biophysics
Florida State University, Tallahassee, FL 32306

Natural abundance carbon-13 nmr linewidths ($\Delta\nu_{\frac{1}{2}}$) and relaxation parameters T_1 and NOE have been measured at 37.7 MHz with proton scalar decoupling on native and LiBr-denatured rabbit skeletal muscle myosin, subfragment 1 (S1) and ROD. S1 and ROD were purified from chymotryptic digests of myosin filaments. NMR sample temperature was 20-25°C.

The spectra of myosin, denatured myosin and S1 are distinct. In carbonyl, alpha and aliphatic spectral regions all preps show narrower peaks superimposed on a broad base. S1 and denatured myosin show much narrower lines. Spectral region relative areas and linewidths of decoupled, unenhanced spectra indicate motional broadening of alpha carbons related to particle size and shape. Lower frequency motional contributions to intensities and linewidths are estimated. Linewidths, T_1 and NOE of spectral regions and narrow peaks are discussed in terms of particle size, shape, sample viscosity and concentration. Ranges for Cα T_1 are 0.1 to 0.3s; for NOE 1.3 to 2.0; for $\Delta\nu_{\frac{1}{2}}$ 260 to 500 Hz. The range of motion probed in these experiments corresponds to correlation times of 10^{-11} to 10^{-7}s. Correlation times (τ_c) of selected carbon resonances are calculated from relaxation parameters using simple models for S1 and denatured myosin. Calculated τ_c's are compared with results from other methods.

T-AM-A3 INTERNAL PROTEIN DYNAMICS, HEMOGLOBIN ALLOSTERY, AND HYDROGEN EXCHANGE MECHANISM. S.W. Englander, J.R. Rogero*, and J.J. Englander*, Dept. of Biochemistry and Biophysics, Univ. of Pennsylvania, Philadelphia, PA.

There is general agreement that the hydrogen exchange (HX) behavior of a protein depends on its internal structural dynamics, but controversy exists concerning the kinds of motion involved, so that the proper interpretation of HX data in terms of structure, structure change, and structural dynamics is uncertain. Alternative models visualize, as the HX rate determining mechanism, either penetration of the native protein by HX catalysts (OH^-,H_3O^+) or transient local unfolding reactions of individual segments.

A differential H-T (tritium) exchange method is being used to study hemoglobin (Hb) structure change. Results show that a small fraction of Hb's peptide H are sensitive to the allosteric form, and these occur in distinct sets of 4 to 18 H. The sets behave as predicted by the local unfolding model, i.e. all the H in a set exchange at about the same rate in the deoxy form, and when the T to R transition occurs, all these H move as a group to a new much faster rate. We are now attempting to determine the structural location of each kinetically defined set by labeling each set one at a time with tritium, fragmenting the protein, and separating fragments by use of HPLC. Results indicate that about half the protons in each set occur on the α-subunits and half on the βs. All the H in each half-set occur together on a given oligopeptide segment. The several sets so far studied are placed along the length of a C-terminal segment of the β-subunit and an N-terminal segment of the α-subunit. It is difficult to reconcile these results with penetration models for the HX process.

T-AM-A4 A MONTE CARLO STUDY OF THE FOLDING PROCESS IN AN IDEALIZED MODEL OF BOVINE TRYPSIN INHIBITOR. S. Miyazawa and R. L. Jernigan, Laboratory of Theoretical Biology, DCBD, NCI, National Institutes of Health, Bethesda, MD 20205

The folding process of reduced bovine trypsin inhibitor in thermodynamic equilibrium is studied by using an idealized model in which simplified interactions between residues are assumed. The protein molecule is regarded as a self-avoiding chain which consists only of C^{α} and C^{β} atoms, except for glycine. Only the backbone dihedral angles are varied and permitted to take discrete values at every 10 degrees. Intra-residue interactions are estimated on the basis of the distributions of (ϕ, ψ) observed in the crystal structures of 20 proteins, which were tabulated by Némethy and Scheraga (1977). Conformations are generated randomly with a bias from these short range probabilities. If contacts closely corresponding to the native conformation are obtained, then that sample is weighted with an additional favorable probability. Various cases from the native state to denatured states are considered by changing the value of the native conformation probability. We estimate S(H) [Gō, 1975], the entropy of the molecule for a given value of enthalpy, H. The S(H) function clearly shows that the folding-unfolding transition in this idealized model is an all-or-none type. In addition to that, we calculate the statistical averages of quantities which characterize the extent of folding at a given value of enthalpy, such as the probabilities of S-S bond formation among the 15 possible cystine pairs and of forming each contact region. We may obtain some information about the folding pathway from these quantities, e.g., the order of S-S bonds formed and of contact regions formed, even though a highly artificial interaction potential has been used.

T-AM-A5 ON THE COMPUTATION OF THE TERTIARY STRUCTURE OF GLOBULAR PROTEINS. Narendra S. Goel, Department of Systems Science, State University of New York, Binghamton, New York 13901.

It is generally believed that the tertiary structure of a globular protein is a configuration of minimal free energy. However, approaches to determine the tertiary structure based on minimization of free energy have not yet been successful.

An alternate approach to the problem will be presented. The approach is based on a geometrical model in which no explicit use of the concept of free energy is made. Instead, energy considerations are implicit in the form of constraints on distances between atoms. Using, as input, information on sequence of amino acids and certain averages of interatomic distances, which can be semi-empirically estimated, structures have been computed for several proteins. These calculated structures resemble those determined by x-ray diffraction methods. It will be shown that the approach presented here is related to the problems of artificial intelligence, image processing and image reconstruction.

T-AM-A6 MOTIONAL AVERAGING OF NMR RELAXATION PARAMETERS IN PROTEINS. R.M. Levy, Rutgers Univ., New Brunswick, N.J., and M. Karplus*, Harvard Univ., Cambridge, Mass.

The nature of the atomic motions in the interior of proteins is currently a topic of great interest. To characterize these motions a wide range of experimental and theoretical techniques are being employed. In spite of the close packed structure of native proteins, significant atomic fluctuations can occur on a picosecond time scale. We make use of recent molecular dynamics simulations of the pancreatic trypsin inhibitor (PTI) to demonstrate the effects of picosecond fluctuations on the observed NMR ^{13}C T_1 values. We show that picosecond averaging has to be included in relating measured T_1 values to other motional properties of the protein (e.g. overall tumbling). For protonated carbons in proteins, ^{13}C NMR relaxation is dominated by dipolar interactions between the ^{13}C nuclei and directly bonded protons. From the protein trajectory studies we conclude that picosecond angular flutuations of the CH internuclear vector do lead to large increases in T_1 values for some of the carbons in PTI. We contrast the extent of motional averaging for protonated carbons on aliphatic residues with the results for aromatic residues. At low field, non protonated carbons in proteins are also relaxed by dipolar interactions with nearby protons. For these carbons, fluctuations in both internuclear distances and angular fluctuations must be considered in order to evaluate the effect of picosecond dynamics on the NMR relaxation.

T-AM-A7 PREDICTED COMBINING SITE STRUCTURE OF IMMUNOGLOBULIN MOPC167.
Steven E. Coutre and Tai Te Wu, Departments of Biochemistry & Molecular Biology and Engineering Sciences & Applied Mathematics, Northwestern University, Evanston, IL 60201.

In our continued effort in trying to predict three-dimensional foldings of the complementarity determining regions (CDR) of antibodies based on their amino acid sequences, the antibody combining site of immunoglobulin MOPC167 was proposed. The basic requirements of the predictive method were: (i) Amino acid sequences of the six CDR's were known, (ii) Each predicted folding of any CDR could be connected onto the framework region of immunoglobulin Newm, and (iii) Steric hindrance should be avoided for all backbone atoms. Since Newm had only five CDR's, slight adjustments of the framework regions bordering on the antibody combining site would be required to accomodate the usual six CDR's. These restrictions were so severe that essentially only one structure was allowed. That for MOPC167 contained a small pocket where the phosphocholine molecule might bind, and was significantly different from our previously predicted structure for the 2,4-dinitrophenol binding site of immunoglobulin MOPC315 (Stanford, J. M. and Wu, T. T. (1981) J. Theoret. Biol., in press.). Our method therefore appears applicable to the prediction of the three-dimensional structure of the antibody combining site of any immunoglobulin so long as the amino acid sequences of its six CDR's are known.

(Supported in part by NIH Grant 5-R01-GM21482, and NIH Contracts N01-RR-4-2147 and N01-RR-8-2158 with the PROPHET computer system.)

T-AM-A8 CONFORMATIONAL ENERGY CALCULATIONS ON GLYCOSYLATED β TURNS IN GLYCOPROTEINS,
C. Allen Bush, Dept. of Chem., Illinois Inst. of Tech., Chicago, IL 60616.

Analysis of the amino acid sequence of glycoproteins has suggested the β turn as a likely site of glycosylation in glycoproteins. According to this model, the peptide chain traverses the interior of a globular protein, reversing its direction at the protein surface, a likely point for the attachment of hydrophillic carbohydrate residues. In order to search for plausible conformations of glycosylated β turns in asparagine linked glycoproteins, we have adapted the conformational energy calculation method of Scheraga and coworkers for use in carbohydrates. The parameters for non-bonded and hydrogen bonded interactions are those which have been published and electrostatic parameters are derived from a CNDO calculation on a model glycopeptide. Our results indicate that the orientation of the glycosyl amide bond having the amide proton nearly trans to the anomeric proton of the sugar has the lowest energy. Although circular dichroism and nmr experiments in our laboratory have consistently found this conformation, our calculations show the conformation having these two protons in a cis relationship to lie very close in energy. Calculations on the glycopeptide linkage model, α-N Acetyl, δ-N(2-acetamido 1,2 dideoxy β-D-glucopyranosyl) N-Methyl-L-asparaginyl amide show that several distinct geometries are allowed for glycosylated β turns. For a type I β turn, three conformations of the glycosylated side chain are found within 4 kcal of the minimum while two conformations of the glycosylated side chain are allowed for a type II turn. The hydrogen bonded C7 conformation is also allowed. Stereo views of the low energy conformations reveal no major hydrogen bonding interaction between the peptide and sugar.

T-AM-A9 GENETIC ANALYSIS OF IN VIVO PROTEIN FOLDING AND SUBUNIT ASSEMBLY. David P. Goldenberg, Donna H. Smith and Jonathan King. Dept. of Biology, MIT, Cambridge, MA 02139

We are studying the in vivo pathway of folding and assembly of newly synthesized polypeptide chains into multimeric proteins,using mutations which interfere with these processes. The tail spike protein of bacteriophage P22 is a trimer of 76,000 dalton polypeptide chains coded for by gene 9 of P22. The mature protein is thermostable, requiring 90°C incubation for inactivation, and is resistant to detergent denaturation and to protease digestion. No covalent modifications have been associated with its maturation.

By pulse labeling infected cells, it has been possible to identify a kinetic intermediate in the folding and assembly of the tail spike which is sensitive to SDS and to protease. This precursor matures into SDS resistant trimers with a half time of five minutes at 30°C. The population of precursors may include unassembled monomers, dimers, or subunits which have associated into trimers but have not completely folded.

Temperature sensitive mutations have been mapped to more than 30 sites in gene 9. These amino acid substitutions prevent the formation of active tail spikes at 39°C, but not at 30°C. Once the mutant proteins have been matured at 30°C, their function and stability is indistinguishable from that of the wild type protein.

The inactive polypeptide chains which accumulate at 39°C are SDS and protease sensitive. They fail to react with antibodies to the mature protein, but are precipitated by antibodies to the denatured protein. On shifting mutant infected cells from 39°C to 30°C, in the absence of new protein synthesis, these chains mature into stable trimers. These results suggest that the ts amino acid substitutions act by kinetically blocking the pathway of folding, perhaps by destabilizing some intermediate structure essential for further folding, but not essential for the stability of the mature protein.

T-AM-A10 GLYCOSYLATION-INDUCED CONFORMATIONAL CHANGE IN α-CRYSTALLIN OF BOVINE LENS. J.N. Liang and B. Chakrabarti, Eye Research Institute of Retina Foundation and Harvard Medical School, Boston, MA 02114.

Observed cataract formation followed by nonenzymatic glycosylation of lens protein has led several investigators to suggest that extensive in vivo glycosylation may be a cause of the disease. It is not known, however, whether glycosylation produces a protein conformational change responsible for the lens opacity. We used circular dichroism (CD) to investigate glycosylation-induced conformational change in α-crystallin isolated from bovine lens. In the near-ultraviolet (UV) region, four major CD bands —at 286, 274, 266, and 258 nm — can be observed. All these bands are presumably contributed by aromatic amino acid residues. The CD spectrum below 250 nm is typical of the β-conformation of the protein. Upon glycosylation, there is a large increase in the magnitude of near-UV CD bands, whereas far-UV CD bands remain unchanged. This indicates that although glycosylation may not alter the secondary structure of the protein, it can change the environment and/or orientation of the chromophore groups, which in turn changes the protein's tertiary structure (as manifested in the near-UV CD spectrum). In absorption spectra, no significant difference was observed between glycosylated and unglycosylated protein. Kinetic studies indicate that glucose-6-phosphate is more effective in glycosylation than is glucose itself.

T-AM-A11 EFFECTS OF LIGAND BINDING AND SUBUNIT ASSOCIATION ON THE HYDROGEN EXCHANGE KINETICS OF E. COLI ASPARTATE TRANSCARBAMYLASE. M. Lennick and N.M.Allewell, Wesleyan University, Middletown, CT 06457.

We have used tritium exchange to examine alterations in the structural dynamics of E.coli aspartate transcarbamylase (c_6r_6) and its catalytic subunit (c_3) produced by ligand binding and subunit association. Contrary to expectation, the most striking effects are observed with c_3, rather than c_6r_6, under the experimental conditions employed (0.04M KH_2PO_4-K_2HPO_4, 2mM β-ME, 0.2mM EDTA, pH 7.0; exchange in at 25°C for 18 hr, exchange out at 0°C for 5 hr).

Binding of the bisubstrate analog PALA (N-phosphonacetyl-L-aspartate) to c_3 produces a substantial decrease in the rate of exchange. (Least squares fitting of data obtained in the presence and absence of PALA to the equation $H_{rem}/c\ chain = \sum_{i=1}^{2} N_i e^{-k_i t}$ yielded values for N_1, N_2, k_1, k_2 of 24 H, 127 H, 1.27 hr^{-1}, 0.02 hr^{-1}, and 58 H, 103 H, 2.24 hr^{-1}, 0.07 hr^{-1}, respectively.) Exchange from c_3 is also slowed by binding of carbamyl phosphate (CP), although the magnitude of the change is ~1/3 that seen for PALA. Addition of succinate (10mM) to c_3 saturated with CP has negligible effect. In contrast, binding of ATP (10mM) to c_3 accelerates the rate of exchange, although CTP (10mM) produces no change.

The same pattern of effects results from binding of PALA, CP, and succinate to c_6r_6, although their magnitudes are reduced two to three-fold. Experiments carried out with reconstituted c_6r_6 in which only one type of subunit is labeled indicate that reassociation of labelled c_3 with unlabelled r_2 slows exchange from c_3 and that the perturbations produced by PALA binding are largely confined to the catalytic subunits. These results suggest that c_3 is conformationally constrained by its interactions with r_2 and that these constraints diminish the effects of PALA on its structural dynamics.

Supported by NIH Grant AM-17335.

T-AM-A12 EFFECTS OF LIGANDS ON THE SELF-ASSOCIATION OF PHOSPHOFRUCTOKINASE. Michael A. Luther, Lyndal K. Hesterberg, and James C. Lee. Department of Biochemistry, St. Louis University School of Medicine, St. Louis, MO 63104.

The self-association of rabbit muscle phosphofructokinase (PFK) has been studied and the mass distribution of the polymeric species was calculated. At 23° C, pH 7.00 and at PFK concentrations less than 200μg/ml the equilibrium can best be described as a rapid equilibrium between monomer and tetramer with a $K_4^{app}=5.06\times10^5$ $(ml/mg)^3$.

In the presence of substrates the self-association is dramatically enhanced, e.g. in 1.0 mM fructose 6-PO_4, the K_4^{app} increased by 10^4 fold; in 0.1 mM ATP, a 2×10^2 fold increase was observed, whereas in 1.0 mM fructose 6-PO_4, and 0.1 mM AMP-PNP, the K_4^{app} increased by 10^6 fold. The effect of the kinetic activator, ADP, is to enhance the tetramerization by 10^3 fold. In contrast, the allosteric inhibitor, citrate, altered the mode of association. It is best described as monomer $\rightleftharpoons$ dimer $\rightleftharpoons$ tetramer.

Results of active enzyme sedimentation studies reveal the tetramer as the only detectable active form under all the experimental conditions tested. Thus, assuming that the tetramer of PFK is the smallest active form, then the amount of activity observed under steady-state kinetic conditions must be proportional to the amount of tetramer present.

To test this assumption this study correlated the mass distribution of the enzyme under steady-state kinetic conditions to the activity observed in kinetic assays. The effects of various ligands have also been correlated to the physical state of the enzyme. (Supported by NIH grants NS 14269, AM 21489, HLO 7050, and the Council for Tobacco Research, Inc.).

T-AM-B1 DIPHTHERIA TOXIN IN PLANAR LIPID BILAYERS: LIPID DEPENDENCE OF PROTEIN INSERTION INTO MEMBRANES. James J. Donovan, Melvin I. Simon, and M. Montal. U.C.S.D., La Jolla CA 92093

Diphtheria toxin (DT) does not interact with planar bilayers at neutral pH. However, at acidic pH (<5.0) DT binds to soybean phospholipid membranes. This is consistent with earlier studies of the binding of DT to liposomes (1). Further, if a negative potential is applied across the membrane, DT inserts into the bilayer and thereby increases the membrane conductance by forming transmembrane, voltage-dependent, anion-selective channels. These channels, once formed, are permanent entities in the membrane (2). The rate of channel formation depends upon the lipid composition of the membrane. DT appreciably increases the conductance only of membranes containing the lipid phosphatidylinositol (PI) or its derivative, phosphatidylinositol phosphate (PIP, see figure). The extent of interaction of DT with the bilayer at acidic pH (as measured by the increase in conductance) is greatest for PIP and follows the sequence: PIP > PI >> phosphatidylserine ≃ phosphatidylcholine > phosphatidylethanolamine ≃ oleoylphospahte. Thus, the presence of a sugar phosphate in the bilayer seems to be essential for the insertion of DT into the membrane. This illustrates how a specific lipid can influence the insertion of a soluble protein into the bilayer.

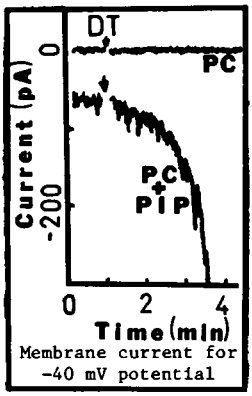

Membrane current for -40 mV potential

1. Alving, Iglewski, Urban, Moss, Richards, and Sadoff. PNAS (1980) 77:1986-1991.
2. Donovan, J., M. I. Simon, R. Draper, and M. Montal. PNAS (January 1981, in press).
This work was supported by grants from the NIH and the ONR.

T-AM-B2 COMPARISON OF A THEORY FOR CARRIER-MEDIATED PERMEATION WITH EXPERIMENTS ON BILAYERS IN THE PRESENCE OF PV. S. Ciani. Dept. of Physiology, UCLA, CA, 90024.

Benz et al. [B.B.A. 445 (1976) 665] studied the electrical properties of bilayers mediated by the carrier PV, a molecule thought to react with ions in water (solution complexation), rather than at the membrane boundaries (interfacial complexation). Comparing their conductance data with our theory for "solution complexation", it was possible to infer approximate values for the dissociation rate constant of the PV-K^+ complex, k_D^a, as well as for the membrane permeability to the neutral carrier, P_s. These are: $k_D^a \simeq 3 \times 10^3$ s^{-1} and $P_s \simeq 8 \times 10^{-4}$ cm/s. However, using these numbers in the equation for the zero-current potential in gradients of carriers, it was found that consistency between the theory and the experiments could be obtained only by postulating an exchange of carriers between the membrane surface and the torus. Alternatively, a consistent interpretation of the data, even without that assumption, is also possible in terms of "interfacial complexation", and is actually preferable, in that it allows for lower k_D^a values, as suggested by independent data (even though taken in methanol instead of in water) [Davis et al. Biochemistry 15 (1976) 768].
Supported by NS 13344.

T-AM-B3 HALOFLUORESCEIN DYE AND pH GRADIENT INDUCED PHOTO-VOLTAGES IN BILAYER MEMBRANES. Jay S. Huebner and W. E. Varnadore, Jr., Department of Natural Sciences, University of North Florida, Jacksonville, Florida 32216, U. S. A.

Halogenated fluorescein dyes, such as erythrosin, ethyl eosin and rose bengal, induce voltage transients across bilayer membranes in response to light flashes and pH gradients. The waveforms vary with membrane lipid, aqueous solution salt concentration and pH. The waveforms have their simplest form in ≥ 1 M NaCl solutions with 10 ns light flashes, in which case the high pH solution is driven positive several mv in 50 ns (the apparatus speed as used here) and returns to the base line in $\lesssim 1$ μs. These effects are observed with glycerol monoolein, phosphatidylcholine and phosphatidylethanolamine, but not with oxidized cholesterol membranes. The polarity is reversed by reversing the pH gradient. More complex and slower waveforms are observed with phosphatidylethanolamine membranes and < 0.1 M NaCl solutions, which will be described elsewhere. The fast transients are explained by a theory which considers that dye; i) permeates bilayers and sorbs in the glycerol regions where it is partially exposed to the solution pH values, ii) releases phenolic protons on illumination, providing the solution pH is approximately between the pK_as of the ground and excited states and iii) reabsorbs protons from the adjacent solution $\lesssim 1$ μs later. The photo-voltage amplitudes are larger for dyes which incorporate the more massive halides. This and the $\lesssim 1$ μs fall time suggest triplet states are involved. Light flashes and erythrosin produce bursts of $\sim 5 \times 10^8$ protons/mm^2 at the membrane interface. This may be useful for comparison to rhodopsin and for studying kinetics of pH gradient and transient induced reactions.

Support from Eastman Kodak Co., the National Institute of General Medical Sciences (grant GM 23250) and the Naval Medical Research Institute is acknowledged.

T-AM-B4 SURFACE BILAYER FORMATION IN LECITHIN DISPERSIONS: TEMPERATURE OF FORMATION DEPENDENCE ON ACYL COMPOSITION. K. Tajima* and N. L. Gershfeld, LPB/NIAMDD, National Institutes of Health, Bethesda, MD 20205.

At the air/water interface of nonsonicated aqueous lecithin dispersions single bilayers form spontaneously at a specific temperature T_f. At temperatures above and below T_f surface bilayers do not form. T_f depends on the fatty acid composition of the lecithin, e.g., lecithins bearing the following fatty acids have these values: 18:1/18:1, < 0°; 14:0/14:0, 29°; 16:0/16:0, 43°. In mixtures T_f depends on the relative proportion of the components in the bulk dispersion. For example, in the mixed lecithin dispersion 18:1/18:1 + 14:0/14:0 (1:1), T_f is approximately 10°, intermediate between the temperature for each pure component. The surface pressures also have characteristic values at these temperatures. In principle, these surface phenomena should be reflected in some property of the equilibrium bulk dispersion. A discussion of these properties will be presented.

* Present address: Tokyo Metropolitan University, Tokyo, Japan.

T-AM-B5 MODIFICATION OF BILAYER MEMBRANE DIPOLE POTENTIALS BY AMINE-BORANES. L. J. Bruner†, M. Mark Midland*, and Janet Wisniewski*. Departments of Physics† and of Chemistry*, University of California, Riverside, CA 92521.

Hydrophobic anions of dipicrylamine (DpA^-) have been used as probes of bilayer membrane dipole potential changes brought about by introduction of amine boranes. In a typical experiment dioleoyl phosphatidyl choline membranes are formed at 25°C in unbuffered 1.0M NaCl containing 10^{-7}M DpA^-. The initial low field conductance, λ_{oo} and relaxation time, τ_o, of the DpA^- transient are determined[1]. Then sufficient triethylamine borane is added to saturate the stirred aqueous phases. Ensuing changes of λ_{oo} and of τ_o are monitored. Typical results are: before amine borane addition, $\lambda_{oo}=2.2\times10^{-3}\ \Omega^{-1}cm^{-2}$, $\tau_o=1.50$ msec, $\lambda_{oo}\tau_o=3.18\times10^{-6}\Omega^{-1}cm^{-2}$sec. One hour after addition: $\lambda_{oo}=4.59\times10^{-3}\Omega^{-1}cm^{-2}$, $\tau_o=1.12$ msec, $\lambda_{oo}\tau_o = 5.14\times10^{-6}\Omega^{-1}cm^{-2}$sec. These results are consistent with amine borane orientation in the membrane/solution interfaces as illustrated.

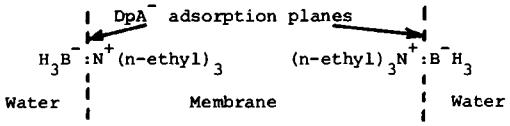

The configuration shown would be expected to facilitate both adsorption and translocation of DpA^- ions. Additional results with other amine boranes will be discussed.

Supported by PHS Grant GM-27626.

1. Ketterer, B., Neumcke, B., and Läuger, P. 1971. J. Membrane Biol. 5:225.

T-AM-B6 ST-EPR DISPERSION STUDY OF SPIN-LABELLED, ORIENTED LIPID MULTIBILAYERS. Colin Mailer*, Dept. of Physics, University of New Brunswick, Fredericton, Canada and A.J. Dammers and M.A. Hemminga, Fysich Laboratorium, Rijksuniversiteit Utrecht, Utrecht, Holland.

We report the results of a study of the anisotropic motion of cholestane spin-label in macroscopically oriented multi-bilayers of dipalmitoyllecithin and cholesterol, using dispersion ST-EPR. The data were obtained in the temperature range +25°C to -30°C with a specially designed TM_{110} bimodal induction EPR cavity, that reduces klystron FM noise effects below the crystal detector noise level (1). Comparison will be made with conventional EPR signals (V_1) and the more commonly used ST-EPR signals (V_1^1) as regards sensitivity to motional processes and size of signals. Operational aspects of bimodal EPR induction spectroscopy will be discussed, with emphasis on the modifications necessary to standard commercial EPR instruments.

This work was supported by the National Science and Engineering Research Council of Canada, the University of New Brunswick Research Fund, the University of Utrecht and the Netherlands Organization for the Advancement of Pure Research (Z.W.O.)

(1) C. Mailer, H. Thomann, Bruce H. Robinson, and L.R. Dalton. Rev. Sci. Inst. Dec. 1980 (in press).

T-AM-B7 X-RAY DIFFRACTION AND CALORIMETRIC STUDY OF ANHYDROUS AND HYDRATED N-PALMITOYL GALACTOSYLCERAMIDE. Martin Ruocco*, D. Atkinson, D.M. Small, R. Skarjune, E. Oldfield and G.G. Shipley, Biophysics Division, Boston University School of Medicine, Boston, MA.

Scanning calorimetry over the 20°-143°C temperature range and x-ray diffraction of anhydrous NPGC demonstrates three crystal phases and one mesophase at 143°C before melting to an isotropic liquid at 180°C. The mesophase → crystal reversibility of anhydrous NPGC is contrasted in the NPGC-water system which exhibits a rate dependent cooling transition resulting in a metastable state. The existence of the metastable structure is indicated by the presence of an exotherm at 52°C during heating. The main transition in excess water occurs at 82°C with an enthalpy of 17.5 ± 1Kcal/mole. X-ray diffraction gives evidence of an ordered chain packing arrangement which, in addition to hydrogen bonding generated at the galactose-water interface, may account for the unusually high enthalpy of this transition.

The thermodynamic model proposed for the NPGC-water system involves states dependent on the rate of cooling from the liquid crystal. Slow rates result in a reversible stable crystal → liquid crystal transition. No exotherm during reheating is observed in this case. The rapid cooling cycle gives a metastable structure that returns to the stable form when reheated through the exotherm or after prolonged storage at ambient temperatures. The exotherm may be associated with the conversion to the stable structure by concommitant headgroup matrix rehydration and chain packing rearrangements.

From kinetic x-ray diffraction and calorimetric studies it is proposed that molecular forces which act synergistically during the chain melt are separated on cooling giving a metastable state. This separation results in hydrocarbon chain freezing which preceeds a time and temperature dependent rearrangement of the hydrogen bonding matrix involving NPGC-NPGC and NPGC-water interactions.

T-AM-B8 SOLVENT-FREE LIPID BIMOLECULAR MEMBRANES OF LARGE SURFACE AREA
Vitaly Vodyanoy and Randall B. Murphy, Department of Chemistry, and Laboratory of Radiation and Solid State Physics, New York University, 4 Washington Place, New York, NY

A method of successive transfer of lipid monolayers onto a hydrostatically closed chamber has been developed which allows the construction of large (2 mm^2), solvent-free bimolecular membranes. The approach is a modification of the conventional Montal-Mueller method. A hydrostatically closed chamber is utilized, which greatly increases the ability of the membrane to resist mechanical disturbances, and produces hydrostatic equilibrium necessary for electrical measurements. The electrical properties of the bimolecular lipid membrane are similar to those prepared by conventional Montal-Mueller techniques. Electrical and hydrostatic compressibility measurements have been performed on both solvent-containing and solvent free membranes prepared by the above methods. The modulus of compressibility as determined by both approaches is identical within the limits of experimental precision.

T-AM-B9 The Amplitude of Rippling in the P_β Phase of Dipalmitoyl Lecithin
J. Stamatoff, B. Feuer, H. Guggenheim, G. Tellez, and T. Yamane
Bell Labs, Murray Hill, NJ 07974

We have investigated the small angle diffraction of dipalmitoyl lecithin at variable temperature and water content using high purity lipids, precision temperature control, and unusually high angular resolution X-ray diffraction methods. In an earlier abstract (Fed. Proc. 39, p. 1834 [1980]) we noted the appearance of several peaks in the region about the first diffraction order due to multilayering. We now report that this diffraction order splits into two peaks throughout the P_β region. Our results agree with earlier studies of the P_β phase by others showing (1) diffraction peaks (d ∿ 150Å) due to rippling and (2) an increase in the multilayer d spacing and disorder.

Splitting of the first order does not imply a new phase as demonstrated using Gibbs phase rule and specimens in excess water. Splitting of this order does imply a zero in the structure factor curve for the rippled bilayer.

Using a very general model, the position of this zero may be used to measure the amplitude of the ripple in the P_β phase. We find that the amplitude is ∿50Å (peak to peak). This amplitude is large enough to suggest a mechanism for rippling. As shown by McIntosh, hydrocarbon tails tilt in order to match headgroup and tail surface areas. In the P_β phase Rand has shown that the chains straighten and become parallel to the stacking direction. Our measurement of a large ripple amplitude permits the headgroup to be displaced out of the bilayer plane permitting matched surface areas with straight chains. Thus, the pretransition marks the transition to an alternative solution to the area mismatch problem.

T-AM-B10 MOLECULAR ORIENTATIONAL ORDER IN STRUCTURES OF THE RIPPLE PHASE: A DMR STUDY, M.J. Vaz, J.W. Doane, and P.W. Westerman, Liquid Crystal Institute and Department of Physics, Kent State University, Kent, Ohio 44242 and Northeastern Ohio Universities College of Medicine, Rootstown, Ohio 44272.

The ripple ($P_{\beta'}$) phase in aqueous multilamellar dispersions of 1-myristoyl-2-[14',14',14'-d_3] myristoylphosphatidylcholine, (DMPC-d_3) and 1-palmitoyl-2-[16',16',16'-d_3] palmitoylphosphatidylcholine, (DPPC-d_3) is found to be characterized by several different structures each exhibiting different orientational order of the terminal segment of the 2-hydrocarbon chain. Each of these structures is identified by a different deuterium spectral pattern with a differently time averaged quadrupole coupling constant and different motionally induced asymmetry parameter. The spectral pattern which appears immediately below the upper phase transition exhibits a large asymmetry parameter, $\eta \simeq 1$ indicating biaxial orientational order. This feature is consistent with either a cooperative tilt of the phospholipid hydrocarbon chain in the bilayer or a cooperative rotational freeze out about the molecular long axis. At slightly lower temperatures in the $P_{\beta'}$ phase other spectral patterns appear which have little apparent asymmetry but different time averaged coupling constants. One of these uniaxial patterns is continuous into the gel ($L_{\beta'}$) phase while the other disappears at the $P_{\beta'}$-$L_{\beta'}$ phase transition. Molecular models for the ripple phase will be discussed.

(Supported in part by the National Institute of General Medical Sciences under Grant No. GM 27127-01)

T-AM-B11 ON THE REVERSIBLE AGGREGATION OF VESICLES: Na^+, Mg^{2+} AND VESICLE CONCENTRATION. J. Bentz, S. Nir, and N. Düzgüneş.

The cation (Na^+ and Mg^{2+}) induced aggregation of sonicated phosphatidylserine vesicles has been studied with respect to both the initial kinetics and the equilibrium state. Using the DLVO theory to compute the initial rate constant of dimerization (which requires explicit consideration of cation binding and hydrodynamic corrections) we have discovered that the aggregation is dynamical: aggregates continuously form and break up, and it is the net rate of this process which is measured as the aggregation rate. Furthermore, using the general mass action kinetic equations to model the aggregation kinetics we have discovered that the higher order aggregates (trimers, etc.) form rapidly enough (<1 sec) to significantly affect light scattering measurements. Aggregation induced by Na^+ ($\geq$ 500mM) or by Mg^{2+} (2-5mM) plus Na^+ (200mM) is shown to be completely reversible and qualitatively equivalent. That is, at subfusion concentrations of Mg^{2+}, the DLVO theory will predict the threshold concentrations of these cations needed to induce fast aggregation. To facilitate the analysis of these types of data we have constructed a flexible classification system for aggregation (using the general mass action kinetic equation) which yields simple approximate formulas for the mass average aggregate size and other aggregate size distribution parameters. Simulations of the turbidity curves using this approach (which includes the scattering interference effects) clearly follow the corresponding experimental curves. Rate constants and equilibrium constants used in these simulations are then used to estimate the depth of the primary energy minimum which holds aggregates of sonicated vesicles together. This work was supported by Grants NIH-GM-23850 and NCI-IN-54R17.

T-AM-C1 SLOW INWARD CURRENT CARRIED BY Ca^{2+} OR Ba^{2+} IN SINGLE ISOLATED HEART CELLS
Kai S. Lee, Esther W. Lee and Richard W. Tsien, Department of Physiology, Yale University School of Medicine, 333 Cedar Street, New Haven CT 06510.

Isolated and internally perfused heart cells offer a promising system for studying the regulation of membrane channels by intracellular ions and messenger molecules. We have begun analysis of slow inward Ca channels (I_{si}) in single myocytes from guinea pig and rat heart ventricle using the method of Lee et al. (Nature, 278, 269, 1979). Single cells are enzymatically dissociated, then voltage clamped by a suction pipette which contains the internal perfusion fluid. To minimize interference from Na or K channels, the internal solution typically contained (in mM): 114 Cs-aspartate, 37 CsF, 5 K_2HPO_4, 5.5 glucose, pH=7.2 with Tris. External solution: 85 Cs-aspartate, 2.85 $MgCl_2$, 5.4 $CaCl_2$ or 5.4 $BaCl_2$, 146 sucrose, 5.5 glucose, pH=7.6 with Tris. Experiments were carried out at room temperature. Under these conditions, the inward current resembles I_{si} seen in multicellular preparations. The inward current begins activating near -35 mV, and reaches a peak near 0 mV (left panel). It vanishes in Ca-free solution and increases if Ca_o is increased or replaced by Ba_o. It is not blocked by 30 μM TTX, nor inactivated by prepulses to -40 mV. The right panel shows a surprising but consistent feature of records taken with external Ba (but not external Ca): the time-dependent current reverses at strong depolarizations.

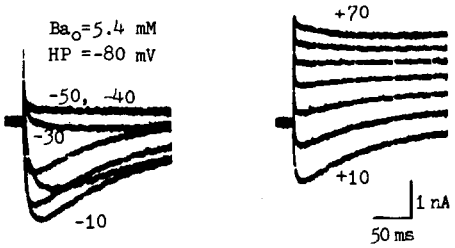

T-AM-C2 IS THE SLOW INWARD CALCIUM CURRENT OF HEART MUSCLE INACTIVATED BY CALCIUM?
Eduardo Marban and Richard W. Tsien, Department of Physiology, Yale University School of Medicine, 333 Cedar Street, New Haven, CT 06510.

It is widely assumed that the slow inward Ca current (I_{si}) in heart muscle is governed by independent processes of activation and inactivation. We have tested this proposition in calf Purkinje fibers under two-microelectrode voltage clamp. To inhibit transient outward current, intracellular K was replaced by Cs using nystatin. This procedure unmasked a large I_{si} with minimal contamination by outward current components. Inactivation produced by a variable conditioning pulse (PI) was assayed by reduction of I_{si} during a subsequent test pulse (PII). Less inactivation occurs as PI is increased from +20 to +80 mV, contrary to expectations of a Hodgkin-Huxley type voltage-dependent mechanism. This result is consistent with the hypothesis that Ca entry leads to inactivation, since Ca influx should diminish as PI approaches E_{Ca}. When Ca is replaced by Ba, both the degree and rate of inactivation decrease, arguing against changes in driving force as a major factor. These results are consistent with earlier findings in Paramecium, Aplysia neurons, and stick insect skeletal muscle, where Ca currents seem to be inactivated by intracellular Ca.

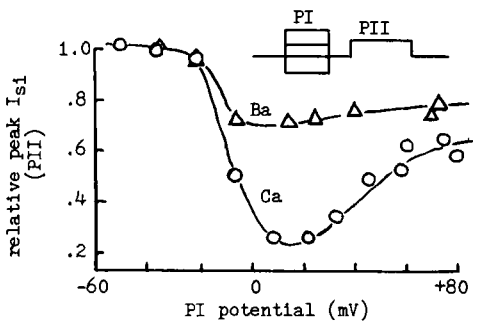

T-AM-C3 ISOLATION OF CALCIUM CURRENT IN INTERNALLY DIALYZED SNAIL NEURONS. Lou Byerly, USC, Los Angeles, CA 90007, and Susumu Hagiwara, UCLA Medical School, Los Angeles, CA 90024.

When neurons of the snail Lymnea stagnalis are dialyzed with Cs^+, Asp^-, EGTA and HEPES on the inside and bathed in a Na-free external solution, inward Ca currents are evoked by depolarization of the membrane to potentials above -20 mV. These inward currents reach a maximum amplitude at +20 mV and then decrease with further depolarization, reversing direction near +50 mV. External Cd^{++} (1 mM) completely blocks the inward current and greatly reduces the outward current. Difference currents obtained by subtracting currents before and after Cd^{++} reverse around +60 mV. We reject the interpretation that the current through Ca channels reverses at +60 mV, since the time course of the outward difference current is quite different from that of the inward and the difference current is not zero at all times for any one potential. In order to do tail current studies, we have speeded up the voltage clamp by recording membrane potential from an intracellular microelectrode and isolating the cells several hours before studying them so axon stubs have rounded into the soma. When the membrane is stepped back to -50 mV after a positive pulse, the inward tail currents decay with more than one time constant. Most of the Ca current decays in less than 500 μsec, too fast for us to accurately measure. However, the remaining inward current decays with a time constant of about 5 msec. This slower tail current increases in amplitude as the preceding pulse is made more positive, even up to +100 mV. It also increases with the duration of the positive pulse, even at +20 mV where the Ca current appears to decrease during the positive pulse. These slow tail currents may allow us to study the properties of the non-specific currents that overlap the Ca current in ths membrane.

This work is supported by U.S.P.H.S. NS09012 and NS15341.

T-AM-C4 EFFECTS OF INTRACELLULAR Ba ON Ca CURRENTS, Y. Tsuda, K. Morimoto and A. Brown, University of Texas Medical Branch, Galveston, Texas 77550.

Increases of intracellular Ca activity, Ca_i, above 10^{-6}M reduce or abolish Ca currents, I_{Ca}. With 10^{-7}M Ca_i, I_{Ca} inactivates at two rates, a fast one and then a much slower one. Addition of EGTA intracellularly in doses of 1-10mM slows the faster inactivation process and the time course of I_{CaEGTA} resembles that of Ba currents produced by equimolar substitution of Ba for Ca extracellularly. The results are consistent with Ca current-dependent inactivation of I_{Ca} (Tillotson, PNAS, 76: 1497, 1979). These doses of EGTA suppress Ca-activated K currents completely and in the solutions used presently (see below) non-linear outward currents are insignificant at potentials of +60 to +100mV. The role of Ca_i on I_{Ca} was examined further by adding Ba in mM amounts to the intracellular solution perfusing isolated voltage-clamped nerve cell bodies of Helix aspersa. Na currents were suppressed by tris substitution and K currents were supressed by Cs substitution, TEA and 4-AP. Ba_i at 0.1 to 10mM concentrations does not activate K or Cs currents and has no effect on the time course of I_{Ba}. The amplitude of I_{Ba} was reduced at the higher intracellular concentration. In the case of I_{Ca}, Ba_i slowed the faster inactivation process and I_{Ca} now had a time course similiar to that of I_{Ba} or I_{CaEGTA}. The results show that inactivation of the Ca channel is voltage- as well as current-dependent. We suggest that a site near the inner mouth of the Ca channel enhances block of I_{Ca}. The site can be occupied by Ba but does not enhance inactivation in this condition.

(Supported by NIH Grant NS-11453.)

T-AM-C5 ACTIONS OF CALCIUM ON ACTIVATION OF THE Ca CHANNEL AND CURRENT FLOW THROUGH IT, K. Morimoto, D. Campbell, Y. Tsuda, D. Wilson, N. Akaike and A. Brown, University of Texas Medical Branch, Galveston, Texas 77550

It is well-known that changes in the concentration of extracellular Ca ion, Ca_o, shift the voltage relationships of activation and inactivation for Na and K channels. Shifts in the relationship between conductance of Ca channels and voltage have also been reported. In addition, increases in Ca_o are associated with saturation of Ca currents, I_{Ca}, at potentials where g_{Ca} is maximal. We compared shifts in activation of I_{Ca} with saturation of I_{Ca} in voltage-clamped, internally-perfused isolated nerve cell bodies of Helix aspersa. Ca_o's ranged from 2.5 to 40 mM. Ba_o was substituted mole for mole for Ca_o. Steady state activation, m_∞, was calculated from peak currents or from tail currents at or near peak currents. In plots of voltage shift of m_∞ versus log concentration, there is for I_{Ca} an initial slowly rising phase which then ascends linearly with a slope of approximately 24 mv/decade Ca_o at extracellular concentrations above 10 mM. For I_{Ba}, there is much less shifting and it only becomes apparent at concentrations above 10 mM. These features are generally consistent with the Stern theory for the diffuse double layer with binding; we assume that Ca binds and Ba does not. Theory predicts that the divalent concentration at the membrane surface will be independent of the bulk concentration at concentrations where the maximal change in surface potentials occurs, given in this case by the peak shifts in m beginning at 10-20 mM Ca_o. Peak I_{Ca} saturates at concentrations above 20 mM, whereas I_{Ba} shows less saturation. It is concluded that saturation of I_{Ca} at high Ca_o's is explained at least in part by the consequences of altered surface charge.

(Supported by NIH Grant NS-11453)

T-AM-C6 DEPOLARIZATION AND Ca ENTRY IN SQUID AXONS. L. J. Mullins and J. Requena, University of Maryland School of Medicine, Baltimore, Maryland, 21201, and Centro de Biofisica y Bioquimica, IVIC, Caracas, Venezuela.

The application of 200-465 mM K^+, 50 mM Ca seawater to aequorin-injected squid axons leads to a phasic entry of Ca that is virtually totally dependent on $/Na/_i$. Both the peak response to depolarization and that of the steady state are enhanced about 8-fold by a doubling of $/Na/_i$ and the response is decreased 8-fold by a halving of $/Na/_i$. If an axon is depolarized with 465 mM K^+ seawater that is Ca-free for 4 min. and then tested with 465 mM K^+, 50 mM Ca seawater, the response is larger than normal so that inactivation of Ca entry occurs not as a result of a change in membrane potential but as a result of Ca entry. In contrast to the results obtained with steady depolarization, repetetive stimulation of an axon at 60/s leads to a small Ca entry that is not affected by a reduction in $/Na/_i$. The results obtained are consistent with the idea that repetetive stimulation leads to Ca entry via Na (and possibly K) channels while steady depolarization leads to Ca entry via an electrogenic Na/Ca exchange where the rate limiting step for Ca entry is the binding of multiple Na^+ to a carrier at the inside of the membrane. Supported by NIH Grant NS 14800 and by CONICIT Grant 31.26.S1-0602.

T-AM-C7 INFLUX OF Ca, Sr, AND Ba, THROUGH Ca CHANNELS IN SYNAPTOSOMES. Daniel A. Nachshen, Dept. of Physiology, University of Maryland School of Medicine, Baltimore, Maryland, 21201

Depolarization-induced (potassium stimulated) influx of ^{45}Ca, ^{85}Sr, and ^{133}Ba, was measured in synaptosomes prepared from rat brain. There are two phases of divalent cation entry, "fast" and "slow"; each phase is mediated by channels with distinctive characteristics. The fast channels inactivate (within one sec.) and are blocked by low concentrations (<1 μM) of La. The slow channels do not inactivate (within one min), and are blocked by high concentrations (> 50 μM) of La. Divalent cation influx through both channels saturates with increasing concentrations of permeant divalent cation; in addition, each permeant divalent cation species competitively blocks the influx of other permeant species. These results are consistent with the presence of "binding sites" for divalent cations in the fast and slow channels. The Ca/Sr/Ba permeability ratio, determined by measuring the influx of all three species in triplelable experiments, was 6:3:1 for the fast channel, and 6:3:2 for the slow channel. A simple model for ion selectivity, based on the presence of a binding site in the channel, could account for slow, but not fast, channel selectivity date. One possible explanation for the discrepancy is that the model does not take into account specific effects of Ca, Sr, and Ba on fast channel activation and inactivation kinetics.
Supported by NIH grants NS-16106 (to M.P. Blaustein) and NS-16461 (to D.A. Nachshen).

T-AM-C8 Ca-MEDIATED Ca CHANNEL INACTIVATION DETERMINED FROM TAIL CURRENT MEASUREMENTS. Roger Eckert and Douglas Ewald. Department of Biology, UCLA, Los Angeles, CA 90024

Inactivation of the Ca channel reportedly depends on an intracellular action of Ca^{2+} following its entry during depolarization (Brehm and Eckert, Science 202:1203, 1978; Tillotson, PNAS 76:1497, 1979; Brehm, Eckert and Tillotson, J. Physiol. 306:193, 1980). We now have utilized Ca tail currents in measuring inactivation so as to avoid contaminating K currents. Axotomized Aplysia neurons L2-L6 were voltage clamped in ASW containing (mM) 268NaCl, 20KCl, 20$CaCl_2$, 45$MgCl_2$, 200TEA, 0.045TTX, and 10Tris-HCl, pH 7.8, 13°C. Currents evoked by depolarization were summed digitally with currents evoked by equivalent hyperpolarization to eliminate symmetrical capacitive and leakage currents. The Ca tail current relaxed with a large fast (τ=1-1.5ms) and a small slow (τ=20-30ms) exponential component. Tail current amplitudes, measured 500μs after pulse termination from prepulse baseline current level, grew sigmoidally to a maximum with increasing pulse voltage, and were reduced 90% or more by Mn substitution for Ca. The relaxation was slowed by reduced temperature, but was unaffected by Ba substitution for Ca. No Ca-dependent K tail was evident at potentials and gains employed. However, the tail current applitude depended on prior Ca entry. To show this a conditioning pulse (P_1) of variable amplitude or duration (10-300ms) was delivered ending 1000ms prior to the 10ms test pulse (P_2) of fixed voltage. Reduction of the P_2 tail paralleled total Ca entry during P_1. This occurred irrespective of whether the tail currents were measured at potentials more negative or more positive than E_K, and so the results cannot be attributed to a facilitated activation of the Ca-dependent K current. The Ca-dependent reduction in tail current amplitude (i.e., inactivation of Ca conductance) was fully eliminated by injected EGTA. These results provide further evidence that inactivation of the Ca channel population is mediated by intracellular Ca^{2+} independent of membrane voltage. Supported by USPHS NS08364.

T-AM-C9 TWO CALCIUM CURRENTS IN EGG CELLS. A.P. Fox and S. Krasne. Dept. of Physiology, UCLA, CA, 90024.

Two distinct types of voltage-activated calcium conductances have been found in the unfertilized egg of the marine polychaete Neanthes arenaceodentata under voltage-clamp conditions. These two conductances differ markedly. In ASW, a calcium current, I_{CaI}, which activates at negative potentials (around -45 mV) is observed. With prolonged depolarization I_{CaI} relaxes with a single exponential decay having time constants in the 10 to 50 ms range. This relaxation of I_{CaI} is due to a voltage-dependent inactivation of the calcium conductance. This current is blocked by cobalt, 10 mM cobalt reducing I_{CaI} to approximately 45% of its normal value. Both barium and strontium can replace calcium as the permeant divalent carrying this current. If the eggs are depolarized to potentials above 0 mV and I_{CaI} is removed with an inactivating prepulse, a second calcium current, I_{CaII}, is observed. At these more positive potentials, under maintained depolarizations, the net inward currents are found to relax with time constants on the order of 300 to 600 ms. These relaxations are not dependent on the absolute membrane potential but rather, they are a function of the net inward current. Cobalt is a more effective blocker of I_{CaII} than of I_{CaI}, reducing the current to less than 5% of its original value at concentrations of 10 mM. Barium and strontium are both permeant in this second channel. This evidence for the existence of two distinct types of calcium conductance in the same preparation may be of importance in resolving conflicting observations on calcium conductances in different preparations.
Supported by MDA grant (C791127), NIH grant (HL20254) and MDA of Canada Fellowship (C7790501).

T-AM-D1 TROPONIN I PHOSPHORYLATION MODULATES THE CALCIUM BINDING PROPERTIES OF CARDIAC TROPONIN. S.P. Robertson, J.D. Johnson, M.J. Holroyde, E.G. Kranias, R.J. Solaro and J.D. Potter. Departments of Pharmacology and Cell Biophysics and Physiology. University of Cincinnati College of Medicine, Cincinnati, Ohio 45267.

The effect Troponin I (TnI) phosphorylation has on the Ca^{2+} binding properties of Troponin C (TnC) in the whole troponin complex reconstituted from bovine cardiac troponin subunits has been measured. To selectively follow Ca^{2+} binding at the Ca^{2+}-specific site of TnC, this subunit was labeled with the fluorescent probe IAANS before reconstituting the troponin complex (TN_{IA}). Phosphorylated TN_{IA} complexes were obtained by either phosphorylating (with cAMP dependent protein kinase) the TN_{IA} complex (0.9±0.3 moles P/mole) or by first phosphorylating TnI (1.7±0.3 moles P/mole) and then reconstituting TN_{IA}. Non-phosphorylated samples contained ~0.1 moles P/mole TnI. Autoradiograms of polyacrylamide slab gels run in the presence of SDS showed that more than 98% of the ^{32}P incorporated into TN_{IA} was associated with TnI. Phosphorylated TN_{IA} complexes formed by both methods required more Ca^{2+} to achieve 50% of the maximal Ca^{2+}-induced fluorescence change in TN_{IA} than did the non-phosphorylated samples. The decrease in $pCa_{50\%}$ was linearly related to the TnI phosphate content, equalling about -0.35 pCa units for 2 moles/mole of P incorporated. The rate of removal of Ca^{2+} from TN_{IA} as judged by stopped flow fluorometry was also found to increase with TnI phosphorylation consistent with the decrease in $pCa_{50\%}$. These results suggest that TnI phosphorylation may have a unique and important regulatory role in controlling cardiac function. A model is presented which illustrates the role this phosphorylation may have in the inotropic response to catecholamines. Supported by grants from the NIH (HL 22619-3A, B, E, HL 22231), the Muscular Dystrophy Associaton and the American Heart Association (78-1167 and 79-1001).

T-AM-D2 THE INTERACTION OF TROPONIN-I WITH TROPONIN-C STUDIED BY SURFACE LABELLING. R.C. Lu, E. Gowell, A. Wong and P.C. Leavis. Department of Muscle Research, Boston Biomedical Research Institute and Department of Neurology, Harvard Medical School, Boston, MA 02114.

Limited reductive methylation of the lysine residues of troponin-I (TnI) was carried out to provide information on the surfaces of TnI interaction with other thin filament proteins. TnI, by itself and in its binary complex with troponin-C (TnC), was labelled in the presence of $NaCNBH_3$ with [^{14}C] and [^{3}H]formaldehyde, respectively (cf. Jentoft and Dearborn, J. Biol. Chem. 254, 4359, 1979 and Lu et al., Fed. Proc. 39, 724, 1980). [^{14}C]TnI and [^{3}H]TnI, isolated from the complex, were mixed and digested with cyanogen bromide and chymotrypsin to separate lysine-containing peptides. Differences in the ratio of the ^{14}C and ^{3}H counts in each peptide are interpretable in terms of alterations in the accessibility of the lysine residue(s). Of the 24 lysines in TnI, two, Lys-31 and Lys-40, show a decrease in reactivity upon complex formation with TnC. Three other closely spaced residues, Lys-98, Lys-105 and Lys-107, exhibit an increase in incorporation of label, indicating that their local environments are affected by complex formation although they are not directly involved in binding. The observations in this work are consistent with the earlier report of Syska et al. (Biochem. J. 153, 375, 1976) who used proteolytic fragments of TnI to show that two regions of the molecule interact with TnC; viz. the N-terminal portion including residues 31 and 40 and a peptide comprising residues 96-116. Studies carried out on TnC by chemical modification (Hitchcock, in Calcium Binding Proteins and Calcium Function, Eds. Siegel et al., Elsevier, 1980, in press) and by proteolytic fragmentation (Leavis et al., J. Biol. Chem. 253, 5452, 1978) also support multiple sites of interaction between the two subunits. (Supported by grants from NIH, MDA, and AHA.)

T-AM-D3 KINETIC STUDIES OF Ca^{++}-BINDING TO TROPONIN C. S.S. Rosenfeld and E.W. Taylor, Dept. of Biophysics and Theoretical Biol., University of Chicago, Chicago, IL 60637

The fluorescence of troponin C labelled primarily at position 98 with 4-[N-(2-iodoacetoxy)ethyl-N-methyl]amino-7-nitrobenzo-2-oxa-1,3-diazole (IANBD-TnC) shows a 2.3-fold enhancement when Ca^{++} occupies the high-affinity sites. At free [Ca^{++}] < 10μM, the majority of this fluorescence increase (80%) occurs with an apparent second order rate constant of $2x10^6 M^{-1}s^{-1}$ at 4°C. The majority of the fluorescence decrease associated with Ca^{++} dissociation from IANBD-TnC occurs with a rate constant of $0.1s^{-1}$. Addition of tropopin I to IANBD-TnC increases the apparent second order rate constant of Ca^{++}-binding to $7x10^6 M^{-1}s^{-1}$, and reduces the rate constant of the major component of the dissociation reaction from 0.1 to $0.06s^{-1}$. When the free [Ca^{++}] is > 10μM, we observe that the fluorescence change associated with Ca^{++}-binding occurs via a different sequence--a rapid, diffusion-controlled rise in fluorescence intensity of approximately 3.5-fold, followed by a decline which occurs with an apparent second order rate constant of $1.5x10^6 M^{-1}s^{-1}$ at 4°C. The rate of this fluorescence decline appears to saturate at a value of $500s^{-1}$. Digestion of IANBD-TnC with trypsin yields two peptides--TR1, containing the two low-affinity sites, and IANBD-TR2, containing the high-affinity sites and the bound fluorophore. Both this mixture as well as isolated IANBD-TR2 show a 2.1-fold fluorescence enhancement when Ca^{++} binds to the high-affinity sites. At all free [Ca^{++}] used in this study (0.001-1000μM), the binding of Ca^{++} to either of these preparations produces a time-dependent increase in fluorescence intensity that is qualitatively similar to that for IANBD-TnC at free [Ca^{++}] < 10μM, and with rate constants for the major components of the fluorescence change that are similar to those for IANBD-TnC. We conclude that under appropriate conditions, a transient state of troponin C can be produced in which Ca^{++} occupies only the low-affinity sites.

T-AM-D4 COOPERATIVE INTERACTIONS IN THE Ca^{2+}-DEPENDENT ACTIVATION OF ACTOMYOSIN ATPase. Z. Grabarek, J. Grabarek, J. Gergely, and P.C. Leavis, Dept. of Muscle Res., Boston Biomed. Res. Inst. and Depts. of Neurology and Biochemistry, Harvard Med. School, Boston, MA 02114.

Activation by Ca^{2+} of Mg^{2+}-ATPase of reconstituted regulated actomyosin containing either intact TnC or its proteolytic fragments was compared to that of myofibrils. Both the cooperativity (cf. Murray et al., FEBS Letters 114, 169, 1980) expressed as the Hill coefficient, n, and the transition midpoint ($pCa_{1/2}$) was lower in actomyosin (n=4.3, $pCa_{1/2}$=6.8) than in myofibrils (n=6, $pCa_{1/2}$=6.2). These parameters were unaffected by variations in Mg^{2+} concentration in the range 0.05 to 4 mM. If in the reconstituted system TnC is replaced by various proteolytic fragments containing sites I+II, sites III+IV or sites I+II+III, the Ca^{2+} activation curves are essentially identical to that of the intact protein even though the isolated fragments bind Ca^{2+} with different affinities (Leavis et al., J. Biol. Chem. 253, 5452, 1978). These findings imply that the transition midpoints and degree of cooperativity seen in the activation curves result from interactions among myofibrillar proteins rather than among the Ca^{2+} binding sites themselves, as recently proposed (Hill et al., Proc. Nat. Acad. Sci. USA 77, 3186, 1980). In order to further examine this point we are currently measuring Ca^{2+} binding to TnC that has been labeled with fluorescent probes and incorporated into the thin filament. (Supported by grants from NIH, MDA and AHA.).

T-AM-D5 DIFFERENCES IN STRUCTURE AND FUNCTION AMONG TROPOMYOSINS FROM SMOOTH AND SKELETAL MUSCLES. M. Yamaguchi, A. Ver, S. Wong, S.S. Lehrer, and J.C. Seidel. Boston Biomedical Research Institute, Boston, MA 02114.

Preparations of tropomyosin made essentially by the method of Bailey from rabbit skeletal muscle, chicken gizzard and bovine arterial muscle, differ from each other in the migration rates and relative amounts of α and β chains observed on SDS gels. The migration rates of tropomyosins from aorta or pulmonary artery are the same but the relative amounts of α and β chains vary from one preparation to another, suggesting that the α chain may be a proteolytic fragment of the β chain. All three smooth muscle tropomyosins bind to skeletal muscle F-actin and all three enhance the actin-activated ATPase of myosin, heavy meromyosin, or subfragment-1 from skeletal muscle, under conditions where tropomyosin from skeletal muscle inhibits these activities. Gizzard tropomyosin approximately doubles activity with 2 or 10 mM $MgCl_2$ while arterial tropomyosins activate with 10 mM $MgCl_2$ but have only a small effect with 2 mM $MgCl_2$. The actin-activated ATPase of gizzard myosin is activated by all four tropomyosins when gizzard myosin kinase is present. Tropomyosins from smooth and skeletal muscles differ inherently in their ability to modulate actomyosin ATPase activity but this modulation also depends qualitatively on the type of myosin. The results also indicate that structurally different forms of tropomyosin which differ in their effects on ATPase activity can be obtained from vertebrate smooth muscles. (Supported by grants from NIH (HL 15391, HL 23249, and HL 22461) and from the MDA.)

T-AM-D6 THE DUAL EFFECT OF TROPOMYOSIN ON THE ACTOMYOSIN-SUBFRAGMENT-1 MG^{2+}-ATPase. S.S. Lehrer, Dept. of Muscle Research, Boston Biomedical Research Institute, 20 Staniford St., Boston, MA 02114.

Several reports have indicated that tropomyosin (Tm) bound to F-actin can either inhibit or activate the acto-S-1 Mg^{2+}-ATPase depending upon assay conditions (Bremel et al. (1973) CSHSQB 37, 361; Eaton et al. (1975) Biochemistry 14, 2718). In order to clarify this dual effect, pH-stat activity studies were performed as a function of [S-1] with 3.2 μM F-actin in 0.05M NaCl, 5 mM Mg^{2+}, at pH 7.9 using saturating amounts of ATP (1 mM). Over a range of [S-1] where the actin-activated activity was proportional to [S-1], excess skeletal Tm (reduced with DTT) produced either inhibition or activation, depending on the S-1/actin molar ratio: When S-1/actin $\lesssim$ 2, inhibition was observed; when S-1/actin $\gtrsim$ 2, activation was observed. The inhibition approached 100% as S-1/actin$\rightarrow$0, and the activation was $\sim$100% when S-1/actin$\sim$4. In the presence of troponin (Tn), similar limiting values of activity were obtained in the absence and presence of Ca^{2+}, respectively. Titrations with Tm showed that both effects were maximal when stoichiometric amounts were bound (1 Tm:7 actin). Thus, there are two Tm-dependent states of the thin filament, inhibited and activated, which do not require Tn to be manifested. Furthermore, from extrapolation to [S-1] = 0, the actin-Tm thin filament appears to be in the inhibited state. These results are consistent with recent binding studies of labeled S-1 to Tn-Tm-actin (Greene and Eisenberg (1980) PNAS 77, 2616) in that the filament state is determined by the S-1/actin ratio. That is, their weak binding state may correspond to the inhibited state and their strong binding state would correspond to the activated state. Our results would predict similar cooperative binding of S-1 to Tm-actin with behavior intermediate between the binding to Tn-Tm-actin in the presence and absence of Ca^{2+}. (Supported by NIH grant HL 22461 and the MDA.)

T-AM-D7 THE AMINO ACID SEQUENCE OF A 34,000 DALTON FRAGMENT FROM S-2 OF MYOSIN.
Jean-Paul Capony and Marshall Elzinga, Biology Dept., Brookhaven Natl. Lab., Upton, NY 11973

A fragment having two 34,000 dalton chains was isolated, by fractional precipitation and gel filtration, from a limited tryptic digest of rabbit skeletal muscle heavy meromyosin. The amino acid sequence was determined from studies on peptides formed by splitting at arginine and methionine; its amino-terminal 258 residues are: SAETEKEMANMKEEFEKTKESLAKAEAKRK ELEEKMVALMQEKNDLQLQVQAEADSLADAEERQDLIKTKIQLEAKIKEVTERAEDEEEINAELTAKKRKLEDECSELKKDIDDLELTLAKV EKEKHATENKVKNLTEEMAGLDETIAKLTKEKKALQEAHQQTLDDLQAEEDKVNTLTKAKTKLEQQVDDLEGSLEQEKKIRMDLERAKRKLE GDLKLAQETSMDIENDKQQLDEKLKKLEFMTNLQSKIEDEQALM. This fragment is a dimer, and its spectroscopic properties indicate that it is α-helical; based upon its apparent similarities to tropomyosin (Tm) it is assumed to exist in solution as a coiled-coil. Evaluation of the sequence by the method of Chou and Fasman predicts that it is α-helical (av. value of 118.6, vs. 118.2 for Tm), and that its helix forming tendency is rather constant throughout its length. Two-stranded coiled-coils are assumed to be stabilized by interactions between non-polar residues located at intervals of 3,4,3,4... residues in the sequence. In this molecule the 3,4,3,4... spacings (underlined above) are observed, but 17 of the 74 "non-polar positions" (23%) are occupied by polar sidechains. This is far higher than in a 17 kd peptide from LMM (5%) or in Tm (4%). These charged sidechains are distributed rather uniformly throughout the molecule. They would be expected to repel each other at the interface between the two chains, and the result could be that the binding between the two chains of S-2 is not as strong as between the two chains of Tm or LMM. In such a postulated "loose" S-2, the two α-helices of S-2 could function more independently than in a tightly constrained coiled-coil; this arrangement may enable the S-2 region of the myosin molecule (the "neck") to exhibit spring-like properties. (Supported by the U.S.D.O.E. and the NIH.)

T-AM-D8 THE MYOSIN HEAVY CHAIN: CANDIDATE FOR THE LOCUS OF THE AVIAN MUSCULAR DYSTROPHY GENETIC DEFECT. Julie Ivory Rushbrook*, Anna I Yuan* and Alfred Stracher* (Intr. by E. McGowan), Dept of Biochemistry, S.U.N.Y.-Downstate Medical Center, Brooklyn, N.Y., 11203.

Muscular dystrophy in humans and in animal models is a genetically determined condition specific for fast white skeletal muscle fibers, with onset during development. Although much attention is currently focused on the sarcolemma, there is no compelling evidence that the primary defect resides in this membrane. The existence of an isozyme of myosin specific for fast white fibers and the evidence emerging for a progression of myosin isozymes during development suggest a reconsideration of the myosin molecule as the locus for the primary defect.

Recently we noted a small difference in the one dimensional peptide maps of myosin heavy chains from fast white muscle fibers of normal and dystrophic chickens (J.I. Rushbrook and A. Stracher (1979) Proc. Nat. Acad. Sci. 76, 4331). Prompted by the report of myosin heavy chain gene differences in cloned genomic DNA from normal and dystrophic chickens (G.A. Freyer et al, (1980) EMBO Workshop on Muscle Cell Culture, Shoresh, Abst., p. 23), we have investigated this finding further. Using a modified form of the one dimensional peptide mapping procedure, we have analyzed a total of 18 myosin preparations from four strains of dystrophic chickens and their normal controls. Two clearly different heavy chain peptide map patterns were found, one present in all dystrophic strains, the other in all normal strains. No dystrophy-specific peptide map differences were found in the light chains. Evidence is presented for a neonatal form in addition to an embryonic form of the heavy chain in the chicken; within each of these forms the normal and dystrophic maps are identical. These results constitute preliminary evidence that the adult dystrophic myosin heavy chain may be the expression of the avian muscular dystrophy gene. (Supported by M.D.A. Inc.)

T-AM-D9 ACTIVE SITE TRAPPING OF SPECTROSCOPICALLY CONVERSANT DIVALENT METAL-NUCLEOTIDE COMPLEXES OF MYOSIN SUBFRAGMENT ONE. Ross E. Dalbey, James A. Wells and Ralph G. Yount, Biochemistry/Biophysics Program, Washington State University, Pullman, WA 99164

Recent experiments [J. Wells and R. Yount (1979) PNAS 76 4966] have shown it is possible to trap Mg ADP and other nucleotides stably at the active site of myosin by crosslinking two thiol groups. A variety of crosslinking reagents including chelation of the two thiols by Co(III)phenanthroline or covalent reaction with N,N'-p-phenylene dimaleimide (pPDM) are effective trapping agents. No trapping of nucleotides occur in the absence of divalent metals. Thus far Mg^{2+}, Mn^{2+}, Co^{2+}, Ni^{2+} and Ca^{2+} all function to promote trapping of the 1:1 divalent metal ADP complex and to enhance the rate of ATPase inactivation. While the stability of the trapped divalent metals vary, e.g., $t_{1/2}$ of 0.5 to 6 days at 0°C, they are stable enough to permit accurate spectral measurements of the Mn^{2+} and Co^{2+} trapped complexes. EPR measurements of Mn^{2+} bound to AMP-PNP (β-γ,imidoATP) or complexed to SF-1 indicate that the metal is bound at the active site. CD and visible absorption studies of the Co^{2+}·ADP trapped complex indicate the metal ion is in an asymmetric octahedral environment. EPR and CD measurements show that the environment of both the metal nucleotide is the same whether bound reversibly or stably trapped at the active site. Supported by grants from MDA and NIH (AM-05195).

T-AM-D10 FLUORESCENCE STUDIES OF THE CONFORMATION OF MYOSIN SUBFRAGMENT ONE (SF_1) CROSS-LINKED WITH p-PHENYLENEDIMALEIMIDE (pPDM) IN THE PRESENCE OF ADENINE NUCLEOTIDES. William J. Perkins, James A. Wells and Ralph G. Yount, Biochemistry/Biophysics Program, Washington State University, Pullman, WA 99164

The crosslinking reagent pPDM has been shown in the presence of MgADP to crosslink the two critical thiols of SF_1, SH-1 and SH-2 [Burke and Knight, J. Biol. Chem. (1980) 255, 8385] and to concomitant trap MgADP at the active site [Wells and Yount (1979) PNAS 76, 4966]. The steady state intrinsic fluorescence of SF-1 in the presence of MgADP at 20°C shows a 10% increase which does not change upon addition of pPDM, indicating crosslinking does not alter the MgADP·SF_1 conformation. Similar studies with MgATP and MgAMP-PNP show fluorescence enhancements of 29% and 21%, respectively, which decrease to 10% upon addition of pPDM. Modified Stern-Volmer fluorescence quenching studies using I^- show that the MgAMP-PNP·SF_1 conformation is similar to that of the MgATP·SF_1 but different from that of MgADP·SF_1. However, upon crosslinking with pPDM all three systems show the same solute quencher accessibility. These data suggest that the only conformation of SF_1 that is stabilized by crosslinking is M*ADP. Moreover, the MgAMP-PNP·SF_1 must exist in more than one conformation, one of which is identical to M*ADP. The crosslinked enzyme binds to F-actin stoichiometrically at low ionic strength and high temperature (4 mM TES, 2 mM $MgCl_2$, 20°C), but not at high ionic strength and low temperature (0.1 M KCl, 0.5°C). Upon binding to F-actin the stability of the trapped magnesium nucleotide is dramatically decreased ($t_{1/2}$ < 30 min). This shows that crosslinking of SH_1 and SH_2 does not prevent the formation of the actin MgADP·SF_1 ternary complex, nor does it prevent the actin-induced conformational change which promotes the release of bound nucleotide. Supported by grants from MDA, AHA and NIH (AM 05195).

T-AM-D11 KINETICS OF THE DISSOCIATION OF RABBIT SKELETAL ACTOMYOSIN-S1 BY MgAMPNP. Howard White, Dept. of Biochemistry, University of Arizona, Tucson, AZ 85721

The kinetics of dissociation of rabbit skeletal myosin-S1 by MgAMPNP have been measured by the decrease in light scattering at 340 nm with a stopped flow fluoremeter. The decrease in scattering intensity is fit well by the equation $I = I_o e^{-k_{obs}} + C$ over a range of MgAMPNP concentrations from 0.25 to 5.0 mM. At high concentrations of MgAMPNP a maximum k_{obs} of 16 s^{-1} is approached (experimental conditions - 100 mM KCl, 10 mM Tris, 5 mM $MgCl_2$, pH 8.0, 20°C). The extent of dissociation measured under these conditions is >90% at 5 mM MgAMPNP. A minimal two step mechanism for the dissociation is given below.

$$\text{Acto·S1} + \text{MgAMPNP} \underset{\text{c}}{\overset{1.4 \times 10^3\ M^{-1}}{\rightleftharpoons}} \text{A·S1·MgAMPNP} \xrightarrow{16\ s^{-1}} \text{A} + \text{S1·MgAMPNP}$$

In contrast, the maximal k_{obs} for the dissociation of acto-S1 by Mg ATP under identical conditions is too rapid to be measured by the stopped flow technique and is likely to be greater than 1000 s^{-1}.

A separate experimental approach was to try to measure the inhibition by MgAMPNP of the dissociation of acto-S1 by MgATP. The rate of acto-S1 dissociation by MgATP was unaffected by MgAMPNP (0.25-2.5 mM) but the amplitude of the scattering change decreased with a 50 percent loss at 0.8 mM MgAMPNP. These results indicate the lack of a detectable (less than 10 percent) ternary A·S1·MgAMPNP complex and require that the binding of S1·MgAMPNP to actin has a dissociation constant less than or equal to 1.2×10^{-4}M. (Supported by PHS Grant #AM25113-02 and the Muscular Dystrophy Association of America).

T-AM-D12 A SEPARATION OF THE EFFECTS OF ATP NUCLEOTIDE ANALOGS ON THE MECHANISMS OF Ca^{2+} REGULATION AND ACTOMYOSIN TENSION GENERATION IN SKINNED SMOOTH MUSCLE. P.S. Cassidy and W.G.L. Kerrick. Dept. Physiology & Biophysics, Univ. of Washington, Seattle, WA 98195.

Onishi and Watanabe (J. Biochem. (Tokyo) 86:569, 1979) reported that when ITP was substituted for ATP in their smooth muscle actomyosin superprecipitation system, it failed to lead to Ca^{2+}-activated superprecipitation or myosin phosphorylation. We have used skinned smooth muscle preparations (chicken gizzard and rabbit ileum) to study the effects of replacing ATP with ITP, GTP, and their thiophosphorylated analogs on Ca^{2+}-activated tension generation. First, we confirmed that ITP and GTP can serve as substrates for Ca^{2+}-activated tension generation in striated muscle fibers (rabbit soleus and adductor). However, both ITP and GTP failed to generate Ca^{2+}-activated tension in skinned smooth muscle. We have previously shown that ATPγS can irreversibly activate tension in skinned smooth muscle by irreversibly thiophosphorylating myosin LC_{20} light chains. Treatment of skinned smooth muscle with ITPγS or GTPγS did not lead to irreversible activation of tension except when the incubation time was extended. We believe these effects are due to the great specificity of the smooth muscle myosin light chain kinase for ATP relative to the rather low substrate specificity of the actomyosin ATPase for tension generating substrates. The similar specificity shown for ATPγS over ITPγS and GTPγS is another indication that the irreversible activation of skinned smooth muscle seen with ATPγS is mediated through myosin light chain kinase and is not due to some non-specific formation of a smooth muscle rigor state due to the exposure of the muscle to any thiophosphorylated nucleotide. (This study was supported by fellowships to Dr. Cassidy from the Muscular Dystrophy Assn. and NIH (HL 07090) and by grants to Dr. Kerrick from the Muscular Dystrophy Assn. and the American Heart Assn. (79-664)).

T-AM-E1 COMPARISON OF OPTICAL SIGNALS IN FROG MUSCLE OBTAINED WITH THREE CALCIUM INDICATOR DYES. S.M. Baylor, W.K. Chandler, and M.W. Marshall, Departments of Physiology at University of Pennsylvania Medical School, Yale Medical School and Newcastle Medical School.

Singly dissected frog twitch fibers were injected with one of the calcium indicator dyes Arsenazo III, Antipyrylazo III or Dichlorophosphonazo III. Changes in dye absorbance were measured following action potential stimulation using light plane polarized at 0° and at 90° with respect to the fiber axis (sarcomere spacing 3.8-4.3 μm, temperature usually 16°C). With all three dyes the earliest changes in dye absorbance were isotropic and varied with wavelength approximately according to the Ca^{++} difference spectra measured in cuvette calibrations. Thus, the earliest signal appears to be due to the formation of Ca^{++}-dye complex. Furthermore, the early time course of this Ca^{++} signal virtually superimposed the time course of the intrinsic birefringence signal, indicating that all three indicator dyes track the myoplasmic Ca^{++} transient with similar speed. Soon after the early Ca^{++} signal at least two other kinds of dye-related signals can be detected: (1) a dichroic signal easily seen with Arsenazo III (Baylor, Chandler & Marshall, 1979) and with Dichlorophosphonazo III and (2) a second isotropic signal easily seen with Antipyrylazo III and with Dichlorophosphonazo III. Experiments with Arsenazo III indicate that the dichroic signal involves a change in orientation of some of the dye molecules. After 0.2 sec the Ca^{++} and the dichroic signals appear to have returned to baseline. The remaining isotropic signal, best seen with Antipyrylazo III and with Dichlorophosphonazo III, has a spectrum which is consistent with a small increase in myoplasmic Mg^{++} and/or pH. Small increases in both quantities would be expected to accompany the breakdown of phosphocreatine. (Supported by Am. Heart 79-630, PCM 77-25163, and NS 07474.)

T-AM-E2 BIREFRINGENCE SIGNAL RELATED TO E-C COUPLING IN HEART MUSCLE. R. Weiss and M.Morad Department of Physiology, University of Pennsylvania, Philadelphia, PA, 19104

An intrinsic birefringence signal was measured in rat ventricular muscles (dia.100-200μm) before the onset of contraction. The signal was found to be a decrease in light intensity with two components which occurred before sarcomere shortening as monitored by laser diffraction and transmitted incandescent light. Both components were verified as arising from changes in optical retardation by their obeyance of Fresnel's equation. The first component occurred simultaneously with the action potential upstroke recorded optically with the voltage sensitive dyes NK 2376 and WW 444. These dyes are non-penetrating and reliably measure the action potential generated by the sarcolemma and T system membranes. The second component was larger, slower and in the same direction as the first component. The onset of the second component occurred with the initiation of the plateau of the action potential. The full time course of the birefringence signal was disrupted by light scattering caused by muscle shortening. Interventions such as changes in $[Ca]_o$, addition of epinephrine, and replacement of H_2O with D_2O altered the rate of development of the second component and isometric twitch tension in similar fashion. On the other hand, variation of the muscle rest length had no significant effect on the second component even when developed tension changed by 2-3 fold. The second component was consistently seen in all mammalian hearts tested (cat atrium, neo-natal cat ventricle, guinea pig), but was absent in frog atrium and ventricle. The appearance of the second component correlates closely with the presence of well developed SR and the electromechanical data for releasable calcium stores in the various mammalian and amphibian hearts. These results suggest that the second component of the birefringence signal reflects the activity of the SR prior to sarcomere shortening which may be related to a step in E-C coupling processes of the mammalian heart.

T-AM-E3 DIFFUSION OF THE Ca^{2+} INDICATOR DYE ARSENAZO III IN AQUEOUS SOLUTION AND IN FROG SKELETAL MUSCLE FIBERS. R.F. Rakowski and J.C. Sommerer*, Department of Physiology and Biophysics, Washington University School of Medicine, St. Louis, MO 63110.

High speed cine film recordings were made of the diffusion of the metallochromic indicator dye arsenazo III after iontophoretic injection into frog skeletal muscle fibers and into a Ca^{2+}-free frog Ringer's solution. Glass capillary microelectrodes were filled with a 60 mM solution of the Na^+ salt of arsenazo III (Sigma, No. A-8891). A brief (50-100 msec) current pulse was applied to electrodes placed in a Ca^{2+}-free frog Ringer solution containing 0.15 mM EGTA. The diffusion of the dye away from the electrode tip was filmed through a compound microscope at 100 frames/sec. The spatial distribution of the dye was obtained by measuring the optical density of the film using an image-processing computer system. A non-linear least squares curve fitting procedure was used to obtain the variance of the spatial distribution function and to calculate the diffusion coefficient. The diffusion of the dye was also studied in the cutaneous pectoris muscle of the frog, Rana pipiens. Since muscle fibers will not tolerate the large currents required to produce a unit impulse injection of the dye, it was necessary to record the response to a step of iontophoretic current. The injection was filmed at a rate of 20 frames/sec and the spatial distribution of the dye determined by measuring the optical density along the length of the fiber. The data were corrected for variations in the background optical density. The apparent diffusion coefficient of the dye in the myoplasmic space was determined from the variance of the spatial distribution function for a step input. The data were analyzed further to determine if the measurements could be explained by concentration dependent binding of the dye. Supported by the Muscular Dystrophy Association and by NIH grant No. NS-14856.

T-AM-E4 THE Ca^{++} CHANNEL IN FROG MUSCLE CELL MEMBRANE: A PHARMACOLOGICAL PROFILE. P.T. Palade and W. Almers (Intr. by C.E. Stirling), Dept. Physiology and Biophysics, Univ. of Washington, Seattle, WA 98195.

Slow Ca^{++} inward (I_{Ca}) and K^+ outward (I_K) currents were recorded with a vaseline-gap voltage clamp technique from fibers with 80 mM intracellular K_2EGTA and (100 mM TEA^+ + 10 mM Ca^{++})CH_3SO_3 in the extracellular solution. Various drugs were applied externally, and currents measured before, during, and after presence of drug. Local anesthetics, nifedipine, barbiturates and D-600 all block I_{Ca}, with half-blockage concentrations (BD_{50}) for I_{Ca} as given. All of these drugs also block I_K as if I_{Ca} and I_K were linked. One type of linkage can be ruled out, however. Replacing external Ca^{++} with Mg^{++} abolishes I_{Ca} but increases I_K. Since in this situation there is no Ca^{++} inside or out, I_K in our experiments cannot flow through a channel activated by internal Ca^{++}. (Supported by NIH grant AM-17803. PTP was supported by a MDA postdoctoral fellowship.)

Drug	BD_{50} ± SEM (n)
Dibucaine	8.6 μm (2)
Tetracaine	.16 ± .04 mM (7)
Lidocaine	1.37 ± .33 mM (6)
Procaine	1.56 ± 0.35 mM (5)
QX-314	32.9 mM (2)
Benzocaine	> 10 mM (1)
D-600	13.4 ± 2.4 μM (7)
Nifedipine	0.28 ± 0.6 μM (10)
F-Nifedipine	.015 mM (2)
Pentobarbital	0.56 ± 0.11 mM (9)
Secobarbital	0.44 ± 0.19 mM (5)
Phenobarbital	2.04 ± 0.58 mM (3)

T-AM-E5 Ca^{++} CURRENTS AND Ca^{++} DEPLETION IN FROG MUSCLE TUBULES. P.T. Palade, R. Fink, and W. Almers (Intr. by P. Verdugo), Univ. of Washington, Seattle, WA 98195.

We have studied membrane currents with a vaseline gap voltage clamp technique under conditions where the intracellular space contained 80 mM $(TEA^+)_2EGTA$, and the external solution contained 90 mM TEA^+, 110 mM $CH_3SO_3^-$ and 10 mM of either Ca^{++}, Ba^{++}, Sr^{++} or Mg^{++}. Under this condition, membrane depolarization elicits divalent cation currents that are inward, rise to a peak within ∿ 0.1 to 0.7 s and then decline with time constants of 1 to 5 s. We believe these currents to be largely uncontaminated by the flow of other ions, since internal and external solutions contain only large and probably impermeant organic ions. The rate of decline is linearly proportional to peak current, no matter whether peak current is varied by changing membrane potential, by block with drugs or by substituting for Ca^{++} other divalent cations that are relatively less (Mn^{++}) or more (Ba^{++}, Sr^{++}) permeant. We conclude that the decline of I_{Ca} depends on the magnitude of I_{Ca} itself and only indirectly on potential. Further, the decline appears to be due to Ca^{++} depletion from the transverse tubules (TTS), because 1) the charge carried by the transient portion of inward current closely agrees with the charge on the Ca^{++} expected to be in the TTS, and 2) decline is slowed roughly in proportion to the Ca-buffering strength of the external medium. On this basis, we calculate that a) between 93% and 100% of all Ca^{++} channels reside in the TTS; b) the Ca^{++} diffusion coefficient in the TTS is 3×10^{-6} cm^2/s after correction for tortuosity; c) depletion may lower $[Ca]^{++}$ in the TTS into the micromolar range, and d) any organic material contained in the TTS cannot have large Ca-buffering capacity. (Supported by NIH grant AM-17803 (to WA), MDA (to PTP) and Deutsche Forschungsgemeinschaft (to RF).)

T-AM-E6 SODIUM CURRENTS IN MUSCLE FIBERS. Julio Vergara. Dept. of Physiology, UCLA.

The existence of a secondary component of sodium inward current attributed to a sodium conductance in the T-system in voltage-clamped skeletal muscle fibers has already been reported by Mandrino [J. Physiol. 269:605(1977)]. Experiments in frog single skeletal muscle fibers voltage-clamped and internally perfused with Cs-containing solutions have been done to verify and complement these observations. The three vaseline gap voltage clamp techniques originally described by Hille and Campbell [J. Gen. Physiol. 67:265(1976)] were slightly modified in these experiments. Special emphasis was made in obtaining close to full series resistance compensation and extracellular isopotentiality in the solution immediately surrounding the fiber. Leak and capacity subtraction was implemented with subtracting pulses. Two components of inward current (early and late) were clearly distinguished in experiments with external Ringer's solution and they were still identifiable with ½ Na external solutions. The early component could be attributed to a surface sodium conductance and showed a voltage dependence compatible with the Q-V distribution of gating charge movement recorded in the same preparation. The second component can be accounted for by activation of a tubular sodium conductance. It was analyzed integrating the partial differential equation for the radial propagation of potential in the T-system including a nonlinear sodium conductance. According to the model, the T-system potential was not well controlled by the surface voltage suggesting that the second component of the current recorded in voltage clamp experiments cannot be analyzed as a direct sodium conductance activation in the tubular membrane. However, the magnitude of the sodium conductance in the T-tubules can be obtained comparing experimental results with computed values. This comparison is dependent on several tubular parameters, other than sodium conductance.
Supported by USPHS grant AM-25201 and MDA grant F6-JLNRC.

T-AM-E7 EFFECT OF DANTROLENE SODIUM ON CHARGE MOVEMENT IN FROG TWITCH MUSCLE FIBERS. Chiu Shuen Hui. Dept. Physiol., Yale Med. Sch., New Haven, CT 06510 & Dept. Biol., Sci., Purdue Univ., West Lafayette, IN 47907, U.S.A.

Charge movements in sartorius muscle fibers of Rana temporaria were studied using the 3-microelectrode voltage clamp technique. Fibers were bathed in solutions containing TEA and TTX to block ionic currents and 350 mM sucrose to minimize contraction. For small membrane depolarizations, Q_{on} in this solution shows two components, the familiar main component (Q_β) that decays more-or-less exponentially, followed by a second component (Q_γ) that is roughly bell-shaped. The time-to-peak (t_p) of Q_γ decreases sharply with increasing depolarizations until Q_γ merges with Q_β (see also Adrian and Peres, J. Physiol. 289, 83, 1979). Perfusion with a test solution having identical ionic contents plus saturated amount of dantrolene sodium abolished Q_γ completely, did not alter the value nor the shape of Q-V distribution of Q_β, but slowed down the kinetics of Q_β by approximately 30%.

In the voltage range where Q_γ is separable from Q_β, the steady-state voltage distributions of Q_β and Q_γ can be individually fitted by $Q(V)=Q_{max}\{1 + \exp(-(V-\overline{V})/k)\}^{-1}$. The values of k and Q_{max} for Q_γ are about ½ and ¼ of those for Q_β, respectively. $1/t_p$ increases linearly with voltage. It is speculated that Q_γ is closely associated with calcium release from the sarcoplasmic reticulum. If so, the finding reported here is consistent with the hypothesis that dantrolene sodium suppresses muscle contraction by affecting calcium release. (Supported by Grants: NIH NS15375, AHA 79634 and MDAA 31557; early part of this work supported by a NIH Grant to Dr. W. K. Chandler).

T-AM-E8 DEUTERIUM OXIDE (D_2O) AND DANTROLENE SODIUM REDUCE TWITCH TENSION IN CALF CARDIAC PURKINJE FIBERS. Kevin J. Malloy and Robert S. Kass, Dept. of Physiology, University of Rochester, Rochester, N.Y. 14642 (Sponsored by Martin F. Schneider).

Contractile activation in mammalian heart muscle is thought to involve two processes: (1) a voltage-dependent transmembrane Ca influx via the slow inward current (I_{si}) and (2) release of Ca from the sarcoplasmic reticulum. These mechanisms cannot be distinguished by inhibition of I_{si} as this leads to depletion of internal calcium and subsequent elimination of step (2). We report attempts to dissect these processes by blocking tension development with agents which might interfere with internal Ca release. In action potential (AP) studies, we find that D_2O (75%) and dantrolene sodium (30 μM) reversibly reduce twitch tension by 75% with little effect on the height of the action potential plateau. This suggests a mode of action which is independent of I_{si}. Because AP results can be misleading, the effects of these agents on membrane current and tension were studied with a conventional two-microelectrode voltage clamp. In agreement with the AP experiments both D_2O and dantrolene reduced peak tension by 75-90% at all voltages. However, each treatment produced a different effect on membrane current. D_2O caused a non-selective reduction and slowing of plateau and pacemaker currents whereas dantrolene appears to rather selectively reduce outward plateau currents without significant effect on I_{si}. Despite the encouraging action potential results, the effects of D_2O on current argue against its use as a selective uncoupler. On the other hand, the experiments with dantrolene suggest that this compound may inhibit internal Ca release in these preparations and may thus be a useful tool in isolating the steps of contractile activation in the heart.

Work supported by NIH 2 T 32 GM07136-06.

T-AM-E9 SOLUTE DISTRIBUTION IN SKINNED MUSCLE FIBERS. Elizabeth W. Stephenson, Laboratory of Physical Biology, NIAMDD, National Institutes of Health, Bethesda, MD 20205

During activation of vertebrate twitch fibers, Ca efflux from sarcoplasmic reticulum (SR) to myofilament-containing space (MFS) increases by an unknown mechanism. Application of permeant anions to skinned fibers stimulates Ca release, but the site of ionic depolarization is unclear. The possibility of a voltage-dependent change in SR Ca permeability raises the question of SR resting potential. If the SR compartment is polarized, the steady-state distribution of permeant ions between skinned fiber and bathing medium should be influenced by its charge. To evaluate this distribution, the simultaneous uptake of ^{14}C-urea + ^{3}H-deoxyglucose (^{3}H-DOG) or S^{14}CN$^-$ + ^{3}H-DOG was measured in segments of bullfrog semitendinosus fiber skinned by the Natori method in mineral oil. ^{14}C-urea served as total solvent marker, ^{3}H-DOG as MFS marker, and S^{14}CN$^-$ as a permeant anion marker. Skinned segments, mounted isometrically, were exposed under mineral oil to 10 μl solution containing K propionate, imidazole, Mg, Na_2ATP, EGTA, and 40 μC ^{14}C/ml + 80 μC ^{3}H/ml. Fiber tracer contents were expressed as a space, i.e. the equivalent volume of bathing solution. In 21 fibers, the ^{14}C-urea space and ^{3}H-DOG space correlated well with the protein content (assayed by a Coomassie Blue method), validating the tracer methodology. The difference between these spaces was 10% of the urea space, similar to the volume fraction of membrane-bounded compartments estimated morphometrically in frog fibers. The ratio SCN$^-$:DOG was 1.17, with a calculated ratio SCN$^-$:solvent of 1.08 in one study (n=10). In a second study, the ratio SCN$^-$:DOG was 1.13 (n=7) and hardly altered by pretreatment with Triton-X100 (n=3), suggesting SCN$^-$ binding. These results imply that anion accumulation by the SR due to resting polarization is small or absent, and support the conclusion that the similarity of elemental Na and Cl in SR and MFS detected by electron probe microanalysis (Somlyo et al., Nature 268:556 (1977) reflects the ionic content.

T-AM-E10 QUANTITATIVE X-RAY MICROANALYSIS OF FREEZE-DRIED RAT SOLEUS MUSCLE
K. L. Monson and T. E. Hutchinson (Intr. by J. B. Bassingthwaighte)
Center for Bioengineering, University of Washington, Seattle, Washington 98195

Resting rat soleus muscle was quick frozen, then thin sections were cut and freeze-dried without thawing. These methods make the tissue vacuum compatible while preserving its structural and compositional integrity, as the usual methods of fixation and dehydration for electron microscopy induce chemical modifications and elemental losses, which make them unacceptable for microanalysis. The sections were examined in a scanning transmission electron microscope, using a liquid nitrogen cold stage at -180°C to minimize or eliminate loss of mass from the analyzed area. Ultrastructure of the unfixed and unstained cryosections was in general quite comparable to the morphology of control specimens prepared by the conventional methods, except that mitochondria were very electron dense, showing no internal structure. Various regions of the muscle cells were irradiated with electrons, and the x-rays produced were collected using an energy-selective x-ray spectrometer system, with a minicomputer interface for spectral processing. Mass fractions of the elements of biological interest in selected regions of the specimens were calculated by the continuum normalization method. Concentrations of all elements analyzed were similar in the A and I bands. The concentration of P was elevated in the nucleus, mitochondria, and sarcoplasmic reticulum (SR). Concentrations in the SR indicate that it is not in direct communication with the extracellular space, as levels of Na and Cl were low, while K was at cytoplasmic levels. The amounts of S measured in the A and I bands are consistent with handbook values for homogenized whole muscle, and with calculations of concentrations of protein-bound S based on deductions from biochemical measurements. (Supported by NSF Grant PCM77-09032. Keith L. Monson is a USPHS Postdoctoral Fellow. The technical assistance of Eunice S. Wang is gratefully acknowledged).

T-AM-E11 POST-DENERVATION CONTRACTILE PROPERTIES OF RAT MUSCLE, Albert C. Kirby and Barry D. Lindley, Department of Physiology, Case Western Reserve University, School of Medicine Cleveland, Ohio 44106.

Isometric contractions of rat soleus (SOL) and extensor digitorum longus (EDL) muscles were examined as a function of time after denervation. 150-200 gram female Sprague-Dawley rats were operated upon under light ether anesthesia. 1 cm of sciatic nerve was removed. Animals were sacrificed at 24 hour intervals beginning at 1 day after operation and up to 57 days. Total contractile force diminishes with time after denervation since the muscle mass dwindles rapidly to 50% control with 2 weeks. EDL twitch tension when normalized for cross-sectional area is increased 35-50% with the increase being apparent in the first day. SOL twitch tension decreases slightly with time after denervation. EDL twitch/tetanus ratio increases after denervation while that of SOL is little changed. Both EDL show changes in post-tetanic potentiation (PTP). PTP of EDL is characterized by increase in twitch tension and slowing of relaxation. As early as 24 hrs EDL PTP shows diminished peak tension and less marked slowing of relaxation. Within the next few days post-tetanic twitches become indistinguishable from pre-tetanic ones. A "running-in" period is found in both EDL and SOL; i.e., the first twitches seen are weak and equilibrium at maximum force is reached only after a considerable period of time which is approximately proportional to the length of the period of denervation. (Supported by NS-10196)

T-AM-E12 ACTION OF ANTHRACENE-9-CARBOXYLIC ACID ON THE MECHANICAL RESPONSE OF SINGLE SKELETAL MUSCLE FIBERS. S. H. Bryant and J. R. Valle*, Department of Pharmacology and Cell Biophysics, U. of Cincinnati College of Medicine, Cincinnati, Ohio 45267.

Anthracene-9-carboxylic acid (A-9-C) is known to block chloride conductance in skeletal muscle membranes, to induce abnormal repetitive firing (myotonia), and to potentiate the twitch. Mechanical studies have previously been restricted to bundles of muscle fibers. In this study single fibers were isolated from frog (Rana pipiens) m. semitendinosus, and were mounted in a Hodgkin-Horowicz chamber. Mechanical responses were monitored by an isometric transducer (RCA 5734). Stimulation was by 0.5 msec square pulses delivered near one tendon of the fiber. All experiments were performed at 23° C. The peak twitch tension is increased 100% over that of the control by 5 x 10^{-5} M A-9-C. There is no detectable decrease in chloride conductance or repetitive firing at this concentration. On the other hand the tetanic tension developed to stimuli at 50 Hz was only increased by less than 20%. Action potentials recorded from these fibers with microelectrodes were not detectably altered by the A-9-C. Voltage-dependent charge movement was also recorded from cut fibers with the three-vaseline-gap voltage clamp following the method of Vergara (personal communication). A-9-C at 5 x 10^{-5} M increased the amount of charge moved over that of the controls. Our findings suggest that the mechanical response phenomenon in A-9-C is not related to changes in the action potential but to alterations of voltage-dependent charge movement and/or calcium kinetics.

(This work was supported by USPHS NIH Grant NS-03178, an MDA Grant to S.H.B. and an MDA postdoctoral fellowship to J.R.V.)

T-AM-Po1 A THEORY FOR NUCLEAR MAGNETIC RELAXATION OF PROBES IN ANISOTROPIC SYSTEMS: APPLICATION TO CHOLESTEROL IN PHOSPHOLIPID VESICLES. J.R. Brainard and A. Szabo (Intr. by J.D. Morrisett), Baylor College of Medicine, Houston, TX 77030 and Indiana University, Bloomington, IN 47405.

The nuclear magnetic relaxation of a nucleus in a cylindrical probe embedded in a membrane suspension is considered. The probe is assumed to diffuse freely about its unique (C_∞) symmetry axis with an effective correlation time, $\tau_\parallel$, and the C_∞ axis moves in a potential which is azymuthally symmetric about a director, with an effective correlation time, $\tau_\perp$. The overall isotropic rotational correlation time of the membrane is τ_M. An expression for the appropriate correlation function is derived which depends on the above effective relaxation times, on the order parameter of the C_∞ axis of the probe and on the angle, in the case of dipolar relaxation of a protonated ^{13}C nucleus, between the ^{13}C-H vector and the C_∞ axis of the probe. A significant feature of this formulation of the dynamics is that no assumptions need be made concerning the relative order of magnitudes of the effective correlation times and the Larmor frequencies. The model can be used not only to describe the dynamics of probes in membranes but is also applicable to certain anisotropic internal motions in proteins. As an application, ^{13}C nuclear magnetic relaxation experiments on cholesterol in sonicated egg yolk phosphatidylcholine vesicles are interpreted within the framework of the model. The remarkable observation that the protonated C6 carbon has a linewidth which is much narrower than those of other methine carbons and in fact comparable to the linewidth of the nonprotonated C5 carbon is shown to be the consequence of (1) the anisotropic nature of the cholesterol motion in the bilayer (2) the fact that the angle between the $^{13}C6$-H vector and the long axis of cholesterol is very close to the "magic" value of 54.7°. (Supported by HL 05696 and HL 21483).

T-AM-Po2 ^2H AND ^{13}C SPECTRA OF THE GEL STATE OF DPPE D.M. Rice, A. Blume, R.J. Wittebort, R.G. Griffin, National Magnet Lab., M.I.T., Cambridge, MA 02139.

Solid state ^2H and ^{13}C NMR spectra of specifically labeled dipalmitoyl-3-SN-phosphatidylethanolamine (DPPE) have been used to examine the structure of DPPE-water multilayers below the gel to liquid crystal phase transition. Uncomplicated by the presence of a pretransition spectra of DPPE lead to an anambiguous model for the gel state which is characterized by rotation perpendicular to the bilayer surface and a nearly all-trans configuration for the acyl chains.

DPPE has been labeled with ^2H at the 4, 8, and 12 positions of the 2 acyl chain, at the 1 position of the ethanolamine headgroup, and with ^{13}C at the 2 position of the 2 acyl chain. The spectra have been observed of pure lipid water multilayers. Deuterium quadrupole echo spectra of the 4, 8, and 12 positions of DPPE multilayers show η=0 powder spectra with nearly one half the rigid lattice splitting. Correlation times, determined from the spectral lineshapes, decrease with increasing temperature from the rigid limit to about 10^{-6} sec just below the phase transition. ^{13}C chemical shift powder spectra also reveal this motion.

Deuterium spectra of the ethanolamine headgroup exhibit at 9 kHz splitting above the phase transition, and below the phase transition a single broad line with a 20 kHz width. The gel state spectrum must result from low frequency conformational transitions which occur in addition to the fast motions of the head group.

(Support NIH GM25505, GM23289, RR00995, DFG BL182/2)

T-AM-Po3 NUCLEAR MAGNETIC RESONANCE STUDIES OF CATION TRANSPORT ACROSS VESICLE BILAYER MEMBRANES: David Z. Ting, P.S. Hagan, J.D. Doll, S.I. Chan, and C.S. Springer; Departments of Chemistry, Cal. Tech.; Pasadena, CA 91125, and SUNY Stony Brook, Stony Brook, NY 11794.

We will present an analysis of an increasingly popular NMR method, employing vesicles, which is analogous to the BLM noise analysis and isotopic tracer experiments for the study of mediated cation transport. It involves the preparation of vesicles with an environment asymmetric in the sense that there are paramagnetic metal ions only outside the vesicles. This asymmetry is manifest in the NMR spectrum as two distinct resonances for magnetic nuclei in outside and inside lipid headgroups. As mediated transport begins the inner headgroup resonance line shifts and changes shape as the paramagnetic metal ions enter the vesicles. The time course of the shift and shape change of this inner resonance contains much information on the actual mechanism by which the ions are transported. Processes by which the ions enter the vesicles one or a few at a time (such as via a diffusive carrier) are easily distinguishable from those by which the ions enter in large bursts (such as by pore activation). The limiting case where intervesicular mediator exchange is slow (the situation for integral membrane proteins) relative to cation transport has been treated analytically. Computer simulated curves indicate conditions necessary for certain changes in the line shape which are analogous to the "current jumps" observed in BLM conductance studies. The theory we have derived allows an analysis of the time course of this line shape to yield the average number of ions which enter in the first few bursts, how often the bursts occur, and how they depend on the concentration of the mediating species in the vesicular membrane. The cases for intermediate and fast intervesicular mediator exchange have been simulated by a Monte Carlo method. Preliminary experimental spectra illustrating some of the various possible line shape behaviors will be presented.

T-AM-Po4 THE MOTIONAL STATE OF LIPIDS IN PHOSPHOLIPID VESICLES AS REVEALED BY PROTON MAGNETIC RESONANCE STUDIES AT 500 MHz. Utpal Banerjee, Joseph R. Schuh, Luciano Müller, and Sunney I. Chan. Caltech, Pasadena, CA 91125.

Proton magnetic resonance spectra of saturated phospholipids in small, unilamellar vesicles have been recorded at 500 MHz on a Bruker WM500 spectrometer. The additional spectral dispersion revealed new structure in the acyl group resonances. The methylene and methyl peaks were split, both showing a broad and a sharp component. Magnetization transfer experiments, together with studies in the presence of manganese ions outside the vesicles, showed that the sharp component is to be assigned to the protons from the chains in the inner half of the bilayer and that the broad one arises from chains in the outer monolayer of the vesicles. Results from these experiments indicate that the outer and inner lipid chains exist in markedly different states of flexibility, probably due to differences in the packing arrangement brought on by surface curvature. (Supported by USPHS NIH Grant GM22432 and American Cancer Society Grant PF-1628.)

T-AM-Po5 DISPERSION STEPR OF SPIN LABELED LIPIDS.

C. Mailer and B. H. Robinson
Department of Physics, University of New Brunswick
Department of Chemistry, University of Washington

The study of the mobility of lipids in membranes by linear EPR is generally limited to correlation times smaller than 10^{-7} sec. Absorption second harmonic quadrature STEPR has extended the sensitivity down to 10^{-9} sec. However in the range of 10^{-8} to 10^{-6} sec the STEPR signal intensity is significantly diminished. Signal intensities are now observed with dispersion first harmonic quadrature STEPR which have signal to noise comparable to linear EPR and retain sensitivity to motion in the range from 10^{-8} to 10^{-4} sec. These signals are obtained with a novel bimodal cavity,[1] and avoid the need for large modulation amplitudes. Spin labeled lipids in model membrane are examined. Data are analysed in terms of spectral ratio parameters. Correlation times obtained from theoretical aniosotropic motional models[2] are compared with correlation times obtained from reference curves of isotropic motion. The validity of using reference curve obtained from molecules whose motion is isotropic for obtaining correlation times for anisotropically moving molecules will be discussed; possible modified correlation times will also be considered.

[1]C. Mailer, H. Thomann, B. H. Robinson and L. R. Dalton, Rev. Sci. Inst. 51, 69(1980).

[2]B. H. Robinson and L. R. Dalton, J. Chem. Phys. 72, 1312(1980).

T-AM-Po6 ELECTRON SPIN RESONANCE STUDY OF THE INTERACTION OF CATIONS WITH LIPOPOLYSACCHARIDE. R. T. Coughlin, A. Haug, and E. J. McGroarty. Michigan State University, East Lansing, MI. 48824

Native lipopolysaccharide isolated from *E. coli* W1485F$^-$ has been studied using 5-doxyl stearate and a cationic spin probe (CAT_{12}). CAT_{12} at low concentrations detected an exceptionally rigid environment from 0 to 50° C in qualitative agreement with results using 5-doxyl stearate.

At higher CAT_{12} concentrations the well resolved hyperfine extrema and the highly negative surface charge of the lipopolysaccharide enabled us to measure the partitioning of this spin probe as a function of temperature. A dramatic increase in partitioning was observed at 15.5 ± 1.5° C. This event was also marked by an increase in the broadening of the low field peak. Thus lipopolysaccharide in this K12 strain is thought to undergo a restructuring at 15.5° C.

CAT_{12} partitioning and line shape changes were also examined in electrodialysed lipopolysaccharide using Ca^{2+}, Mg^{2+}, and spermidine.

T-AM-Po7 AN FT-IR SPECTROSCOPIC STUDY OF THE THERMOTROPIC PHASE BEHAVIOR OF PHOSPHATIDYLSULFOCHOLINES.

H.H. Mantsch, D.G. Cameron, P.A. Tremblay and M. Kates.

Ottawa University (P.A.T. & M.K.) and National Research Council of Canada, (H.H.M. & D.G.C.) Ottawa, Ontario, K1A 0R6, Canada.

Fourier transform infrared (FT-IR) spectroscopy has now matured to a powerful method for the study of molecular organization and the dynamics of membrane lipids. We have developed a methodology whereby infrared frequencies and bandwidths are routinely determined with uncertainties of less than 0.1 cm^{-1}, which allows one to monitor extremely small changes in the vibrational parameters of localized groups or sites, even in highly diluted aqueous systems. In the present study we discuss the temperature-induced changes observed in the infrared spectra of dimyristoyl-, dipalmitoyl-, and distearoyl phosphatidylsulfocholines. The gel to liquid-crystalline phase transition and the "pretransition" are considered in detail, and the thermotropic phase behavior is compared with that observed in the corresponding phosphatidylcholines.

T-AM-Po8 RAMAN AND CALORIMETRIC STUDIES OF SMALL UNILAMELLAR PHOSPHOLIPID VESICLES OF CHAIN LENGTHS 14-20. Bruce P. Gaber and James P. Sheridan, Bio/Molecular Optics Section, Optical Probes Branch, Code 6510, Naval Research Laboratory, Washington, D.C. 20375.

Raman spectra taken in the CH_2 stretching region (2750-3050) CM^{-1}) are useful in assessing the degree of lateral chain packing within the phospholipid bilayer. We use an order parameter (S_{lat}) which permits normalization of the Raman data on a scale such that n-alkane liquids have S_{lat} = 0 and crystalline alkanes, S_{lat} = 1. Viewed in this way, it has been shown that S_{lat} for DPPC small unilamellar vesicles (SUV) differs substantially from the corresponding large multilamellar vesicles (LMV). These comparisons now have been extended to include DMPC, DSPC and DAPC. For S_{lat} measured at 10°C below the relevant T_m, the trend with increasing chain length is for LMV values to decrease slightly while the those for SUV increase substantially. To correct for the effect of temperature, the ratio of S_{lat} for SUV and LMV was determined. Plotted versus chain length, these ratio fall on a straight line. For chains greater than C20 the ratio extrapolates to one. Thus the extent of chain-chain packing interaction above C20 is the same for SUV as it is for LMV. At about C-12 the ratio extrapolates to zero, indicating a chain order for SUV comparable to a liquid hydrocarbon. These data are consistent with the results of calorimetric measurements. Transition enthalpies for SUV when plotted versus chain length fall on a line lower than, and parallel to, that for the enthalpies of LMV and extrapolate to ΔH = 0 for C-12. These data reflect well the chain length dependence we have previously reported for the relative stability of SUV against fusion. (Supported, in part, by a contract from the Office of Naval Research Biophysics Program)

T-AM-Po9 A METHOD FOR DETERMINATION OF TRANS/GAUCHE RATIOS FROM RAMAN LINE INTENSITIES. James P. Sheridan and Bruce P. Gaber, Bio/Molecular Optics Section, Optical Probes Branch Code 6510, Naval Research Laboratory, Washington, D.C. 20375.

The most convenient quantitative measure of organization in the interior of a phospholipid bilayer is the fraction of bonds in the alkyl chains which are gauche. We have reinvestigated the problem of obtaining such information from the analysis of Raman skeletal mode intensities. Examination of the Raman spectrum of crystalline and gel phase dipalmitoyl phosphatidylethanolamine (DPPE) reveals that these phases are orthorhombic in nature and that they are highly ordered in terms of % trans bonds. The evidence for this is the existence of a relatively strong longitudinal acoustic mode (LAM) and a single methyl deformation band at ∿890 cm^{-1}. On the other hand, the Raman spectrum of dipalmitoyl phosphatidylcholine gel phase reflects the existence of an hexagonal phase and a fairly disordered one at that as evidenced by a very weak LAM and methyl deformation modes at ∿860 and 840 cm^{-1} indicative of specific gauche bonds at positions 14 and 13. Thus a measureable fraction of the chain ends in the DPPC gel phase at 25°C are in the gauche conformation and the relative intensity changes in the methyl deformation modes give a quantitative measure of this fraction. These data together with intensity measurements of the 1130 cm^{-1} as a function of temperature in an isotropic environment (where the % gauche bonds can be calculated) provides us with a means of establishing a calibration curve for the dependence of the Raman intensity at 1130 cm^{-1} upon % gauche bonds in the lipid bilayer.

T-AM-Po10 A LASER RAMAN STUDY OF THE CONFORMATIONAL CHARACTERISTICS OF SINGLE COMPONENT SPHINGOMYELIN BILAYERS J. P. Sheridan, S. D. Merajver and B. P. Gaber, Optical Probes Branch, Code 6510, Naval Research Laboratory, Washington, D.C. 20375, and Y. Barenholz, Dept. of Biochemistry, Hebrew University, Jerusalem (Israel) and Dept. of Biochemistry, U. Va. School of Medicine, Charlottesville, Va.

The structural properties of the synthetic sphingolipids, N-palmitoyl (N-C16), N-stearoyl (N-C18), and N-lignoceryl sphingomyelin (N-C24) have been investigated in the crystalline, gel, and fluid phases by Raman spectroscopy. Significant differences are observed between all three chain lengths in terms of chain packing and conformation in the crystalline and gel phases, and in the melting behavior at the first-order gel-fluid phase transition. For example, N-C16 displays a sizeable number of gauche bonds in the gel phase - indicative of considerable disorder at the bilayer mid-plane; on the other hand the highly asymmetric N-C24 possesses very few gauche bonds below the main transition, reflecting, perhaps, interdigitation occurring at the bilayer mid-plane. The melting curve for N-C24 shows a high-temperature asymmetry which further reflects interdigitation and the persistence of an excess of trans-bonds into the fluid phase, while that for N-C16 exhibits no such anomaly.

N-C18 possesses two gel phases - a stable and a metastable one. The Raman data indicate that the stable gel phase is of a fairly highly ordered orthohombic nature while the metastable one is a more loosely packed hexagonal phase. There are also differences in the head group vibrations suggestive of different levels of hydration between the two phases which may contribute significantly to the disparate ΔH values observed for the gel-fluid phase transition of the two species.

T-AM-Po11 ION INTERACTIONS WITH DIPALMITOYLPHOSPHATIDYLCHOLINE: A RAMAN SPECTROSCOPIC STUDY. **J.W. Kauffman, D. Hess* and D. Boston*, Biomedical Engineering Center, Northwestern University, Evanston, Illinois 60201, and L.J. Lis, Department of Physics, Illinois Institute of Technology, Chicago, Illinois 60616.**

We have re-examined the effect of ions on dipalmitoylphosphatidylcholine bilayer arrays using Raman spectroscopy. The effect of high ionic solution concentrations of various mono and di-valent salts on DPPC bilayers was previously examined by this same technique (L.J. Lis, J.W. Kauffman and D.F. Shriver (1975) Biochim. Biophys. Acta 406, 453-464). Concentrations as low as 1mM $CaCl_2$ have now been found to cause significant changes in the 'trans' order but not the 'lateral' order as determined by various Raman spectroscopic order parameters, which agrees with the findings of Loshchilova and Karvaly (Biochim. Biophys Acta 514 (1978) 274-285). In addition, vortexed DPPC samples show some changes in the DPPC Raman head group bands, particularly the phosphate stretch at ca. 760 cm^{-1}, in the presence of $CaCl_2$ at these low solution concentrations. The interaction of 1M solutions of Na and K salts of monovalent anions with DPPC was also examined. Our results indicate that although Na^+ and K^+ salts have no apparent difference in their interaction with DPPC, anions, particularly Cl^-, have some effect on the packing of the lipid in the bilayer arrays.

T-AM-Po12 APPLICATION OF INFRARED SPECTROSCOPY IN PROBING MEMBRANE ASSEMBLIES: UNIQUE BILAYER STRUCTURES OF DIDODECYLDIMETHYLAMMONIUM BROMIDE (DDAB) AND DIPALMITOYL PHOSPHATIDYLGLYCEROL (DPPG). R. G. Adams and I. W. Levin, Laboratory of Chemical Physics, NIAMDD, National Institutes of Health, Bethesda, Md. 20205.

Two model bilayer systems, didodecyldimethylammonium bromide (DDAB), a completely synthetic bilayer membrane, and dipalmitoyl phosphatidylglycerol (DPPG) were investigated by vibrational infrared spectroscopic procedures. Since DDAB membranes form modified headgroup and interfacial regions, in comparison to phospholipid molecules, the characterization of the gel and liquid crystalline structures for this system provide information on the various contributions toward bilayer stability from specific lipid structural elements. Infrared spectroscopic frequency shifts of the 2850 and 2920 cm^{-1} C-H stretching modes were used to monitor the phase transition processes for DDAB multilamellar and single shell vesicle assemblies. Temperature profiles for the multilayers display a gel to liquid crystalline phase transition at 17.7°C, but exhibit no pretransition effects as observed in phospholipid bilayers. Temperature profiles were also determined for both the uni- and multilamellar systems containing 15 mol % cholesterol. The phase transition temperature for the multilayers was depressed to 7.5°C, while that for the unilamellar system decreased to only ∿16°C from 17.0°C, suggesting different structural reorganizations within the two types of assemblies. Completely hydrated bilayers of DPPG were examined in the methylene C-H stretching mode region, the carbonyl C=O stretching mode region and the methylene CH_2 deformation region, respectively. Comparisons with DPPC multilayers provide evidence for DPPG bilayers undergoing chain interdigitation below ∿41°C in which the CH_3 termini from one monolayer significantly perturb the interfacial region of the opposing monolayer.

T-AM-Po13 1-[4'-TRIMETHYLAMINOPHENYL]-6-PHENYL-HEXA-1,3,5,-TRIENE (TMA-DPH): USE AS A FLUORESCENCE PROBE OF LIPID BILAYERS. Prendergast, F. G. and Haugland, R. P., Department of Pharmacology, Mayo Foundation, Rochester, MN. and Molecular Probes, Plano, TX.

Diphenylhexatriene (DPH) has been widely used as a fluorescence probe of lipid bilayer structure and dynamics but the precise location of DPH in the bilayer, especially at temperatures (T) > T_c the thermal transition temperature of the lipid. We reasoned that a cationic derivative such as TMA-DPH should be tethered at the lipid-water interface and allow us to probe a defined region of the bilayer. The photophysical properties of TMA-DPH and DPH are generally similar -- absorption and fluorescence spectra are identical, although the molar extinction for TMA-DPH is significantly less than that of DPH. Fluorescence lifetimes (τ) of TMA-DPH in all solvents is < 1.5 nsec. However, when incorporated in vesicles of dimyristoylphosphatidylcholine (DMPC) at T < T_c, τ is increased to $\sim$ 7 nsec but decreases sharply at T_c. Values for r_∞ were determined for this probe in several lipid systems by measurements of differential polarized phase lifetimes. Profiles of changes in r_∞ with temperature are broadly similar for TMA-DPH and DPH, but the minimum r_∞ for the former in DMPC at T >> T_c is $\sim$ 0.14 (cf for DPH 0.03). Electrostatic interactions of the cationic probe with negatively charged phospholipid headgroups do not seem to significantly influence the motions of the probe. Values for order parameters and cone angles of fluorophore diffusion were calculated from measurements of r_∞. Because of the predictable location of the probe in bilayers, models of its motion are more readily derived and seem more plausible than comparable models for DPH. This work was supported by grants from the Muscular Dystrophy Association and the National Science Foundation. F.G.P. is an Established Investigator of the American Heart Association and a Searle Foundation Scholar.

T-AM-Po14 ALTERATION OF FLUORESCENCE POLARIZATION GRADIENTS IN EGG AND DIPALMITOYL LECITHIN MULTI-LAMELLAR VESICLES INDUCED BY n-ALKANOLS. G.B. Zavoico and H. Kutchai, Dept. of Physiology, University of Virginia Medical School, Charlottesville, VA. 22908

The lipid soluble fluorescent probes 2-, 7-, and 12-(9-anthroyloxy) stearic acids (2-AS, 7-AS, & 12-AS) have been used to study the polarization ("fluidity") gradient of egg lecithin (EggL) and dipalmitoyl lecithin (DPL) multi-lamellar vesicles. By partitioning into the bilayer with their carboxyl groups near the phospholipid head groups and their alkyl groups parallel to the phospholipid acyl chains the fluorescent anthroyloxy moiety reports from well-defined depths in the bilayer. The n-alkanols are believed to partition into the bilayer with their hydroxyl groups near the phospholipid head groups and their alkyl chains parallel to the phospholipid acyl chains. In this study pentanol, heptanol, and decanol were used to perturb the bilayer to different depths. The polarization gradient in EggL at 25° and 38°, and of DPL at 47° are very similar. Polarization of 2-AS is slightly greater than of 7-AS, which is considerably greater than of 12-AS indicating an increasing "fluidity" towards the bilayer center. Addition of each n-alkanol to about 30 mole % only decreased the absolute values of polarization without altering the profile of the gradient indicating a general "fluidizing" effect of n-alkanols. In contrast, the polarization gradient in DPL at 25° is not as steep, and the n-alkanols have a "solidifying" effect. The polarization of 2-AS and 7-AS is increased with each n-alkanol studied, but that of 12-AS is increased only with decanol. It appears that above the phase transition n-alkanols have a non-specific "fluidizing" effect, whereas below the phase transition there is a "solidifying" effect that is dependent on the chain length of the perturbing n-alkanol. (Supported by NIH Grant GM24168).

T-AM-Po15 THE INTRINSIC LUMINESCENCE OF LIPID PEROXIDATION PRODUCTS AS PROBE OF STRUCTURAL STATES OF LIPOSOMES. S.N. Cherenkevich and A.I. Khmelnitzky, Department of Biochemistry & Biophysics, University of Pennsylvania, PA 19104 and Department of Biophysics, Byelorussian State University, Minsk, USSR.

Data are presented to demonstrate the possibility of the use of luminescence properties of lipid peroxidation products for the study of model membrane systems (liposomes). The magnitude of anisotropy and the position of the spectrum of intrinsic fluorescence of peroxidized egg lecithin, total lipid, and total phospholipid of rat liver, as well as of fluorescent parameters of 1-anilino-8-naphthalenesulfonate (ANS) bound to liposomes were measured using the single-photon detection technique. The intrinsic fluorescence properties of lipid peroxidation products (LPP) have been used to monitor thermal transition of vesicles. It was shown that there were correlations between temperature dependent changes of fluorescence properties of ANS and LPP. Measurement of intrinsic fluorescence of LPP is useful to the study of kinetics and mechanism of lipid peroxidation. It was established that the fluorescence parameters reflect the nature of the microenvironment of LPP and depend on the medium conditions of measurement. The phosphorescence properties at 77°K and room temperature of LPP of a number of lipids were measured and were found to depend upon the nature of the lipid. Thus, intrinsic luminescence of LPP appear to be well suited to the study of structural organization of lipids in biological membranes without the use of an extrinsic fluorescent probe. Sponsored by J.M. Vanderkooi.

T-AM-Po16 X-RAY STUDY OF A MONOBROMINATED ANALOG OF PALMITOYL LECITHIN
R. K. Lytz, J. C. Reinert, E. W. Dilsworth and H. H. Wickman, Chemistry and Agricultural Chemistry Departments, Oregon State University, Corvallis 97331.

Hydrated multibilayers of 1-palmitoyl-2-monobromopalmitoyl lecithin, where the β-chain is brominated in either the 9- or 10-position, have been studied by low angle x-ray diffraction methods. Samples were prepared in two forms: (1) oriented multibilayers on glass substrates and (2) multibilayer vesicle suspensions. The variation with temperature of the long spacing was followed in the interval -15°C to 80°C. Unlike the parent DPL complex (which shows a solid-liquid side chain transition near 41°C), BrDPL showed no evidence of a sharp structural transition in the temperature interval noted. Instead, a monotonic increase in long spacing from ca 5.0 nm to ca 6.2 nm (28 wt % H_2O) occurred with decreasing temperature. Wide angle scattering showed a diffuse peak corresponding to $(0.45\ nm)^{-1}$. Differential scanning calorimetry measurements for fully hydrated multibilayers (50 wt % H_2O) also showed no evidence for a phase transition. These results suggest a low temperature amorphous (glass) state for the acyl side chains of BrDPL. (Research supported by PHS Grant ES-00040-15).

T-AM-Po17 PHOTON CORRELATION SPECTROSCOPY STUDY ON THE STABILITY OF SMALL UNILAMELLAR DPPC VESICLES. E. L. Chang, B. P. Gaber, and J. P. Sheridan, Bio/Molecular Optics Section, Optical Probes Branch, Code 6510, Naval Research Laboratory, Washington, D.C. 20375.

The growth in size of DPPC SUV below its T_m has been studied by photon correlation spectroscopy (PCS). The data were fitted by single-, double-exponential, and cumulants analysis. The time-dependence of the hydrodynamic diameter, as obtained by single-exponential fitting, showed an initial fast rise followed by a slower increase of the diameter. The time evolution of the two diameters, as obtained by double-exponential fitting, exhibited a "slow" and a "fast"behavior pattern respectively. Concommitant scans with DSC on the SUV sample showed that the slower growing component (the smaller-sized population) is due to the gradual fusion of SUV while the faster growing one is the result of aggregation. The order of the kinetics appears to be higher than the first order. The estimated half-lifetime of fusion is ∿67 hours. The initial diameters for the fast and show processes are 765Å and 266Å respectively, while, in the limit $\tau \to \infty$ the diameters approach 1,570Å and 733Å respectively. The fraction of small to large particles was estimated from the double exponential fitting assuming the scatterers as hollow, spherical shells of isotropic scattering elements.

We analyzed the kinetics of fusion in terms of a condensation model. The effectiveness-of-collision parameter, ρ, was estimated to be 3×10^{-5} fusions/collision for a value of ∿64 fusion events per second per Molar lipid. This research was supported in part by a contract from the Office of Naval Research - Biophysics Program and in part by a grant from the National Research Council.

T-AM-Po18 HEXANE LOCATION IN LIPID BILAYERS DETERMINED BY NEUTRON DIFFRACTION. Glen King and Stephen White, Dept. of Physiology and Biophysics, University of Calif., Irvine, CA 92717

We have examined oriented dioleoyl lecithin (DOL) multilayers containing hexane introduced via the vapor phase. The distribution of hexane across the bilayer is determined by a comparison of the neutron scattering density curve from samples with protonated and deutenated hexane, respectively. The samples were maintained at 66% relative humidity (T = 22.5°C) as the hexane concentration was varied in the experiments. We find that the hexane is located predominantly in a zone about 10 Å wide in the center of the bilayer. At moderate concentrations of hexane (less than 0.4 times the vapor pressure of pure hexane), we find that the d-spacing and hydrocarbon thickness do not change as more alkane is dissolved in the bilayer. Furthermore, the amount dissolved in the lipid is a linear function of the hexane vapor pressure, meaning that we are in the Henry's law region of the bilayer's hexane solubility curve. At higher concentrations of alkane, this linearity is no longer observed. However, the d-spacing remains constant in the non-linear region. The effect of water activity on hexane solubility in the bilayer has also been studied by varying the relative humidity of the samples. (Supported by NIH Grant 23983.)

T-AM-Po19 BRIGHT BLACK LIPID MEMBRANES. Ron Waldbillig, Department of Physiology & Biophysics, U.T.M.B., Galveston, TX 77550

Planar black lipid membranes have been made highly reflective (bright) by modification of the aqueous phase refractive index (n_a). This development stems from the fact that the total light reflection from a thin dielectric film depends upon both its thickness (destructive interference) and interfacial refractive index ratio (reflectance). From these and other considerations an electroptic model has been developed to predict the dielectric thickness and dielectric constant of membranes.

The model predicts an increase in membrane reflectance when the two interfacial n ratios are dissimilar. The results of preliminary membrane reflectance studies support this prediction. For example monoolein bilayers situated between aqueous compartments of different refractive index (1.33-1.50) are highly reflective. The bilayer specific capacitance and therefore thickness and dielectric constant (n_m^2) are not significantly changed by the gradient.

In symmetrical solutions the bilayer reflectance is expected to approach zero (totally black) as n_a approaches n_m. Preliminary results obtained from monoolein/decane bilayers suggest a reflectance minimum as n_a nears 1.4. Either increasing or decreasing n_a about this point yields increased membrane light reflectance. An n_m value of 1.4 corresponds to a membrane dielectric constant near 2.0. An asymmetrical circumstance where one interface has $n_a < n_m$ while the other interface has $n_a > n_m$ is expected to yield constructive interference between the reflected light waves.

(Supported by N.I.H. Grant 1Rol GM-26980.)

T-AM-Po20 ABSENCE OF TRANSBILAYER ASYMMETRY IN SMALL UNILAMELLAR VESICLES COMPRISED OF PHOSPHATIDYLGLYCEROL AND PHOSPHATIDYLCHOLINE. J.R. Nordlund, C.F. Schmidt and T.E. Thompson, Dept. of Biochemistry, University of Virginia, Charlottesville, Virginia 22908.

In contrast to earlier studies, we have found that egg phosphatidylglycerol (PG) and phosphatidylcholine (PC) are equally distributed between the two monolayers in small unilamellar vesicles comprised of PG and PC. These vesicles, which contained 10, 25, 50 or 75 mole percent PG (sodium salt) were formed in borate buffer pH 7.6 by rapid ethanol injection or by sonication. The crude dispersion was centrifuged before use to obtain a homogeneous population of vesicles. Using Mn^{+2} as a broadening agent, the transbilayer distribution of PG and PC was determined by ^{31}P NMR. The vesicles were impermeable to Mn^{+2}. Subsequent elution from a molecular sieve column indicated that the vesicles did not fuse during the NMR experiment. Proton NMR spectra of vesicles containing $Fe(CN)_6^{-}$ were recorded in the presence and absence of Mn^{+2}. The intensity of the N-methyl choline protons corresponding to the PC molecules in the inner monolayer, which were shifted upfield from the outside protons by $Fe(CN)_6^{3-}$, remained constant when Mn^{+2} was added. Thus, Mn^{+2} did not cause transbilayer phospholipid rearrangement. The absence of PG and PC asymmetry in structurally equivalent vesicles made by very different methods suggests that the effective polar head group volumes rather than net charge determine the packing constraints for mixtures of phospholipids with the same acyl chains in highly curved membranes. (This investigation was supported by U.S. P.H.S. Grants GM-14628 and GM-23573).

T-AM-Po21 FREEZE-FRACTURE AND NEGATIVE STAIN ANALYSIS OF MULTILAMELLAR LIPID PHASES CONTAINING N-ALKANES. M.J. Costello and T.J. McIntosh, Department of Anatomy, Duke University Medical Center, Durham, N.C. 27710.

The effect of n-alkanes on lipid bilayer structure has been investigated using freeze-fracture and negative stain electron microscopy. The smooth fracture faces of gel ($L\beta'$) and liquid crystalline ($L\alpha$) state bilayers are unmodified by long chain alkanes such as tetradecane. However, short alkanes, such as hexane, dramatically alter the hydrophobic bilayer interior, producing large (200 to 500 Å) mounds and depressions in the fracture faces. The fracture steps in these multilayer preparations containing short alkanes are variable in thickness and often considerably wider than the corresponding fracture steps in multilayers which contain long alkanes or are solvent-free. These results are consistent with x-ray diffraction data which imply that the long alkanes are primarily located between adjacent lipid hydrocarbon chains in each monolayer of the bilayer, while short alkanes can partition into the geometric center of the bilayer between apposing monolayers. We have also examined the effects of alkanes on the $P\beta'$ or "banded" phase of phosphatidylcholine (PC) bilayers. At temperatures between the pretransition and main transition a periodic banded pattern in the plane of the bilayer can be observed by negative staining as well as by the freeze-fracture technique. The negative stain method provides a view of the hydrophilic surface of these bilayers and provides additional information on the structure of the $P\beta'$ phase. The incorporation of tetradecane into these bilayers removes the banded structure from both the hydrophilic surface and hydrophobic interior of the bilayer.

T-AM-Po22 ELECTRON DIFFRACTION ANALYSIS OF DIHEXADECYL PHOSPHATIDYLETHANOLAMINE. W. A. Pangborn* and D. L. Dorset. Molecular Biophysics Department, Medical Foundation of Buffalo, Buffalo, New York 14203

A major impediment to the use of electron diffraction data in the crystal structure analysis of phospholipids has been the proclivity of these compounds to crystallize with the long molecular axis nearly perpendicular to the best developed crystal face. The electron beam will then be parallel to a long unit cell direction. The data obtained are further complicated in that any crystal bending acts as a coherence restriction, and this effect is most pronounced when the unit cell dimension parallel to the beam is large. As a result, under these conditions only the hydrocarbon chain packing is observable from the electron diffraction data. These factors have recently been obviated by the development of a technique of growing lipid crystals epitaxially by cooling from a molten naphthalene solution. The crystal growth appears to be controlled by the nascent (001) naphthalene crystal face. Intermolecular furrows along the <110> diagonals are separated by 5Å, approximately the hydrocarbon interchaim distance. Evaporation of the crystalline naphthalene leaves phospholipid crystals with the long molecular axis parallel to the best developed crystal face. The long spacing of the ether-linked lipid dihexadecyl phosphatidylethanolamine is 55.6Å. The sideband diffraction is observed at 4.69Å. The 00ℓ(ℓ=16) electron diffraction intensity data have been used in a multilayer structure calculation, using a model derived from dilauryl PE. The best fit yields a crystallographic residual of 0.23, which is lowered to 0.18 when corrected for n-beam dynamical scattering. The data have been extended to a resolution of 1.25Å (ℓ = 45). The multilayer calculation is now being repeated. Supported by NIH grant GM 21047.

T-AM-Po23 PRESSURE EFFECTS ON LIPID BILAYERS AND BIOLOGICAL MEMBRANES, P. L.-G. Chong, M. Shinitzky, A. Cossins and G. Weber (University of Illinois, Biochemistry Department, Urbana, Illinois, and University of Liverpool, Department of Zoology, Liverpool, England)(Intr. by Robert Gennis).

The small, unilamellar vesicles (SUV) and the multilamellar vesicles (MLV) from dimyristoyl-L-α-phosphatidylcholine (DMPC), dipalmitoyl-L-α-phosphatidylcholine (DPPC), dioleoyl-L-α-phosphatidylcholine (DOPC) and L-α-phosphatidylcholine from egg yolk were examined by steady state polarization fluorometry under pressure in the range 10^{-3} to 2 Kbar. Isothermal pressure-induced phase transitions were observed in DPPC and DMPC vesicles labelled with 1,6-diphenyl-1,3,5-hexatriene (DPH). The temperature-to-pressure equivalences, dT/dP, estimated from the transition point, P_t, are 30.4°K $Kbar^{-1}$ for SUV from DPPC, 27.5°K $Kbar^{-1}$ for MLV from DPPC, 22.2°K $Kbar^{-1}$ for SUV from DMPC and 22.5°K $Kbar^{-1}$ for MLV from DMPC. Synaptosomal membranes isolated from goldfish brain, also labelled with DPH, were studied by differential polarized phase fluorometry, in addition to the steady state technique. Our results indicate that the depolarizing motions are hindered as reflected by a decrease of the mean rotation angle $<\theta>$ and an increase of the lower limit anisotropy (r_∞) under pressure, although the exact equivalence of temperature and pressure effects could not be determined in this case. These observations, however, can also be explained in terms of temperature-pressure compensation of magnitude similar to those observed with the pure lipids, therefore in the range of 20-30 °K $Kbar^{-1}$. The magnitude of our dT/dP values is very close to those reported previously on phospholipid dispersions (Ceuterick et al. (1978), Eur. J. Biochem. 87, 401), on n-C-18 alkanes (Würflinger et al. (1973), Ber. Bunsenges. Physik. Chem. 77, 121), on polyethylene (Monobe et al. (1974), Proc. 4th Int. Congr. High Pressure, Kyoto, Phys. Chem. Soc. Jap. 63) and on activity of (Na^+,K^+)-ATPase (Smedt et al. (1979)Biochem. Biophys. Acta, 556, 479).

T-AM-Po24 DEVELOPMENT OF A GENERAL REPRESENTATION OF THE LATERAL ORGANIZATION OF LIPID MEMBRANES: APPLICATION TO PROTEIN-LIPID SYSTEMS. Ernesto Freire and Brian Snyder, Dept. of Biochemistry, University of Virginia, Charlottesville, Virginia 22908.

Our method of Monte Carlo calculations of the lateral distribution of molecules in lipid bilayers (Freire and Snyder, Biochemistry 19, 88 (1980); Biochim. Biophys. Acta 600, 643 (1980))has been generalized to include molecules of different cross sectional areas and various interaction potentials. These results have allowed us to investigate the dependence of the lateral distribution of membrane proteins on the protein size, the protein/lipid ratio and the magnitude of the interaction energies. A precise description of the resulting computer generated distributions has been obtained by calculating the state of aggregation of the protein molecules, the radial distribution and the pair connectedness function. The radial distribution function measures the distribution of intermolecular distances whereas the pair connectedness function measures the physical extension of compositional domains. These quantities have been calculated for three different types of domains: protein domains, protein + annular lipid domains and pure lipid domains. As the protein/lipid ratio increases, the protein + annular lipid as well as the protein domains grow in size; however, at a characterisitc protein/lipid ratio, the annular lipid becomes connected forming a single network that contains all the protein molecules and extends over the entire bilayer surface. This process is accompanied by the isolation of the pure lipid domains into small, disconnected areas dispersed over the bilayer surface. Additional dynamic calculations show that these changes in the lateral connectivity of compositional domains might play an important role on the regulation of diffusional processes along and across the plane of the bilayer. (Supported by USPHS, NIH grants GM-27244 and GM-26894).

T-AM-Po25 LIPID MELTING AND NOISE IN THE STEADY-STATE LEVEL OF FLUORESCENCE OF 5-IUDO-ACETAMIDOFLUORESCEIN LABELLED Ca^{2+}-ATPase RECONSTITUTED IN VESICLES ENRICHED IN DIMYRISTOYL PHOSPHATIDYLCHOLINE. Carlos Gutierrez-Merino and Rodney L. Biltonen, Dept. of Pharmacology, University of Virginia, Charlottesville, Va. 22908.

Ca^{2+}-ATPase from rabbit skeletal muscle sarcroplasmic reticulum reconstituted into liposomes chemically enriched in dimyristoyl phosphatidylcholine according to a protocol recently developed in this laboratory [C. Gutierrez-Merino and R.L. Biltonen (1980) Fed. Proc. 39, 1980] was labelled with 5-iodoacetamiadofluorescein following the procedure of Vanderkooi et al.[Biochem. 16, 1262-1267 (1977)]. A large and typical noise in the fluorescence of this chromophore was noticed within the temperature range in which the lipid matrix of these vesicles is undergoing its melting process. The extent of this noise relative to the signal size as well as its frequency is markedly dependent on the lipid physical state. This noise, which under the proper conditions reaches (20-30)% of the total fluorescence intensity, was found to be markedly affected by factors that decrease the cooperativity of the lipid melting process, such as the local anesthetics procaine and dibucaine. Data obtained on studies carried out to clarify the physical nature of this noise are reported. (Supported by NIH grant GM-26894)

T-AM-Po26 EFFECT OF LOCAL ANESTHETIC CHARGE STATE ON THE DIPALMITOYL PHOSPHATIDYLCHOLINE PHASE TRANSITION. T.G. Conley and R.L. Biltonen, Dept. of Pharmacology, University of Virginia, Charlottesville, Va. 22908.

Perturbations to the gel-to-liquid crystalline phase transition of dispersions of multilamellar dipalmitoyl phosphatidylcholine liposomes (DPPC) produced by the local anesthetic tetracaine were studied as a function of the charge state of the anesthetic molecule using differential scanning calorimetry. Multilamellar aqueous dispersions of DPPC were prepared in the presence of varing concentrations of tetracaine (pka = 8.5) in 0.05 M TES (N-tris-[hydroxymethyl] methyl-2-aminoethanesulfonic acid) buffer at either pH 6.8 or pH 8.2. The enthalpy change (ΔH) of the DPPC phase transition was unaffected by the presence of tetracaine, averaging 8.7 kcal/mole lipid. Both the transition temperature (t_m) and the maximum value of the heat capacity function (ΔC_{Pmax}) versus the total anesthetic concentration exhibited biphasic behavior. At low anesthetic-to-lipid ratios a small linear decrease in t_m and the maximum heat capacity change is observed followed by an abrupt, rapid decrease in both t_m and ΔC_{Pmax} at an anesthetic-to-lipid ratio of about 0.2. This was observed regardless of the pH of the solution. While the value of t_m at a given anesthetic concentration was independent of the pH, the phase transition at pH 8.2 was significantly broader than at pH 6.8. These results suggest a significant dependence of the cooperative unit size of the DPPC phase transition on the charge state of tetracaine. (Supported by NIH grants GM-07561 and GM-26894).

T-AM-Po27 THERMOTROPIC PROPERTIES OF CYCLOPENTANOID ANALOGS OF DIPALMITOYL LECITHIN. H.J. Pownall, W.W. Mantulin, H.Z. Sable, M.D. Lister, and A.J. Hancock. Department of Medicine, Baylor College of Medicine and The Methodist Hospital, Houston, Texas 77030 and the Department of Chemistry, University of Missouri, Kansas City, Missouri 64110.

A series of dipalmitoyl lecithin analogs in which the 1 and 3 carbons of the glyceride moiety are connected by a bridge of two methylene units has been synthesized. Of the seven possible isomers six have been synthesized and their thermal properties studied by differential scanning calorimetry and by the temperature dependence of the depolarization of fluorescence of the probe, 1,6-diphenyl-1,3,5-hexatriene (DPH). All six isomers exhibit reversible acyl chain melting and a decreased microviscosity between a low value of 36.2° C to a high value of 45.5°C. None exhibited a pretransition. This behavior compares with L-α-dipalmitoyl lecithin (DPH) which melts at 41°C and has a pretransition at about 37°C. The enthalpy of melting of 4 of the analogues was similar (8-10 Kcal/mol) to that of DPH (8 Kcal/mol) but two of the analogues had melting enthalpies of about 19 kcal/mol. We suggest that the unique acyl chain structure of the latter pair of analogues contributes to its unusually high enthalpy.

T-AM-Po28 THERMAL STUDIES OF THE SINGLE PHASE REGIONS OF PHOSPHOLIPIDS. D.A. Wilkinson and J.F. Nagle, Department of Physics and Biological Sciences, Carnegie-Mellon University, Pittsburgh, PA 15213

Previous calorimetric studies of lipid bilayers have focused on the phase transition and the apparent specific heats, C_p, in the single phase regions have been set equal to zero. In contrast, dilatometric studies have shown a non-zero coefficient of thermal expansion. We have performed measurements on lipid dispersions (2 to 3%) in water using a highly sensitive differential scanning calorimeter (Microcal). For saturated phosphatidylcholines and phosphatidylethanolamines, we find that C_p increases with temperature in the low temperature phase (below the lower transition in the PC's) whereas it is nearly constant above the phase transition. This behavior is similar to C_p data of fatty acids and n-alkanes of comparable chain lengths. In contrast, the coefficients of thermal expansion are nearly constant in the low temperature phase and decrease with temperature in the high temperature phase. From the dilatometric results obtained previously, the change in van der Waals' interaction energy between hydrocarbon chains is therefore constant in the low temperature phase and decreasing above T_m. This interaction accounts for about 1/3 of C_p. The interaction energy responsible for the remainder of C_p has not yet been identified.

T-AM-Po29 LATERAL DIFFUSION IN MULTICOMPONENT MEMBRANES. Brian Snyder, William van Osdol and Ernesto Freire, Dept. of Biochem., University of Virginia, Charlottesville, Virginia 22908.

We have investigated the compositional dependence of the lateral diffusion parameters of multicomponent membranes using dynamic Monte Carlo calculations based upon molecular distributions previously derived for binary mixtures of phosphatidylcholines and cholesterol-phospholipid mixtures (Biochem. 19, 88 (1980); BBA 600, 643 (1980); PNAS 77, 4055 (1980)). In order to estimate the lateral diffusion parameters of these mixtures we have labelled a fraction of the molecules in the original computer distributions so that the position coordinates of these molecules can be monitored as they move within the bilayer. The lateral motion has been assumed to be a biased random walk in which: a) the diffusional jump frequencies are dictated by the intrinsic diffusion coefficients of the compositional domains; and, b) the direction of movement is stochastically determined by the occupancies and partition coefficients of the nearest neighbor positions of each molecule. The lateral diffusion coefficients have been estimated from the time dependence of the mean square displacement of the labelled molecules or by computer simulating photobleaching recovery experiments. These calculations have also allowed us to examine the kinetics of diffusion-controlled bimolecular reactions by directly computing the collision frequency and the average number of diffusional steps per molecular collisions as a function of the composition of the membrane. These studies provide an explicit numerical dependence for the macroscopic diffusion coefficients on the local coefficients and the membrane domain structure. It is shown that changes in the lateral connectivity of the compositional domains, such as in the case of cholesterol-lipid mixtures at 20 mole % cholesterol, might profoundly affect the magnitude of the macroscopic diffusion coefficients and the kinetics of bimolecular and higher order reactions within the plane of the bilayer. (Supported by NIH grants GM-27244 and GM-26894).

T-AM-Po30 ANNEALING STUDY OF IRREVERSIBILITY IN THE CHAIN-MELTING TRANSITION IN LIPIDS, S.G. Black and G.S. Dixon, Oklahoma State U., Stillwater, OK 74078

Differential a.c. calorimetry of multilamellar suspensions of dimyristoyl phosphatidylcholine (DMPC) shows a specific heat peak on cooling through the chain-melting transition that is markedly different from that observed on heating through this transition. Not only is the transition shifted to lower temperatures, but also the profile of the peak is altered. On subsequent reheating the phase transition closely reproduces the original heating run. Similar results are observed for dipalmitoyl phosphatidylcholine. Here, we report results of a detailed investigation of these phenomena in DMPC. Samples were held for 1 hr. at 10°C, heated to an annealing temperature T_h, and then cooled. Data were acquired for various values of T_h and the time of anneal. Heating and cooling rates were approximately 3°C/hr. The a.c. temperature had a frequency of 0.4 Hz and an amplitude of less than 1 millidegree. Preliminary data indicate that the results may be reversible when T_h is within the specific heat peak. This is not the case for samples annealed at higher temperatures. Supported by NSF, Grant Number PCM 7813752.

T-AM-Po31 MECHANICAL CALORIMETRY OF LARGE DMPC VESICLES IN THE PHASE TRANSITION REGION. R. Kwok and E. Evans, Duke University, Durham, N.C.

The physical state of large DMPC vesicles in the phase transition region has been studied with micromechanical techniques. Unstressed DMPC vesicles below the crystallization temperature, T_m, are forced through the phase transition by micropipet aspiration. These experiments are performed at various reduced temperatures close to the phase transition temperature. The data provide membrane tension, $\bar{T}$, versus fractional area dilation, α, isotherms. The thermoelastic relation, $(\partial\bar{T}/\partial T)|_{T_m}$, is derived from the difference between the tension-area dilation isotherms. When multiplied by the total area dilation of the transition and the temperature, T_m, the thermoelastic relation is a form of the Clausius-Clapeyron equation which provides the latent heat of "melting" for the surface material. From a single isotherm, the elastic area compliance of the vesicle bilayer is determined throughout the transition region. The (temperature) breadth of the transition is inversely proportional to the elastic compliance which is observed to be finite in the DMPC phase transition. (Supported in part by USPHS NIH grant HL16711.)

T-AM-Po32 INTERACTION OF NON-STEROIDAL ANTIINFLAMMATORY DRUGS AND SMALL HYDROPHOBIC MOLECULES WITH MEMBRANES: A DIFFERENTIAL SCANNING CALORIMETRIC STUDY, San-Bao Hwang and T. Y. Shen, Merck Sharp & Dohme Research Laboratories, Rahway, New Jersey 07065

Interaction of non-steroidal antiinflammatory drugs (NSAIDS) including indomethacin, diflunisal, flurbiprofen, and the active sulfide metabolite of sulindac with phosphatidylcholine (PC) liposomes was investigated using differential scanning calorimetry (DSC). These biologically active structures decreased the phase transition temperature and also broadened the transition peak without affecting the enthalpy change for the transition on the thermal scan. However, comparison with the effects of the prodrug, sulindac and its inactive sulfone metabolite, suggests that the main action of the NSAIDS on membranes could be the reduction in the degree of cooperative interaction between phospholipid molecules. The likely positions of these active drugs in the bilayer were inferred by comparison with DSC effects of several hydrophobic reference compounds whose binding to the PC bilayer have been described. The active antiinflammatory molecules appeared to insert deeply into the hydrocarbon region of the bilayer and significantly broadened the transition peak of the PC multilamellar dispersions with increasing concentration. In contrast, the DSC effects of inactive compounds are very similar to those induced by reference compounds binding to the carbonyl region. Using purple membrane as the model system to study the drug effects on protein-protein interaction in membrane systems, only active NSAIDS were found to dissociate effectively the bacteriorhodopsin lattice. These results suggest that the active NSAIDS studied here are able to partition deeply into the hydrocarbon region of the bilayer and interact with membrane protein imbedded inside the bilayer. The inactive compounds appeared to imbed only into boundary region of the bilayer.

T-AM-Po33 LECITHIN BILAYERS: A THEORETICAL MODEL WHICH DESCRIBES THE MAIN AND LOWER TRANSITIONS. H.L. Scott, Jr., Physics Department, Oklahoma State University, Stillwater, OK 74078

I present a theoretical model which describes both the main and the lower phase transitions in phosphatidylcholine bilayers. In this model the conformational states of the molecules are characterized by the shadow they cast on the bilayer plane. Various conformations cast shadows of different sizes, and these are modeled as rods of varying lengths with semicircular caps. Statistical weights for the various conformations and the actual rod dimensions are selected in accordance with an earlier theory (Biophys. J. 28, 117, 1979) leaving two free parameters: the cap diameter for the rods and the van der Waals interaction strength. When the hard rod shadows are treated using Scaled Particle Theory, two first order phase transitions occur. One transition involves a melting of the hydrocarbon region and is associated with the main lipid bilayer phase transition. The second transition is weaker in enthalpy change, and involves a nematic to isotropic change in orientations for the rods. For a phospholipid bilayer, this is interpreted as an onset of molecular rotation about the long axis parallel to the hydrocarbon chains (which are still almost entirely in all-trans conformations). This transition is associated with the lower phase transition in bilayers, and the temperature at which it occurs is very sensitive to the cap diameter chosen for the rods. The model will be described in detail and compared with existing experimental data for both transitions, and other theoretical models for the lower transition.

T-AM-Po34 STATISTICAL MECHANICAL MODEL OF MEMBRANES. R. J. Pace and S. I. Chan. (Intr. by John J. Hopfield) Caltech, Pasadena, CA 91125.

A statistical mechanical model of bilayer membranes is developed, based on the two dimensional Ising ferromagnet formalism. Definite average geometries are proposed for the acyl chains in the gel and liquid crystalline states, allowing separation of the chain order parameter contributions arising from intramolecular and bulk motions. The model contains no freely disposable parameters, but the thermodynamic predictions are sensitive to the assumed energy difference (Eg) between gauche and trans states in the acyl chain. Best overall agreement (± ~ 10%) with experimental transition data for C_{12}-C_{22} lipids requires Eg = 2.57 kJ/mol, compared with a reported value of 2.55 ± 0.3 kJ/mol from gas phase conformation studies on alkanes.[1] Molecular order fluctuations deduced from the model are consistent with the results for rigid spin probes in bilayers. The model provides a simple rationalization of the apparent failure of lecithins with chain lengths less than 12 carbons to form stable bilayers. (Supported by USPHS NIH Grant GM22432.)

[1]L. Bartell, D. Kohl, J. Chem. Phys., 39, 3097-3105 (1963).

T-AM-Po35 MEASUREMENT OF THE SURFACE VISCOSITY OF LIPID BILAYERS BY A MECHANICAL TECHNIQUE.
Richard E. Waugh. U. of Rochester Med. Cntr., Rochester, N.Y. 14642.

A mechanical technique has been developed to measure the surface viscosity of a lipid bilayer. Large multilamellar vesicles are formed by adding distilled water to egg phosphatidyl choline dried onto a glass surface. The vesicle suspension is drawn into a large tube (0.5 mm ID) under the microscope. A tether (strand of membrane) is formed by sticking the vesicle to a micropipette at the center of the tube and exerting a fluid drag on the vesicle. The force on the vesicle is proportional to the velocity of the fluid in the tube. The fluid velocity is controlled by adjusting the height of a reservoir. The rate of tether growth is measured as a function of the fluid velocity. Analysis of tether formation (Waugh, 1980, Fed. Proc. 39(6):1834) provides a relationship between the surface viscosity, the rate of tether growth, the force on the vesicle and the force when the tether growth rate is zero. Using this relationship the surface viscosity can be calculated from the data. Because of the multilamellar character of the vesicles, the measured value of the viscosity is expected to vary from vesicle to vesicle depending on the number of layers incorporated into the tether. The smallest measured values provide an upper bound for the viscosity of a single bilayer. Based on the measurements available at this time, the viscosity of a single bilayer appears to fall in the range 0.5 - 1.5 x 10^{-5} dyn sec/cm (surface poise).

T-AM-Po36 PHASE BEHAVIOR OF MIXED BILAYERS CONTAINING SYNTHETIC PHOSPHATIDYLCHOLINE AND SPHINGOMYELIN. B.R. Lentz, M. Hoechli, and Y. Barenholz*. Departments of Biochemistry and Anatomy, University of North Carolina , Chapel Hill, N.C. 27514.

The phase behavior of mixtures of N-palmitoyl sphingosine with dimyristoylphosphatidylcholine has been monitored using the fluorescent membrane probe 1,6-diphenyl-1,3,5-hexatriene (DPH). From these data, we have constructed temperature-composition diagrams which summarize the phase behavior of both small unilamellar vesicles and large multilamellar vesicles composed of these two similar phospholipids. In addition, we have used freeze-fracture electron microscopy to investigate the morphology of multilamellar vesicle membranes frozen from different temperature-composition regions of the diagram. Single or mixed morphologies confirmed the presence of single and two-phase regions in the phase diagram. Significant conclusions are 1) that phosphatidylcholine and sphingomyelin species with similar acyl chains were miscible in the liquid crystalline phase; 2) that the sphingomyelin species demonstrated a gel phase with morphology very similar to the P_{β}' phase of phosphatidylcholine; and 3) that despite the similarity of these two lipids and their similar gel phase freeze-fracture morphologies, their demonstrated gel phase immiscibility suggests that their detailed close-packing arrangements may be considerably different.

Supported by National Science Foundation Grants PCM7523245 and PCM7922733. This work was done in part during the tenure of an Established Investigator Award to BRL from the American Heart Association and with funds contributed in part by the North Carolina Heart Association.

T-AM-Po37 A MULTIPLE EQUILIBRIUM BINDING TREATMENT MODIFIED FOR LIPID-PROTEIN ASSOCIATIONS IN MEMBRANES. P.C. Jost, O.H. Griffith, and J.R. Brotherus, Institute of Molecular Biology and Department of Chemistry, University of Oregon, Eugene, Oregon 97403 and Department of Medical Chemistry, University of Helsinki, Helsinki 17, Finland.

Biological membranes contain a diversity of phospholipids. Proteins embedded in the two-dimensional lipid matrix are in direct contact with these lipids, and lipids at hydrophobic protein boundary are in equilibrium with the bulk phospholipid bilayer. Any influence of lipid composition on protein function is most likely to occur at the lipid-protein interface. In order to characterize any specific sites in the presence of the non-specific lipid-protein contacts, a modification of the classical treatment of equilibrium binding to multiple non-interacting sites has been developed. The starting point is the exchange equilibrium of two types of lipids, solvent (L) and solute (L^*), competing for a hydrophobic site (B_i) on the surface of the membrane protein, i.e., $B_iL + L \rightleftarrows B_iL^* + L$, where the relative binding constant of the solute is defined by $K_i = [B_iL^*][L]/[B_iL][L^*]$. This is then generalized to N binding or contact sites per protein. The concentrated nature of the membrane solution and the choice of experimentally accessible variables lead to equations that differ from the classical dilute solution expressions. One useful linear approximation at low solute to protein ratios is $y = (x/NK_{av}) - (1/K_{av})$, where x is the total solvent lipid per protein, y is the ratio of integrated intensities of bilayer and bound ESR spectra components for the spin-labeled solute lipid, and K_{av} is the average of all individual binding constants. The specific cases of one and two classes of binding sites are treated explicitly and computer generated plots are included to illustrate some specific cases and serve as a basis for experimental design. Within experimental error preliminary experimental binding curves fit the linear approximation. (Supported by NIH GM 25698)

T-AM-Po38 EVIDENCE FOR A PREFERENTIAL BOUNDARY LIPID IN MELITTIN:DMPC-d_0:DMPC-d_{54} LIPOSOMES BY RAMAN SPECTROSCOPY. F. Lavialle, G. J. Bryant and I. W. Levin, Lab. of Chem. Phys., National Institutes of Health, Bethesda, Md. 20205.

Temperature profiles determined from Raman spectroscopic parameters for bilayer systems containing melittin, a polypeptide consisting of 26 amino acid residues, exhibit 2 order-disorder processes.[1] These transitions are associated with the depression of the main lipid phase transition and the melting behavior of the immobilized lipid surrounding the hydrophobic segment of the peptide, respectively. In order both to confirm and to characterize further the properties of boundary lipids, the interactions of melittin with liposomes composed of pure DMPC-d_{54} (1,2-dimyristoyl-sn-glycerol-3-phosphorylcholine-d_{54}) and of a 1:1 mole ratio mixture of DMPC-d_{54}:DMPC-d_0 were investigated by Raman spectroscopy. For the isotopically mixed multilamellar assembly containing melittin, the methylene C-D stretching mode line-width parameters yield 2 order-disorder transitions at ∿12° and ∿27°C; while the methylene C-H stretching mode intensity parameters display a single transition at ∿21°C. Since the main transition for a 1:1 mixture of the normal and isotopic lipids without melittin occurs at 19°C, these data suggest that at least three classes of bilayer lipid exist in the melittin:DMPC-d_0:DMPC-d_{54} lipid-protein system and that DMPC-d_{54} preferentially forms a boundary interface about melittin.

[1] F. Lavialle, I. W. Levin and C. Mollay, Biochim. Biophys. Acta 600 (1980) 62-71.

T-AM-Po39 BILAYER ACYL CHAIN DYNAMICS AND LIPID PROTEIN INTERACTIONS. Bruce Hudson, Paul Wolber and Anthony Ruggiero, (Intro. by Roderick A. Capaldi). Department of Chemistry and Institute of Molecular Biology, University of Oregon, Eugene, OR 97403.

The angular motion of the acyl chains of fluid phase DPPC and DMPC bilayers has been determined by measuring the fluorescence polarization anisotropy of parinaric acid and parinaroyl labeled phospholipids. Synchrotron radiation or the ultraviolet pulses of a cavity dumped synchronously pumped dye laser were used to obtain subnanosecond time resolution. The anisotropy shows that acyl chain reorientation is very rapid but is restricted. The order parameter obtained from the asymptotic anisotropy is in agreement with deuterium NMR results. The temperature dependence of the order parameter and the acyl chain wobbling diffusion coefficient will be discussed. Studies using a parinaroyl chain analog with a shorter methylene chain can distinguish rapid gauche isomerization from rapid rigid body motion. Incorporation of the 50 AA coat protein of the filamentous M13 bacteriophage results in restriction of the range of angular motion of the labeled chains and in reduction of the rate of the chain motion. Energy transfer experiments demonstrate that the chromophore labeled chains are randomly distributed with respect to the coat protein. The order parameter obtained from the samples with coat protein is higher than that in the pure lipid. The corresponding deuterium NMR experiment shows a decreased order parameter. The difference between these two results indicates that, in contrast to the case for the pure lipid, there are important relaxation processes with time constants in the 10^{-7} to 10^{-6} sec time range.

T-AM-Po40 SPIN-LABELING DETERMINATION OF THE SELECTIVITY OF LIPID BINDING TO THE (Na,K)-ADENOSINETRIPHOSPHATASE. J.R. Silvius, J.R. Brotherus, P.C. Jost, L.E. Hokin, and O.H. Griffith, Institute of Molecular Biology, University of Oregon, Eugene, Oregon and Department of Pharmacology, University of Wisconsin, Madison, Wisconsin.

The (Na,K)-adenosinetriphosphatase (ATPase) from the dogfish rectal gland has been reconstituted with a pure synthetic phosphatidylcholine (PC) to give ATPase/PC recombinants free of detergents and of the phospholipids normally associated with the enzyme. Spin-labeled phosphatidylcholine, anionic spin labels such as phosphatidylserine, and single-tailed amphiphilic spin labels of varying charge have been introduced into reconstituted preparations of varying lipid/protein ratio, and the fraction of label that is motionally restricted on the electron spin resonance time scale by the protein has been determined in each case by quantitative spectral analysis. The results have been analyzed using a mathematical treatment appropriate for the analysis of the interaction of one type of lipid, the "solute" species, with a membrane protein in competition with a large molar excess of a second type of lipid, the "solvent" lipid. Our results indicate that the ATPase interacts with the various labels at a common set of sites but exhibits a preference for interaction with anionic lipids at what is probably a small subset of these sites. The detected preferential association of this enzyme with anionic lipid species at a portion of its total lipid-contact sites may be related to the known stimulation of its activity by such lipids in both the native membrane environment and reconstituted systems. (Supported by NIH Grant GM 25698 and by a postdoctoral fellowship award to J.R.S.)

T-AM-Po41 LIPID-PROTEIN INTERACTIONS IN PHOTOSYNTHETIC MEMBRANES AND TRANSBILAYER MOVEMENT OF CHLOROPHYLL SPIN LABELS. G.B. Birrell, S.A. Boyd, J.F.W. Keana, and O.H. Griffith, Institute of Molecular Biology and Department of Chemistry, University of Oregon, Eugene, Oregon 97403

The primary events of photosynthesis occur in a specialized membrane containing the photopigments, lipids, and proteins. Two lines of investigation are being pursued to provide information about the structure and dynamics of these photosynthetic membranes. In one study, lipid spin labels with different polar head groups have been incorporated into chromatophores isolated from the photosynthetic bacterium Rhodopseudomonas sphaeroides. The proteins present in the chromatophore membranes have been shown to bind negatively charged labels to a much greater extent than positively charged labels. The amount of bound spin label varies directly with the bacteriochlorophyll content of the chromatophores, suggesting that a significant fraction of the lipid spin labels is bound to the hydrophobic surfaces of the chlorophyll-binding proteins. The changes in bound lipid with bacteriochlorophyll content and lipid head group suggest that the light harvesting bacteriochlorophyll-binding proteins preferentially associate with negatively charged lipids.

In a second approach, derivatives of chlorophyll have been synthesized to study the rate at which chlorophyll can diffuse from one side of a bilayer to the other, a possible step in the assembly of photosynthetic units. The spin labeled chlorophyll derivative flip-flops rapidly in egg PC vesicles at 0 °C ($\tau_{1/2} \sim$ 1-4 min). This is orders of magnitude more rapid than phospholipid flip-flop under these conditions, but detectably slower than the flip-flop of a model compound, TEMPO palmitate, which lacks the large chlorin head group. Presence or absence of the magnesium does not significantly effect the flip-flop rate.

T-AM-Po42 RELATIONSHIP BETWEEN THE ACTIVITY OF PANCREATIC PHOSPHOLIPASE A_2 AND THE PHYSICAL STATE OF THE PHOSPHOLIPID SUBSTRATE. Moshe Menashe, Dov Lichtenberg, Carlos Gutierrez Merino and Rodney L. Biltonen, Dept. of Biochem., University of Virginia, Charlottesville, Va. 22908 and Dept. of Pharmacology, Hebrew University Hadassah Medical School, Jerusalem, Israel.

When pancreatic phospholipase A_2 is mixed with small unilamellar vesicles made from dipalmitoyl phosphatidylcholine at or above the phase transition temperature (t_m), the time course of hydrolysis exhibits a distinct lag period. On the other hand, if the enzyme is preincubated with substrate for a short period of time below the transition temperature (during which time only limited hydrolysis occurs) and then assayed at high temperature, no lag period is observed. This phenomenon does not appear to be the result of product formation. Moreover, it appears to be unique to small unilamellar vesicles, since in larger unilamellar vesicles ($\simeq$ 900 Å diameter), the high temperature hydrolysis is not affected by preincubation below t_m. These findings lend substantial support to the hypothesis that a relatively slow substrate-enzyme organizational step is required as part of an activation process. This step is most rapid when packing irregularities exist in the membrane, such as those in the gel phase of highly curved membranes. Furthermore, the intrinsic activity (after the initial step of activation) is maximal when the substrate is in the liquid-crystalline state. (Supported by NSF grant PCM80-03645).

T-AM-Po43 QUENCHING OF APOLIPOPROTEIN A-I FLUORESCENCE BY OXYGEN IN SOLUTION AND IN LIPID-PROTEIN COMPLEXES. W.W. Mantulin and H.J. Pownall, Department of Medicine, Baylor College of Medicine and The Methodist Hospital, Houston, Texas 77030 and D.M. Jameson, Department of Biochemistry, University of Illinois, Urbana, Illinois 61801.

Apolipoprotein A-I (apoA-I) is the major protein component of human plasma high density lipoprotein. The isolated, lipid-free protein is soluble, but has a tendency to self-associate in solution. ApoA-I will also form lipoprotein recombinants with phospholipid. We have examined the effects of self-association and complex formation with dimyristoylphosphatidylcholine (DMPC) on the efficiency of apoA-I (tryptophan) fluorescence quenching by oxygen. Dynamic, diffusion controlled, quenching of fluorescence is described by the Stern-Volmer Equation $F_o/F = 1 + k^*\tau_o [Q] = \tau_o/\tau$ where F and F_o and τ and τ_o are the fluorescence intensities and lifetimes in the presence and absence, respectively, of the dissolved quencher [Q] oxygen. k^* is the bimolecular quenching constant. The unquenched fluorescence lifetime of apoA-I (by the phase shift technique, 30 MH_z) is 3.68 nsec. At 0.2 and 0.02 mg/ml of apoA-I $k^* = 2.3 \times 10^9\ M^{-1}\ sec^{-1}$ (25°C). In association with DMPC $k^* = 6.8 \times 10^9\ M^{-1}\ sec^{-1}$. There is no significant deviation from linearity in these plots. From this data we conclude that 1) self-association of apoA-I does not impede the diffusion of oxygen to tryptophan residues buried in interior regions of the protein and 2) association of apoA-I with DMPC either increases exposure of tryptophan residues to oxygen or,perhaps, increases the localized concentration of oxygen in hydrophobic regions of the protein.

T-AM-Po44 STRUCTURE OF HUMAN SERUM HIGH DENSITY LIPOPROTEINS: AN ESR STUDY OF LIPID-PROTEIN INTERACTIONS IN HUMAN HDL_3. D.A. McMillen, P.C. Jost, and A.M. Scanu, Institute of Molecular Biology, University of Oregon, Eugene, Oregon 97403 and Departments of Medicine and Biochemistry, University of Chicago Pritzker School of Medicine, Chicago, Illinois 60637.

Fundamental to understanding the role of human serum lipoproteins in the metabolism and transport of lipids is understanding the structure of the lipoproteins. Spin labels (single chain amphiphiles of varying head group charge, zwitterionic phospholipids and cholesterol analogs) were incorporated into native human HDL_3. On the ESR time-scale all of the lipid labels indicated the presence of at least two lipid domains. Similar composite spectra have been obtained in other biological systems, and there is strong evidence to indicate that the motion-restricted component represents lipid interacting with protein. The fluid spectral component closely resembles spectra of the lipid labels in vesicles formed from lipids extracted from HDL_3 and separated from the core apolar lipids. Quantitative spectral analysis estimates that ~75% of the polar lipid in the human HDL_3 interacts with protein as detected by lipid labels with the nitroxide moiety at the C-14 position of the acyl chains. Changing the head group charge of the lipid labels does not change the observed lipid-protein interactions, unlike the role charge plays in shifting the apparent lipid binding affinities with some membrane proteins. There is also evidence that the lipid head groups contact some stretches of each of the lipoprotein peptides. This was determined by introducing lipids with head groups substituted with the photo-reactive nitroarylazido moiety into the native HDL_3, followed by photolysis. These data are consistent with a model of the serum lipoproteins that allows for some lipid-lipid contacts, lipid head group-protein contacts, and hydrophobic interaction of the lipids with protein. (Supported by PHS grants GM-25698 and HL-18577.)

T-AM-Po45 STATIC AND TIME RESOLVED FLUORESCENCE STUDIES ON HIGH DENSITY LIPOPROTEINS: IMPLICATIONS FOR STRUCTURE. R. D. Ludescher and B. S. Hudson, Department of Chemistry, University of Oregon, Eugene, OR 97403.

Shen, Scanu and Kezdy (PNAS 74(3), 847) have proposed a model for human serum lipoproteins with the following features: an oil drop core of non-polar lipids, a surface monolayer of polar lipids, and a surface layer of protein closely packed with the lipid headgroups. We have begun fluorescence studies of the human high density lipoproteins (HDL) employing the fluorescent fatty acid, parinaric acid. Forster energy transfer is possible from tryptophan to PNA. Analysis of PNA quenching of HDL tryptophan fluorescence using the method of Wolber and Hudson (Biophys. J. 28, 197) is consistent with a random distribution of the tryptophan residues. There are two isomers of parinaric acid; cis PNA (cis, trans, trans, cis) and trans PNS (all trans). Measurements of the static anisotropy ($\bar{r}$) of these probes in HDL indicate a fairly rigid environment: at 37°C $\bar{r}$ is 0.29 for trans PNA and 0.22 for cis PNA. The comparable numbers in EPC:cholesterol vesicles of mole ratio 4:1 (with a lipid composition similar to HDL) are 0.15 and 0.09. We conclude that the polar lipid environment in HDL is constrained. We have also measured the time resolved anisotropy decay of these two probes in EPC vesicles and HDL particles. In vesicles the anisotropy decays rapidly (5 nsec) to an asymptotic value. In HDL the initial anisotropy decay is slower (>10 nsec) and decays to zero due to the rotation of the entire particle. Calculation of the rotational correlation time for the particle from experimental data give values between 50 and 90 nsec at room temperature, numbers in reasonable agreement with 65 nsec, the calculated value for a sphere of HDL radius (40 Å).

T-AM-Po46 LIPOPROTEIN THERMODYNAMICS: THE FREE ENERGY OF ASSOCIATION OF REDUCED AND CARBOXYMETHYLATED APOLIPOPROTEIN A-II(RCM-A-II) WITH PHOSPHOLIPIDS AND LIPOPROTEINS. D.L. Hickson, A.M.Gotto,Jr., and H.J. Pownall. Baylor College of Medicine and The Methodist Hospital, Houston, Texas 77030.

Apolipoprotein A-II is an apoprotein which in human plasma high density lipoproteins(HDL) exists as a disulfide-linked dimer of 17,400 molecular weight. It is known to spontaneously bind phospholipids with an affinity that has so far eluded measurement. We have prepared and isolated ^{3}H-RCM-A-II (MW=8,700) and measured its free energy of association,ΔG_a, by equilibrium methods. The ΔG_a were measured for dimyristoyl phosphatidylcholine (DMPC) multilayers (-7.1±0.4 kcal) and single bilayer vesicles(-8.0±0.2 kcal), bovine brain sphingomyelin vesicles(-7.2±0.4 kcal), brominated egg lecithin in the absence (-8.7±0.4 kcal) and presence of 33 mol % cholesterol (-7.9±0.4 kcal) and human plasma HDL (-7.3±0.5 kcal). With DMPC in 0.3 M guanidine HCl, ΔG_a decreased to -6.1±0.3 kcal. The free energy of association was insensitive to temperature even close to T_c where a large enthalpy of association has been observed by microcalorimetry. These results represent the first quantitative measurement of the affinity of an apolipoprotein for a lipid or lipoprotein; the measured values are much less than the values based upon the sum of the free energy of transfer of the component amino acid side chains. These results suggest that the free energy of association of RCM-A-II with lipids and lipoproteins is entropy driven largely due to the hydrophobic effect; that the enthalpy of association is compensated by an additional entropy term; that the hydrophobic amino acid residues of RCM-A-II associate with a region of the lipid or lipoprotein that is much more polar than the interior of a lipid bilayer. This region must include the bilayer surface and the first 4 or 5 methylene units..

T-AM-Po47 KINETICS OF PENETRATION OF PLASMA APOLIPOPROTEINS INTO PHOSPHOLIPID BILAYERS. H.J. Pownall, D.L. Hickson, Q. Pao, J.T. Sparrow, A.M.Gotto,Jr., W.W. Mantulin and J.B. Massey. Baylor College of Medicine and The Methodist Hospital, Houston, Texas 77030.

We have studied the rate of association of dimyristoylphosphatidylcholine (DMPC) with a series of lipid-associating proteins derived from the human plasma lipoproteins. The variables for this study were temperature with respect to the solid→fluid transition of DMPC (T_c=23.9°), denaturant concentration [guanidinium chloride, 0→2.0 M] and protein size; the proteins used in this study were apoA-I (MW=28,400), apoA-II(MW=17,400), reduced and carboxymethylated apoA-II (MW=8,700), apoC-III(MW=8,800) and LAP-20, a lipid associating peptide of 20 residues which had been modeled after the native apolipoproteins (MW=2,600). We found that the rate of association increased as the molecular weight decreased ($K_{1/2}$=2 and 100 min^{-1} for apoA-I and LAP-20,respectively), that the unfolded proteins associate with DMPC faster than folded proteins which do not have as many exposed hydrophobic residues, and that the rate is always fastest at T_c. These results are consistent with the Kanehisa-Tsong cluster model of phospholipid phase transitions. Our data provide the first convincing evidence of the validity of that model in a homologous series of polypeptides whose rate of association with lipid is a direct function of the permeability of the lipid matrix. Our data suggest that the exposure of additional hydrophobic residues may provide additional sites that may penetrate the lipid matrix after which rapid insertion of the remainder of the hydrophobic residues into the lipid bilayer occurs.

T-AM-Po48 INCORPORATION OF PHOTOACTIVABLE AND FLUORESCENT-LABELED PHOSPHOLIPIDS INTO LOW DENSITY LIPOPROTEIN. Kala V. Shaw*, Michael J. Iwanik*, Jerome E. Laux* and J. Michael Shaw. Virginia Commonwealth University, Medical College of Virginia, Richmond, Virginia 23298

Isolated human low density lipoprotein (LDL) has been modified by insertion or fusion of photoactivable derivatives of phosphatidylethanolamine (PE), [^{3}H] 1,2-diacylglycero-3-(N-4-Azido-2-nitrophenylaminoethyl) phosphate or [^{3}H] 1,2-diacylglycero-3-(N-4-azidophenylamidinoethyl) phosphate, and fluorescent-labeled PE (1,2-diacylglycero-3-(N-4-nitrophenyl-2-oxa-1,3-diazole). A lipid exchange approach utilizing a monolayer device in conjunction with a nonspecific phospholipid exchange protein or 'fusion' of photoactivable or fluorescent-labeled phospholipid vesicles were techniques for introduction of the PE-derivatives into the LDL particle. The modified LDL's were stable at levels of PE-derivative representing about 5-15% of the total phospholipid of LDL. The physical properties of the photoactivable modified-LDL have been monitored by hindered-rotation measurements of a lipid soluble fluorescent reporter molecule and differential scanning calorimetric analysis. The modified LDL's, when incubated in the dark with cultured skin fibroblasts at 4°, were bound to cell surface sites and released by heparin. In addition, the modified-LDL's competed with native LDL for binding to adrenal cortex membrane preparations. (Supported by an American Heart Association Grant-in-Aid (79-882) and Virginia Heart Affiliate.)

T-AM-Po49 ROLE OF SYNEXIN IN MEMBRANE FUSION: ENHANCEMENT OF CALCIUM-DEPENDENT FUSION OF PHOSPHOLIPID VESICLES. K. Hong, N. Düzgüneş, D. Papahadjopoulos. Cancer Research Institute, University of California, San Francisco, CA 94143.

Synexin, a soluble adrenal medullary and liver protein which causes calcium-dependent aggregation of isolated chromaffin granules, was isolated and purified according to published procedures. A new assay for monitoring membrane fusion by following the mixing of aqueous contents of phospholipid vesicles was used to examine the effect of synexin on the kinetics of membrane fusion. The results of fusion studies on large unilamellar vesicles of phosphatidylserine, and a mixture of phosphatidylserine with phosphatidylethanolamine, indicate synexin lowers the threshold of Ca^{2+} concentration required for fusion. In addition, synexin also increases drastically the initial rate of fusion. The initial rate of fusion increases with the quantity of synexin present in the reaction mixture. With a concentration of synexin at 20 to 40 μg/ml (in 50 μM phospholipid) the rate of fusion increases by two orders of magnitude compared to phospholipid vesicles alone at the threshold concentration of Ca^{2+}. Magnesium does not activate synexin in fusion. For several other vesicles containing acidic phospholipids, synexin enhances aggregation in the presence of Ca^{2+}, without promoting fusion. It is, therefore suggested that synexin may play a role in exocytosis by promoting fusion of membranes containing specific phospholipids in the presence of Ca^{2+}.

This work was supported in part by Grants GM-26369 and GM-28117 from the National Institutes of Health.

T-AM-Po50 EFFECTS OF PROTEINS ON PHOSPHOLIPID VESICLE AGGREGATION AND LIPID VESICLE-MONOLAYER INTERACTIONS. S. Ohki & K.S. Leonards, Dept. of Biophysics, SUNY at Buffalo, Buffalo, NY 14214.

Effects of proteins on divalent cation-induced phospholipid vesicle aggregation and phospholipid vesicle-monolayer membrane interaction (fusion) were examined. Glycophorin (from human erythrocytes) suppressed the above membrane interactions more than N-2 protein (from human brain myelin) when these proteins were incorporated in acidic phospholipid vesicle membranes. The threshold concentrations of divalent cations to cause vesicle aggregation were increased by the protein incorporation and the rate of vesicle aggregation was reduced. When these proteins were incorporated in the acidic phospholipid monolayers, however, the interaction (fusion) of lipid vesicle-monolayer membranes induced by divalent cation was not altered appreciably by the presence of the proteins. On the other hand, Synexin in the solution did enhance the Ca^{2+}-induced aggregation of acidic phospholipid vesicles, but seemed not to affect the Ca^{2+}-induced fusion between acidic phospholipid vesicles and vesicle-monolayer membranes.

(Supported by the NIH Grant GM-24840).

T-AM-Po51 REPLACEMENT OF THE PRIMARY UBIQUINONE OF PHOTOSYNTHETIC REACTION CENTERS WITH OTHER QUINONES. M.R. Gunner, R.C. Prince, P.L. Dutton, U. of Penn., Phila., Pa.19104.

There is one tightly bound ubiquinone-10, UQ, associated with the reaction center protein of Rps. sphaeroides. In the isolated protein the UQ accepts an electron from a light activated bacteriochlorophyll dimer, $(BChl)_2$, via a bacteriopheophytin, BPh. The UQ^- thus formed can in turn reduce the light generated $(BChl)_2^+$. We are studying the effect of replacing the UQ with quinones of varying size, shape, substituent, and E_m to characterize (a) the structure and specificity of the quinone binding site and (b) the kinetic and thermodynamic parameters of the reactions involving the quinone. We have found that benzo-, naphtho- and anthraquinones all function as electron acceptor from BPh and donor to $(BChl)_2^+$. Benzoquinones with less than three substituents and benzanthraquinone reconstitute poorly, and this may define the size requirement for the quinone to fit the binding site. Alkyl, thiol, halogen, amino and sulfonate substituted quinones can reconstitute full activity. In contrast, o-hydroxy and nitro substituted quinones work poorly. K_D's have been measured eg. benzoquinone 9 μM, duroquinone 0.1 μM, naphthoquinone 5 μM, anthraquinone 20 nM. The E_m values for the Q/Q^- couple in DMF have been measured and correlate well with the kinetics of the quinone-involved reactions. The reaction of UQ_1^- reducing $(BChl)_2^+$ is a temperature independent tunneling reaction with a rate of 10 s^{-1}. With quinones of E_m lower than UQ this rate increases ten fold per 60 mV decrease in E_m in a thermally activated reaction which we propose involves the back reaction via BPh. The rates for quinones with E_m up to 500 mV higher than UQ lie between 0.3 and 10 s^{-1}, probably measuring electron transfer direct to $(BChl)_2^+$. Systematic failures in quinone reduction are seen at very low and high E_m. These may be explained by a decrease in the rate of electron transfer from BPh to the quinone as predicted by Levich-Marcus electron transfer theory. DOE DE AC02-80-ER10590.

T-AM-Po52 PHYSICAL AND CHEMICAL PROPERTIES OF IRON-SULFUR CENTERS IN THE HALOPHILIC ALGA, DUNALIELLA PARVA Robert Hootkins and Alan Bearden, Department of Biophysics and Medical Physics, University of California, Berkeley, California 94720

Studies with the halophilic alga, D. parva, have proven useful in the examination of bound iron-sulfur centers A and B associated with photosystem I of the photosynthetic "Z-scheme". Four lines of evidence suggest structural differences between these centers and those of spinach photosystem I. First, in membrane fragments from D. parva, it is possible to photoreduce both centers A and B at cryogenic temperatures in non-chemically poised samples. EPR examination at 10K reveals six g-values: 2.072, 2.053, 1.940, 1.925, 1.876, and 1.844. Second, midpoint potentials determined from the oxidation-reduction titration data fit with n=2 Nernst curves yield values of -543mV and -518mV (± 10mV) for centers A and B, respectively. In contrast to spinach preparations, center B is chemically reduced prior to center A in this system and, therefore, permits the assignment of g-values to center B in the absence of center A. Third, an unusual temperature dependence of the EPR signal intensity is observed and suggests unusual relaxation properties for these centers. Fourth, orientation of the magnetic axes of centers A and B, the "Rieske" center, and X has been studied in addition to other, unassigned g-values. These results illustrate both similarities and differences with the orientation data obtained on spinach preparations (1). These data are presented to offer contrast to the experiments performed on other photosynthetic systems.

1. Prince, R., Crowder, M., and Bearden, A.,(1980) Biochim. Biophys. Acta. 592, 323-337
(Research supported by NSF(PCM-78-22245) and DOE through Lawrence Berkeley Laboratory. R.H. acknowledges support by an Associated Western Universities Graduate Fellowship.)

T-AM-Po53 THE EFFECT OF VERY LARGE MAGNETIC FIELDS ON THE TRIPLET YIELD IN PHOTOSYNTHETIC REACTION CENTERS. S.G. Boxer*, C.E.D.Chidsey* and M.G. Roelofs*, Dept. of Chemistry, Stanford University, Stanford, Ca 94305

The triplet yield has been measured in dithionite reduced RC's from R.spheroides, R-26, in the presence of a large magnetic field (0 to 50 kG). In contrast to a reduction in the triplet yield at low field (0 to 500 G), the yield increases as the field is raised further, exceeding its value at zero field. At very high field and low temperatures, the yield levels off, becoming independent of field strength. These measurements have been made both with steady-state and time-resolved detection of the triplet population. This observation is interpreted as direct evidence for a radical pair precursor to the triplet and a g-factor difference in this radical pair ($P^+ I^-$). The density operator for the system is found from the stochastic Liouville differential equation and spin Hamiltonian, including the electron Zeeman, hyperfine, and electron-exchange interactions. The triplet yield is obtained from the density operator, and an analytical solution is derived at high field. This expression is used to calculate a value of $|\Delta g| = 0.0010$ from the data at 200°K. This value is consistent with the assignment of bacteriopheophytin as the primary acceptor (I) in these reaction centers. The temperature dependence of the high field modulation of the triplet yield and its dependence on the state of the quinone (Q^- vs $Q^=$) have been studied to measure the barriers to charge recombination and magnetic field independent (incoherent) mechanisms for singlet to triplet conversion. (Supported by USDA 5901-0410-8-147-0)

T-AM-Po54 SPECTROSCOPIC STUDIES OF SYNTHETIC CHLOROPHYLL-PROTEIN COMPLEXES. S.G.Boxer* and K.A. Wright*, Dept. of Chemistry, Stanford University, Stanford, Ca 94305.

Chlorophyllides a,b, and d and bacteriochlorophyllide a have been inserted in the heme pocket of apomyoglobin. These complexes provide the first well defined 1:1 complexes between the chlorophyll chromophores and a protein. The electronic absorption, CD, MCD, triplet state esr and high-field nmr spectra of these complexes in solution are compared. Striking CD effects are observed and the zero-field splittings in the triplet states increase by approximately 10%, when the chromophore is in the protein. The chemical shifts of the ring-current shifted valine-E11 resonances in the series porphyrin, chlorin, bacteriochlorin suggest the absolute orientation of the chromophore. Doubling of nmr peaks in some complexes is shown to arise from dynamic rather than static disorder, suggesting prosthetic group dependent population of conformational substates of the protein. Orthorhombic single crystals of high quality have been prepared. These have space group $P_{21,21,21}$ and unit cell parameters nearly identical to native myoglobin (collaboration Dr. B.Katz, UCSD). The red absorption maximum of single crystals of chlorophylide a-apoMb is red shifted relative to a solution of the same protein. Comparision of a number of chromophores suggests that distortion of rings IV and/or V may be responsible for the shift. Chlorophyllide a covalently connected to imidazole and a high-potential quinone (see Boxer, Bucks, Chidsey poster) have also been inserted into apo-Mb. (Supported by NSF PCM-7926677 and USDA 5901-0410-8-147-0)

T-AM-Po55 SYNTHETIC MODELS FOR THE PHOTOSYNTHETIC REACTION CENTER, S.G. Boxer*, R.R. Bucks and C.E.D. Chidsey*, Dept. of Chemistry, Stanford University, Stanford, Ca 94305

The doubly linked, relatively rigid cofacial dimer of pyrochlorophyllide a shown below has been prepared by cross-linking opposite edges of the macrocycles. The spectroscopic properties of this dimer are compared with the flexible hinged dimer reported earlier by Wasielewski et al. [J.Am.Chem.Soc.,100,1501(1978)] and with the original singly linked chlorophyll dimer [Boxer & Closs, J.Am.Chem.Soc,98,5406(1976)]. An intense, split, conservative CD spectrum is obtained for the cofacial dimer, characteristic of exciton interaction; the zero-field splittings in the lowest triplet state and the spin polarization are indistinguishable from those of its monomer; the fluorescence quantum yields and lifetimes for metal free, mono-metal (Mg) and dimetal (2Mg) cofacial dimers are about 10% of the monomers. The high-potential quinone shown below has been covalently attached to the glycol ester of pyrochlorophyllide a [$E_{1/2}$(quinone)= -0.79V vs. SCE]. Electron transfer is energetically forbidden from the triplet state and is favorable by about 0.43eV from the singlet state. The fluorescence quantum yield is reduced by 80% relative to the macrocycle alone. The dianion ($Chl^{\bullet}\sim Q^{\bullet}$) has been prepared electrochemically and studied by esr. (Supported by NSF PCM-7926677 and DOE PG02-80-CS84006)

T-AM-Po56 ON THE MECHANISM OF HYDROGEN-DEUTERIUM EXCHANGE IN BACTERIORHODOPSIN, Ajay Pande, A. G. Doukas, T. Suzuki, R. H. Callender, Physics Dept., City College of New York, N.Y., N.Y. 10031; Barry Honig, Dept. of Physiology and Biophysics, Univ. of Illinois, Urbana, Ill. 61801 and Michael Ottolenghi, Dept. of Physical Chemistry, The Hebrew University, Jerusalem, Israel.

Bacteriorhodopsin (bR), the purple membrane protein of H. halobium, uses light to actively transport protons from the inside to the outside of the cell membrane. The chromophore of bacteriorhodopsin is all-trans retinal bound in the form of a protonated Schiff base to the ε-amino group of one of the lysines in the protein. The Schiff base deprotonates and then reprotonates during the course of the light driven photocycle of bR and it is likely that these events are directly associated with the proton pumping mechanism. An understanding of this mechanism is possible, in principle, by the study of the rate of isotope exchange of the Schiff base proton. We have used the continuous-flow resonance Raman technique to study the hydrogen-deuterium exchange kinetics of light adapted bR over a wide pH range. The exchange is found to be complete in 3 msec, the limit of resolution of our instrument. Given the high pK of the Schiff base within the protein matrix, it is clear that these fast exchange times cannot be accounted for by the standard exchange mechanism involving deprotonation of acidic groups. A mechanism involving a concerted exchange with one or more water molecules in the binding site will be presented.

T-AM-Po57 INVOLVEMENT OF CARBOXYL RESIDUES IN THE PHOTOCYCLE OF BACTERIORHODOPSIN. Jeffrey M. Herz and Lester Packer. Membrane Bioenergetics Group, Lawrence Berkeley Lab and the Department of Physiology/Anatomy, University of California, Berkeley, CA 94720.

Purple membranes from Halobacterium halobium were treated with the carboxyl specific reagents 1-ethyl-3-(3-dimethylaminopropyl) carbodiimide (EDC), a water soluble carbodiimide, and N-ethoxycarbonyl-2-ethoxy-1,2-dihydroquinoline (EEDQ), a hydrophobic compound. After modification, laser flash photolysis and difference spectra revealed: (a) Inhibition of the decay of the M_{412} intermediate, but no effect on the kinetics of M_{412} formation; the presence of a nucleophile (glycine methyl ester) during modification partially prevented the inhibition caused by EDC or EEDQ treatment alone. Photostationary steady state levels of M_{412} revealed large increases that correlated with the degree of inhibition of M_{412} decay; modification of lysine residues (5 of 6) with ethyl acetimidate and subsequent carboxyl modification also decreased the inhibition of M_{412} decay. This suggests that in the absence of a nucleophile, EDC and EEDQ may form an intramolecular cross-link between a carboxyl and lysine residue. (b) Absence of the O_{640} intermediate at pH 7.0. At pH 3.0, where the decay of the 'O' intermediate is stabilized, no positive absorbance at 650 nm was detected, although a small negative signal is still observed. (c) The kinetics of M_{412} decay and reformation of BR_{570} were found to be similar. (d) Difference spectra of acid-titrated unmodified membranes showed an A_{max}=640 nm and a pK=3.5. Carboxyl modified purple membranes could not form this blue species. We conclude that a carboxyl residue(s) is required for formation of the O_{640} intermediate of the photocycle and for the formation of the acid-induced species of bacteriorhodopsin.

Research support by the Department of Energy.

T-AM-Po58 A PROVISIONAL ATOMIC MODEL FOR THE STRUCTURE OF BACTERIORHODOPSIN

S. Khan, S. Anderson, E. Gogol, J. Trewhella, G. Zaccai, and D. Engelman. Dept. of MB&B, Yale University (P.O. Box 6666, New Haven, CT 06511) and Institut Laue-Langevin, Grenoble, France.

A model for bacteriorhodopsin has been built using the amino acid sequence[1] and the projected density map obtained from electron microscopy[2]. The locations and tilts of the seven helical segments were varied and predictions made of electron diffraction structure factors. The residual ($R=\frac{\sum||F_{obs}|-|F_{calc}||}{\sum|F_{obs}|}$) was used as a guide for refinement, and the best model gave R = 0.25.

Using the model as a starting point, neutron diffraction measurements were exploited to find the identity and rotational orientation of each helix. These measurements are based on the placement of deuterated amino acids in the structure by biosynthetic incorporation. Intensity changes were obtained by subtracting the observations for samples with and without deuterated amino acids.

A preferred model with regard to both helix assignment and orientation has been obtained by testing predictions for the observed intensity changes resulting from the deuteration of several amino acids.

(1) Gerber et al. (1979) P.N.A.S. 76, 227-231.
(2) Unwin and Henderson (1975) J. Mol. Biol. 94, 425-440.

T-AM-Po59 BACTERIORHODOPSIN STRUCTURE: RETINAL LOCATION AND HELIX CONNECTIONS PROBED BY FLUORESCENCE ENERGY TRANSFER. Robert Renthal, Div. Earth & Physical Sciences, Univ. of Texas at San Antonio, San Antonio, Texas 78285

Two fluorescent labeling sites on bacteriorhodopsin (BR) have been studied in this laboratory. We previously located a highly specific dansyl chloride reactive site at Lys 40. In addition, we coupled dansyl hydrazine (DH) to BR with water-soluble carbodiimide, and I have now found conditions where the only product of this reaction is located between residues 72-118. This peptide includes helix C and part of helix D, which contain at least 5 possible sites for DH. However, functional studies suggest the labeled site is near the cytoplasmic side of the membrane, favoring Asp 102 or 104. I have used these two dansyl sites as probes to study the retinal chromophore location and the helix connection pattern by fluorescence energy transfer. The fluorescence measurements were done in 0.4% Triton X-100, where BR is exclusively monomeric, to eliminate multiple acceptors. Fluorescence in the absence of acceptor was measured after bleaching the retinal absorbance by briefly lowering the pH to 2.3 and then returning to neutral pH. 1) Dansyl-Lys 40 to retinal. The transfer efficiency is 0.81. The limiting anisotropy is 0.20, which indicates that that R_0 could range from 37 to 67 A. Thus, the minimum distance between Lys 40 and retinal is 29 A. The reported location of retinal at Lys 41 is inconsistant with this result. 2) Dansyl-Asp 102/104 to retinal. The transfer efficiency is greater than 0.9, suggesting significantly closer proximity of Asp 102/104 to retinal than Lys 40. Comparison of these results with the location of retinal found by neutron diffraction (King et al., PNAS 77, 4723, 1980) provides two new constraints on helix connection models. Model 3l of Engelman et al. (PNAS 77, 2023, 1980) satisfies the energy transfer constraints as well as many of the density and ion pair requirements.
(Supported by grants from NSF, NIH and The Robert A. Welch Foundation.)

T-AM-Po60 QUANTITATIVE ANALYSIS OF RESONANCE RAMAN SPECTRA OF PURPLE MEMBRANE FROM HALOBACTERIUM HALOBIUM. Pramod V. Argade and Kenneth J. Rothschild. Boston University, Department of Physics and Department of Physiology, Boston, Ma. 02215.

By fitting the resonance Raman spectra of purple membrane to a superposition of Voigtian line shapes, information is obtained about the position, half-width and integrated intensity of bands in the range 1475-1700 cm^{-1}. Spectra were recorded at 2 cm resolution using a spinning cell under a variety of conditions such that only the intermediates preceding M contributed to the spectra in varying proportions. Two bands at 1540 and 1550 cm^{-1} associated with the C=C stretching vibration are clearly resolved. Further, it is found that the integrated intensity changes in the bands at 1540, 1550 and 1640 cm^{-1} (due to the C=NΘH stretch) are linearly correlated with each other. This evidence, along with the resonance Raman enhancement of the 1540 and 1550 cm^{-1} bands at two different exciting wavelengths suggests that these bands originate from a single intermediate, L, and not from two distinct intermediates. A spectrum of the L intermediate obtained from the curve fitting is presented. It is concluded that i) the L intermediate is protonated and ii) the chromophore of the L intermediate is in a configuration similar to 13-cis.

Supported by grants from the NIH and NSF and an Established Investigatorship Award from the AHA to KJR.

T-AM-Po61 DICHROIC RATIO AND FRACTION OF BACTERIORHODOPSIN CYCLING AS FUNCTIONS OF LIGHT INTENSITY. J. F. Nagle and S. M. Bhattacharjee, Depts. of Physics and Biological Sciences, Carnegie-Mellon University, Pittsburgh, PA 15213 and L. A. Parodi and R. H. Lozier, Cardiovascular Research Institute, University of California, San Francisco, CA 94143.

If the chromophore of a photochemical or photobiological system, such as bacteriorhodopsin, does not undergo tumbling during a fast actinic flash, then the approach to saturation with increasing light intensity does not follow a simple exponential. Using the principles of photoselection formulae have been derived for various cases, including plane polarized and unpolarized actinic flashes, thin and thick samples, and with chromophore shifts between bR and K. For the simplest case of a thin sample and plane polarized actinic flash the formulae can be expressed in closed form using the error function, but the more complex cases require numerical integration. When the measuring beam polarization is set at the magic angle, $\cos^2\theta_m = 1/3$, then the asymptotic approach to saturation goes as the inverse square root of the intensity, which is much slower than exponential. Also, the dichroic ration D is computed as a function of light intensity. D exhibits a rapid decrease as I increases from zero, so that experimental values of D significantly less than 3 may often be due to photoselection. Data obtained for bacteriorhodopsin shows that the equations based upon photoselection provide a better fit than a simple exponential theory, and the measured dichroic ratio is consistent with the estimated fraction cycling obtained from analysis of kinetic data.

T-AM-Po62 LASER DOPPLER ELECTROPHORETIC LIGHT SCATTERING STUDIES OF THE CYTOPLASMIC SURFACE OF THE RED BLOOD CELL MEMBRANE. Wei S. Yen, Robert W. Mercer, B. R. Ware, and Philip B. Dunham. Departments of Chemistry and Biology, Syracuse University, Syracuse, New York 13210.

Using laser Doppler electrophoretic light scattering (ELS), we have studied the electrokinetic behavior of the cytoplasmic surface of the red blood cell membrane using inside-out vesicles prepared from red cell membrane ghosts. The vesicle suspension generally consisted of both inside-out (IOV) and right-side-out (ROV) species having a ratio determined by the presence of a small amount of Mg^{+2} in the vesiculation buffer. The ROV have similar electrophoretic mobility to that of whole red cells, while the mobility of IOV is about 15% lower, indicating lower surface charge density for the cytoplasmic surface. Electrophoretic determination of the sidedness and relative proportions of each specie agrees well with those obtained from assay of acetylcholine esterase, an enzyme which resides exclusively on the external surface. Both measurements indicated 80% of the vesicles were IOV when vesiculation was performed in the presence of 1 mM Mg^{+2}. Agreement of the two methods indicates that the vesicles are sealed. Neuraminidase treatment of vesicles caused the ROV mobility to decrease by 60%, while no significant change was observed for IOV. Trypsinization reduced the mobility of the vesicles and concomitantly induced aggregation, as evidenced by a narrowing of the ELS spectrum. Treatment by phospholipase C left the IOV mobility spectrum essentially unchanged; phospholipase D caused an increase in mobility. pH titration of IOV indicated three distinct ionizable species, pK 4, 6.3, 9.2 on the cytoplasmic cell surface. (This work supported by NIH grants, AM27851 to PBD and GM27633 to BRW.)

T-AM-Po63 A NEW THEORY OF CELL ELECTROPHORESIS. D.E. Brooks, S. Levine, M. Levine and K. Sharp, Departments of Pathology and Chemistry, University of British Columbia, Vancouver, B.C., V6T 1W5

Values of RBC membrane surface charge derived from the amount of sialic acid released by neuraminidase treatment and from Smoluchowski's classical cell electrophoresis theory differ by a factor of 2 to 3. A new theory of electrophoresis of RBC's has been developed which is consistent with the neuraminidase results. The cell surface is considered as a layer of polyelectrolyte anchored to the membrane. The net negative charge on the segments of the polyelectrolyte, due mainly to sialic acid, is represented by various different idealized charge distributions: uniform charge density throughout the polyelectrolyte layer, uniform charge plane on the membrane and uniform charge plane at the polyelectrolyte ends. Solvent flow and conterion penetration occur in this layer. The resulting potential profiles are calculated. By solving the Navier Stokes equations, including a friction term describing drag exerted by the polymer chains, theoretical expressions for the mobility are obtained and compared with the experimental results. The results indicate that the potential at the outer edge of the polyelectrolyte is much lower than the usually accepted value, about 3 mV at an ionic strength of 0.1 M.

T-AM-Po64 IONIC STRENGTH AND SURFACE CHARGE DEPENDENT SURFACE WAVE GROWTH ON HEATED ERYTHROCYTES AS AN EXAMPLE OF INTERFACIAL INSTABILITY. W.T. Coakley, J.O.T. Deeley and D. Tilley, Dept. of Microbiology, University College, Newport Road, Cardiff, Wales, U.K. (Intr. by Prof. Floyd Dunn).

Human erythrocytes undergo significant morphological changes when the cells are heated through the thermal denaturation temperature of the structural protein, spectrin. Two principal categories of morphological change can be distinguished. In one case a wavy disturbance develops along the rim of the biconcave disc and vesicles pinch from the crests of the growing waves. In the second case no wave develops on the cell rim, the shape changes occur at the cell dimple and can include membrane invagination. Cells heated in isotonic saline develop an average of ten waves per cell. Vesicles formed within 0.3s of the initiation of a wave when the heating rate is 1.0°C/s. The number of waves per cell decreases as the ionic strength of the suspending phase is decreased or its serum albumin content is increased. Conditions which suppress wave development on the cell rim and encourage changes involving the cell dimple are, (i) low ionic strength, (ii) decreased surface charge or (iii) high serum albumin levels.

Examples of the fragmentation process will be shown. The shape changes will be discussed in the light of interfacial instability theories which include electrical interactions and emphasize the importance, in low interfacial tension systems, of free energy changes associated with membrane curvature changes. Comparisons will be made with ionic strength, surface charge and serum protein effects on membrane curvature in other systems.

Ref. Coakley, W.T. and Deeley, J.O.T. Biochim. Biophys. Acta (in press).

T-AM-Po65 DEFORMABILITY OF YOUNG, OLD, LIQUID STORED, FROZEN AND REJUVENATED RED BLOOD CELLS (RBC) AS MEASURED BY LASER EKTACYTOMETRY. E.N. Serrallach*, K. Colmer, N. Catsimpoolas*, C.R. Valeri, and C.P. Emerson, Naval Blood Research Laboratory and Depts. of Biochemistry and Biobehavioral Sciences, Boston University Medical Center, Boston, MA 02118.

Cellular deformability is an important determinant of RBC life span *in vivo*. The ability to deform is a necessary condition for the repeated passage through capillaries and restricted areas of the spleen. The inability to deform inhibits red cell circulation and their function to deliver oxygen to the tissues.

Laser Ektacytometry measures the light intensity of the diffraction patterns generated by RBC suspension exposed to shear stress at values comparable to those found in the microcirculation. We have measured the light intensity ratio (LIR) which is associated with cellular deformability of different RBC populations. Reticulocyte-enriched (20%) populations obtained by low density phthalate centrifugation (corresponding to the younger RBC) showed a 40% increase in the LIR. High density phthalate fractions (older RBC) showed a minimal change in the LIR. Fresh-frozen RBC had LIR curves identical to the fresh red cells. It was observed that red cells exposed to hypertonic solutions (1.6% NaCl) and red cell fixed in glutaraldehyde had negative LIR values. Hypotonicity (0.6% NaCl) caused a 20% increase in LIR. The effects of rejuvenation on red cell LIR will be discussed. In certain studies, the LIR measurement was correlated to the *in vivo* survival of RBC and to the red cell enzyme (GOT) activity. These data show that the LIR measurement may predict RBC age *in vivo*.

T-AM-Po66 PHYSICOCHEMICAL PROPERTIES OF ERYTHROCYTES FROM RATS OF DIFFERENT AGES. G.V.F. Seaman, Cherry H. Tamblyn* and Harry Walter, Department of Neurology, U.O.H.S.C., Portland, OR 97201, and Laboratory of Chemical Biology and Laboratory Service, VA Medical Center, Long Beach, CA 90822.

Changes have been reported to occur in the physicochemical properties of the rat red cell population during postnatal development of the animal. The changes could have arisen either from a gradual drifting from day to day in cell properties or from a sudden genetic switch such that a new cell line is produced and the existing cell line gradually disappears as the cells age and are eliminated from the circulation. Aqueous solutions of dextran and poly(ethylene glycol) form immiscible two-phase systems suitable for the separation of cells based on differences in their surface membrane properties. Alterations in rat red cell membrane surface properties as a function of differentiation, maturation and age have been detected and monitored by cell partition in two-polymer aqueous phase systems. The partition coefficients of erythrocytes from rats increase with rat age for both charged and uncharged aqueous dextran-poly(ethylene glycol) phase systems implying that both charge and membrane lipid related parameters of the red cells alter as the rat ages. The mean electrophoretic mobility of the rat erythrocytes in standard saline increases with the age of the rat from about -1.12 μm sec^{-1} V^{-1} cm at ten days to -1.23 μm sec^{-1} V^{-1} cm for the adult rat (>90 days) while the mean cell volume decreases from 110 ± 13 μm^3 to 63 ± 5 μm^3 and the sialic acid content increases from 7.9 ± 0.5 fg/RBC to 8.5 ± 0.5 fg/RBC. Analysis of the data indicates that as the rat ages new red cell lines develop with different physicochemical properties from the original red cell line present in the neonatal rat. Supported by USPHS Grant HL 24374 from the NHLBI.

T-AM-Po67 EVALUATION OF RED CELL DEFORMABILITY BY SPIN-LABELING METHOD. S. Noji, F. Inoue, and H. Kon, NIAMDD, National Institutes of Health, Bethesda, MD 20205.

In order to clarify rheological properties of human red blood cells (RBC), various techniques such as membrane aspiration, cell filtration, ektacytometry, microphotography, etc. have been utilized. The mechanisms responsible for the deformability of RBC, however, have not been elucidated yet satisfactorily by the rheological data accumulated so far. In this study, a spin-labeling method was explored to evaluate viscoelasticity of RBC. ESR measurements of RBC suspension spin-labeled with fatty acid (12,3) labels were performed in a flat quartz cell (thickness=0.28 mm) at 35% hematocrit. Two spectroscopic quantities, the bulk ESR anisotropy (Δh) of the flow-oriented cells and its decay time (t) (when the flow is suddenly stopped), were taken as measures of elasticity and ratio of cellular viscosity (η) to elastic shear modulus (μ) (η/μ), respectively. The effects of iodoacetate-induced ATP depletion, the cross-linking of spectrin with diamide and the temperature on both Δh and t were investigated and compared with the data from other methods. The dependence of Δh on shear stress (τ) (0-100 dynes/sq.cm) revealed that the elasticity of diamide-treated RBC becomes low, while the iodoacetate-treatment affects the τ dependence of cell deformation significantly. These ESR results are in good agreement with those from a rheoscope method (Haest et al. Blood Cells, 6, 539 (1980)). The elasticity of the RBC which was heated to 49°C for 2 min and then cooled to 25°C was estimated to be much lower than that heated to 46°C for 7 min and then cooled to 25°C. The latter exhibits almost the same Δh vs τ curve as the control treated at 37°C. This result is also in good agreement with that from a flow channel technique (Rakow et al. Biorheol., 12, 1 (1975)). Furthermore, concomitant changes in t by the chemical or temperature treatments provided information on η. This spin-labeling method is, thus, proven to be successfully applicable to evaluate RBC deformability.

T-AM-Po68 MECHANICAL MEASUREMENT OF MEMBRANE THICKNESS. R.M. Hochmuth, H.C. Wiles and E.A. Evans. Department of Biomedical Engineering, Duke University, Durham, N.C. 27706.

The principle of conservation of mass often permits submicroscopic dimensions (less than the wavelength of light) to be calculated from microscopic measurements. For example, the thickness of a film of oil spread on water may be calculated from a measurement of the surface area of the film and the fixed mass of the oil (and the tacit assumption of constant molecular density). We use this constant-mass principle to calculate the submicroscopic radii of long, thin membrane cylinders or "tethers" which are readily pulled from red cells. In our experiment a "reservoir" of membrane material is created by aspirating a portion of the red-cell membrane into a micropipet of radius R_p (R_p=1μm). The suction pressure is sufficient to create a sphered portion of the red cell external to the pipet. With a second pipet mounted on an electro-mechanical linear translator, we "draw out" a membrane tether attached to the surface of a small bead. We observe that the change in cell projection length in the pipet, ΔL_p, is directly proportional to the change in length of the tether, ΔL_t. Since the volume of the cell is constant, the membrane material in the pipet is exchanged for the material in the tether. The mathematical expression for this conservation principle permits us to directly calculate the submicroscopic radius of the tether from the microscopic measurements; viz, $R_t=R_p(-\Delta L_p/\Delta L_t)$. Typically, R_t=.015μm = 150 Å for tethers as long as 100μm. We are studying the constitutive relation between tether radius and membrane tension. The limit of the tether radius taken as one over the membrane tension goes to zero defines the membrane thickness.

Ackowledgment: Supported by NHLBI Grant No. 23728

T-AM-Po69 ANALYSIS OF RED BLOOD CELL MEMBRANES FOLLOWING SEPARATION BY ISOPYCNIC DENSITY CENTRIFUGATION. M. Griffin, P.E. Swanson, O.J.Bjerrum, and L. Lorand. Northwestern University, Evanston, Il. 60201

Separation of normal RBC membranes upon continuous sucrose gradients of 25-45% w/w revealed a peak buoyant density of 1.146 + 0.003 (Flynn, et.al., Am. Soc. Hematol. Meet., 1979, Abstr., found spec. grav. of 1.155 ± 0.005). Further fractionation of these membranes upon discontinuous sucrose gradients enabled the isolation of two dense subpopulations (peaks at spec. grav. 1.158 and 1.165 ± 0.003) which accounted for between 12-20% of the total population. These dense populations contained decreased amounts of sialic acid and contained thiol-reducible protein polymers when analyzed by SDS gel electrophoresis. Reduction did not alter the densities of the membranes, suggesting an analogy between the physiological ageing of the cell and irreversible increases in membrane density. When RBC's were loaded with Ca^{2+} (Biochemistry 17, 2598, 1978 and J. Supramol. Struct. 9, 427, 1978), an increase in membrane density occured which could be related to the amount of non-reducible polymer present in isolated membranes. This Ca^{2+} induced increase in membrane density could be inhibited by histamine but not by its analogue, $^{\alpha}$N-dimethyl-histamine, indicating that transglutaminase may play a role in the increase in membrane density. Analysis of sickle cell membranes upon continuous sucrose gradients (25-45% w/w) indicated a peak with a buoyant density greater than that of normal RBC's. Electrophoretic analysis of the most dense membranes revealed a non-reducible polymer analogous to that present in membranes following Ca^{2+} loading of normal cells. Further separation and analysis of these dense subpopulations is presently under investigation. (Supported in part by NIH-AM-25412)

T-AM-Po70 FREE FATTY ACID ASSOCIATED PLASMA MEMBRANE PERTURBATION. W.J. Pjura, A.M. Kleinfeld, R.L. Hoover, R.D. Klausner, M.J. Karnovsky. Biophysical Lab. and Dept. of Pathology, Harvard Medical School, Boston, MA 02115 and NIH, Bethesda, MD 20014.

Fluorescent polarization values of anilinonapthalene sulfonate (ANS) and/or diphenylhexatriene (DPH) and fluorescent lifetimes of DPH were measured in plasma membranes isolated from bovine aortic endothelium, platelets, baby hamster kidney, WTS lymphoma and red blood cells, which had been incubated with cis unsaturated and saturated free fatty acids (ffa). These results, obtained at ambient temperature, demonstrate that DPH polarization (P) is decreased by cis unsaturated ffa but unchanged by saturated ffa. Measurements of DPH polarization in aqueous dispersions of ffa indicate that structures exhibiting micelle characteristics occur at micromolar ffa concentrations. In these dispersions the P values of DPH were about 0.1 and 0.3 for the cis unsaturated and the saturated ffa, respectively. Several studies were performed to demonstrate that the micelle contribution does not signficantly affect changes observed in DPH polarization. In one study membranes were washed after incubation with ffa. In another study, acrylamide was used to quench micelle associated DPH fluorescence. In both studies the DPH polarization was unchanged. In addition, at temperatures higher than ambient, DPH polarization in membranes incubated with cis unsaturated ffa was significantly lower than in the control membranes or in an aqueous dispersion of the same ffa. It was also observed that the effect of ffa on the previously observed (Klausner et al, 1980, J. Biol. Chem. 255, 1286) increase in ANS polarization is probably due to the binding of membrane associated Ca^{2+} with micelles. This suggests that ffa perturb phospholipid acyl chains. (Supported in part by NIH GM 26350, HL 26191, and AI 10677 and JFRA-15 from the Amer. Cancer Soc.).

T-AM-Po71 THE EFFECT OF FATTY ACID SUBSTITUTION ON THE LIPID COMPOSITION, FUNCTION AND PHYSICAL STATE OF THE PLASMA MEMBRANE. R.Y. Poon and W.R. Clark. Department of Biology, University of California, Los Angeles, California 90024.

EL4 tumor cell plasma membrane phospholipids (PL) were selectively enriched in various fatty acids (FA) by culture supplementation for 24 hr. Enrichment ranged from 30-50% of total PL FA. This is accompanied by reproducible changes in the FA chain length profile of the two major PL classes, phosphatidylethanolamine (PE) and phosphatidylcholine (PC). Variations in PL headgroup ratios from normal plasma membrane were also measured but no general trend was discernible among the different FA used. The FA effect on two intrinsic PM enzyme activities, adenylate cyclase and ouabain sensitive Na^+-K^+-ATPase, fell into two discrete groups, the saturated FA being inhibitory and the unsaturated FA, both cis and trans, being either enhancing or without effect. Two EPR motion parameters (order parameter and relative rotational correlation time) calculated using the probe molecules 5NS and 12NS were essentially the same in normal and FA substituted plasma membrane and in the PE and PC liposomes prepared from these membranes. It is possible that the failure to detect changes in the physical properties of substituted membranes and their constituent lipids is due to compensatory changes in overall lipid composition. However, we feel it is more likely that the two nitroxide stearic acid probes as used do not give the necessary resolving power to analyze changes in the physical state of the membrane lipid matrix due to the incorporation of exogenous FA, even when such incorporation extensively alters the overall lipid composition. Our data suggest caution in making assumptions about the "fluidity" of biological membranes following experimental manipulation of membrane lipid composition and in attributing modulations of membrane protein functions to presumed alterations in the fluidity state per se.

T-AM-Po72 Cholesterol Movement Between Human Skin Fibroblasts and Phosphatidylcholine Vesicles. Mark J. Poznansky & Sandra Czekanski, Dept. of Physiology, University of Alberta, Edmonton, Alberta.

Cholesterol has been shown to readily exchange between erythrocytes, lipoproteins and/or phospholipid vesicles. The net movement of cholesterol to and from both erythrocytes and lymphocytes has been shown to depend on the cholesterol to phospholipid (C/P) mole ratio in the donor and acceptor membranes. We report here on the movement of cholesterol between fibroblasts and lipid vesicles and an attempt to distinguish between simple exchange and net movement. Five important conclusions can be drawn from our experiments. 1) More than 90% of ^{3}H-cholesterol introduced into fibroblasts by exchange from lipid vesicles remains available for exchange subsequently with non-labelled vesicles. 2) Only 25-35% of ^{3}H-cholesterol labelled endogenously from ^{3}H-mevalonic acid is available for exchange from fibroblasts to unlabelled lipid vesicles. 3) Only 10-15% of the total cellular cholesterol (or 15-20% of the free cholesterol) is available for depletion to cholesterol-free lipid vesicles. 4) ^{14}C-cholesterol introduced into the plasma membrane by exchange from lipid vesicles does not readily equilibrate with ^{3}H-cholesterol labelled endogenously in fibroblasts from ^{3}H-mevalonic acid. 5) ^{14}C-cholesterol introduced into fibroblasts from lipid vesicles does not appear to be available for esterification into cholesterol esters even in the presence of low density lipoproteins. The data suggest that plasma membrane cholesterol and intracellular cholesterol represent very separate and non-interchangeable pools. This may explain how such large C/P gradients are maintained between the plasma membrane and the intracellular organelles. (Supported by the Alberta Heart Foundation)

T-AM-Po73 QUANTITATION OF AFFINITIES FOR AGGREGATION OF RED BLOOD CELLS IN PLASMA AND DEXTRAN SOLUTIONS. K. Buxbaum, E. Evans, and D. Brooks, Duke Univ., Durham, N.C., and Univ. of British Columbia, Vancouver, B.C.

The affinities for aggregation of red blood cells in plasma and dextran solutions have been quantitated by minimum energy analysis of red cell-to-red cell "particle" adhesion experiments. The red cell "particles" are 2-3 μm spherical fragments of red cells produced by vesiculation above 48°C. The red cell "particles" are collected and resuspended with normal red cells in the appropriate solutions. The experimental procedure is to use dual-micromanipulators to position a normal red cell and a "particle" for contact. After contact, the red cell encapsulates the spherical fragment to an extent which depends on the affinity. The surface affinity is the reduction in free energy per unit area of the interface which is associated with formation of surface contact. Thus, the surface affinity is derived from the partial derivative of the elastic free energy of the red cell membrane (at a mechanical equilibrium configuration) with respect to the area of adhesive contact on the "particle". Comparison of a simple model to numerical computations of equilibrium shapes of red cell encapsulation of a spherical particle has shown that the surface affinity normalized by the elastic shear modulus of the red cell membrane depends only on the fractional extent of particle encapsulation. The analytical results are independent of particle size for particles less than 3 μm and for normal red cell surface areas and volumes. With this approach, surface affinities were measured for normal and neuraminidase-treated red cells in plasma and in dextran (28000, 70000, 150000 MW) solutions of various concentrations. Based on a membrane shear modulus of $\sim 7 \times 10^{-3}$ dyne/cm, the measurements of surface affinity ranged from 5×10^{-4} to 3×10^{-2} ergs/cm^2 in these tests. (Supported in part by USPHS NIH grants HL 16711 and HL 24796.)

T-AM-Po74 THERMAL STUDIES ON FROG SCIATIC NERVE. C.R. Worthington and D.A. Wilkinson, Departments of Biological Sciences & Physics, Carnegie-Mellon University, Pittsburgh,PA

In earlier work on frog sciatic nerve performed in this laboratory, it was shown that above a certain temperature (58°C) the normal X-ray repeat period of 171A changed to 435A characteristic of the anomalous swollen state. Differential scanning calorimetry has now been applied to further elucidate the thermal events that occur in the nerve as it is heated. Whole nerves show three endotherms, A(48°), B (54°), and C (62°). However, we find that homogenized myelin (collagen residue removed) does not show any of these transitions. This observation of no thermal transitions is in agreement with previous studies on wet (homogenized) myelin by Ladbrooke et al. (BBA 164:101, 1968). Evidence that the B transition represents the irreversible denaturation of collagen (the collagen shrink point) is presented. It appears likely that the shrinkage of the collagen is an important factor leading to the formation of the anomalous swollen state. Properties of the A and C transitions are also discussed.

T-AM-Po75 COMPARATIVE STUDY OF VARIOUS CELLULAR MEMBRANES USING FLUORESCENT PROBES. R. B. Haugland, T.-I Lin, J-C. Burgun, and R. M. Dowben. Dept. of Pathology, Baylor Univ. Med. Cntr., Dallas, TX 75246 and Dept. of Physiology, Univ. Texas Health Sci. Cntr., Dallas, TX 75235.

Liver plasma membranes (LPM), erythrocyte ghosts (RCM), L-cell (NTC 929) plasma membranes (LCM), synaptosomes, and sarcoplasmic reticulum (SR) have been studied using the fluorescent probes 12-(9-anthroyl)stearic acid (12AS) and tetramethylammonium 1,6-diphenyl-1,3,5-hexatriene (TMA-DPH). Characteristic incorporation kinetics of the probes and differences in excitation and emission spectra, as well as fluorescence lifetimes were found for various membrane types. Fluorescence energy transfer between the aromatic amino acids of membrane proteins and 12AS was found and differed for various membrane types. LMP, SR and synaptosomes from rats (1) irradiated at 10 mW/cm^2 cw or pulsed microwaves 1 hr/day for 9 days, (2) sham irradiated, and (3) temperature controls did not show significant differences in fluorescence and marker enzyme activity within each membrane type. LCM and ascites (Lettre) cell membranes grown in (1) 1 mM cystamine, (2) 0.1 mM dansylcadaverine, or (3) calcium ionophore A-23187 showed inhibition of the transglutaminase that catalyzes the formation of the glutamyl-lysine crosslink in membrane proteins by the first two reagents and enhancement by the third. Differences in the fluorescence parameters were observed in the different membrane types that correlated with changes in membrane marker activities (e.g., Na^+K^+-ATPase, Ca^{2+}-ATPase) and the amount of glutamyl-lysine isopeptide in the membranes. 12AS and TMA-DPH, therefore, are sensitive and useful probes for detecting changes in membrane structure. Supported by a contract from the U.S.A.F. School of Aerospace Medicine and a grant from the National Science Foundation.

T-AM-Po76 SPIN LABELS FOR MEMBRANE-WATER PARTITIONING STUDIES. Philip D. Morse, II, Robert Clarkson, and Donna M. Lusczakoski-Nesbitt. Department of Biological Sciences, Wayne State University, Detroit, MI 48202 and Varian Associates, Palo Alto, CA 94303.

Spin label partitioning using the spin label TEMPO has been widely used as a measure of membrane fluidity in model membrane systems and bacteria. This measurement is more difficult and sometimes impossible in more complex membrane systems such as red blood cells, spinach thylakoids, and mitochondrial membranes. The purpose of this presentation is to introduce spin labels which will partition into these membranes.

These labels are of the general structure:

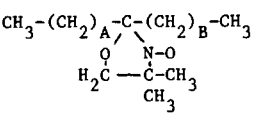

When A=0, B=1,3,5,7,9,or 11; when A=3, B=4; when A=5, B=6. We use the shorthand notation (A+2)N(A+B+3), i.e., A=5, B=6 is 7N14. These labels are synthesized by the method of Keana et al (1). The details of their synthesis and purification will be described in detail. Gas chromatography serves to separate the spin labels from their precursors.

At a spin label to lipid ratio of 1:50, partitioning of the labels in ether and ester linked dipalmityl or dipalmitoyl phosphatidyl choline is dependent on the length of the spin label and, for the shorter labels, on the phospholipid head group linkage. Partitioning differences associated with the pretransition and main transition of DPL are quite evident. X- and Q-band spectra are used to resolve partitioning effects from motional effects. These spin labels seen to be valuable tools for membrane structural studies.

(1) Keana et al. JACS 89, 3055 (1967).

Supported in part by a Wayne State University Faculty Research Award to PDM.

T-AM-Po77 DOSE DEPENDENT EFFECTS OF PROSTAGLANDIN E_1 AND E_2 ON HUMAN ERYTHROCYTE MEMBRANES AS DETECTED BY ELECTRON SPIN RESONANCE SPECTROSCOPY AND HYPOTONIC HEMOLYSIS. D. L. Mazorow, A. Haug, and E. J. McGroarty. Michigan State University, E. Lansing MI 48824

Electron spin resonance spectroscopy studies were carried out in an Earle's salt solution in the presence of prostaglandin E_1 (PGE_1) and prostaglandin E_2 (PGE_2) at various temperatures over many orders of magnitude using 5-doxyl stearate as the probe. PGE_1 at 10^{-9}M increased membrane order by 1.3% in the presence of calcium. PGE_1 was inactive in the absence of calcium. PGE_2 disordered the erythrocyte membrane at 10^{-10}M in the presence of calcium. It also was inactive in the absence of calcium. These studies were repeated in a phosphate buffer. PGE_1 disorders rather than orders the membrane in the presence of calcium. Dose response hypotonic hemolysis curves were established over several orders of magnitude in the presence and absence of calcium. In a hypotonic Earle's salt solution, PGE_1 was lytic or nonprotective at all levels in the presence of calcium. PGE_1 was inactive in the absence of calcium. PGE_2, however, in a hypotonic Earle's salt solution was inactive in the presence of calcium and very protective in the absence of calcium. Maximal protection occurred at 10^{-9}M PGE_2. (Funded in part by a General Research Support Grant from the College of Osteopathic Medicine, Michigan State University.)

T-AM-Po78 THE RESISTANCE OF LIVER MITOCHONDRIAL MEMBRANES AND PHOSPHOLIPIDS FROM CHRONIC ALCOHOLIC RATS TO DISORDERING BY ETHANOL. A. Waring, H. Rottenberg and E. Rubin, Dept. of Pathology and Laboratory Medicine, Hahnemann Medical College, Philadelphia, PA 19102.

The fatty acid spin labels 5-doxyl and 12-doxyl stearic acid were used to probe the response of hepatic mitochondrial membranes and isolated phospholipids from rats fed a chronic alcoholic diet to perturbation by in vitro ethanol. At 35°c the order parameter of mitochondrial membranes from rats fed ethanol chronically and from their pair-fed controls were similar as calculated from the hyperfine splittings of the EPR spectra. The addition of ethanol in vitro to mitochondria from control animals appeared to "fluidize" the membranes, as evidenced by a pronounced decrease in the order parameter. By contrast, in membranes from rats fed ethanol chronically, there was no effect on the order parameter after addition of ethanol in vitro, in concentrations up to 0.5M. The resistance of the mitochondrial membranes from chronically intoxicated animals to the disordering effects of ethanol appears to result from an alteration in the physical properties of the phospholipids, because the same differential response to ethanol was observed using vesicles of mitochondrial phospholipids extracted from control and chronically treated rats. At lower temperatures the order parameter of both membranes and phospholipid vesicles from chronically treated animals were higher than in controls Suggesting an increased "rigidity" of these membranes. These findings point to the underlying molecular mechanism for the previous observation that mitochondria from chronic alcoholic rats are more resistant to uncoupling by ethanol at physiological temperature (Rottenberg,Robertson, Rubin, Lab Invest. 42:318, 1980) and suggest that an adaptive change in the phospholipid composition leads to structural alterations, which result in increased resistance to disruption of the mitochondrial membranes by ethanol.

T-AM-Po79 EFFECT OF ACETYLCHOLINE ON FLUIDITY OF PLASMA MEMBRANES OF ADRENAL CHROMAFFIN CELLS. Darlene Rimle,* Philip D. Morse II, and David Njus, Department of Biological Sciences, Wayne State University, Detroit, Michigan 48202.

The chromaffin cell of the adrenal medulla secretes catecholamines upon stimulation by acetylcholine, but the mechanism of this stimulus-secretion coupling is poorly understood. Acetylcholine apparently increases the fluidity of chromaffin cell plasma membranes above 30°C as measured by fluorescence depolarization (Schneeweiss et al., Biochim. Biophys. Acta 555, 460, 1979). Hexamethonium, a cholinergic blocker, reportedly inhibits the acetylcholine induced fluidization. We used electron spin resonance spectroscopy to investigate membrane fluidity changes caused by acetylcholine and hexamethonium. Chromaffin cell plasma membranes were isolated from bovine adrenal medullae by density gradient centrifugation. Two nitroxide spin labels, 2N14 and 7N14, were used to monitor changes in membrane fluidity. 2N14 probes the part of the membrane close to the polar region, while 7N14 probes the hydrophobic interior. Arrhenius plots of rotational correlation time τ_c showed a change in slope reflecting a change in the phase behavior of the component lipids around 29°C for 2N14 and 31°C for 7N14. The Arrhenius plot of acetylcholinesterase activity showed a change in slope around 28°C confirming the existence of a phase transition in the membrane around 30°C. Acetylcholine caused a small decrease in fluidity measured using 2N14 and a large decrease in fluidity measured using 7N14. Hexamethonium plus acetylcholine caused a large increase in 2N14-measurable and a smaller increase in 7N14-measurable fluidity. Thus, the effects of acetylcholine and hexamethonium seem to depend on the probe used to monitor membrane fluidity.

Supported by NSF Grant BNS-7904752.

T-AM-Po80 MEMBRANE LIPID FLUIDITY OF HUMAN LYMPHOCYTES IS UNAFFECTED BY CONCANAVALIN A STIMULATION: A FLUORESCENCE POLARIZATION STUDY WITH A LIPOPHILIC PROBE.

A. H. Parola[†], J. H. Kaplan, S. H. Lockwood, E. E. Uzgiris, General Electric Research and Development Center, P. O. Box 8, Schenectady, NY 12301

The notion that membrane lipid fluidity is altered following mitogen stimulation has been supported by a number of observations on rat and mouse lymphocytes. Some studies have indicated short term fluidity alterations; other studies, on the contrary, report no changes up to 20-24 hours of incubation with mitogen and then, with further incubation, rather sizable relative decreases of fluoresence polarization using a lipid probe. We find that for human peripheral blood lymphocytes, purified on Ficoll-Hypaque, concanavalin A stimulation is accompanied by incorporation of radiolabeled thymidine into new DNA, as is to be expected, but that there is no concomitant lipid fluidity change as measured by fluoresence polarization of the lipid probe 1-6-diphenyl-1,3,5-hexatricne (DPH), either after a short period of mitogen application or after 24, 48, or 72 hours of incubation. Therefore, we infer that a lipid probe is relatively insensitive to membrane changes produced by concanavalin A stimulation, at least in human lymphocytes. However, we note that the membrane changes following stimulation produce a decline in cell electrophoretic mobility of up to 20% after 48 or 72 hours of incubation.

[†]G.E. Research Fellow, Permanent Address: Department of Chemistry, Ben-Gurion Univeristy of the Negev, Beer-Sheva, Israel

T-AM-Po81 LACK OF A CORRELATION BETWEEN HYPERTHERMIC CELL KILLING AND MEMBRANE LIPID FLUIDITY. J.R. Lepock and J. Kruuv (Intr. by R.A. Snyder), Departments of Physics and Biology, University of Waterloo, Waterloo, Ontario, Canada N2L 3G1. - An increase in membrane lipid fluidity to a critical value, above which death ensues, has been proposed as the primary event during hyperthermic killing of mammalian cells. This has been investigated by studying the relationship between 1) the hyperthermic sensitization of V79 Chinese hamster lung cells by short chain alcohols and the effect of these alcohols upon lipid fluidity as determined with spin labels, 2) the membrane fluidizing ability of butylated hydroxytoluene (BHT) and its effect upon hyperthermic killing and 3) the membrane fluidity of untreated cells and cells in which thermotolerance has been induced by heating. The alcohols methanol, ethanol, 2-proponal and t-butanol increase the rate of cell killing of V79 cells by the ratios 1:1.3:1.8:3.1, respectively, where the sensitization of methanol has been normalized. However, the effect of these same alcohols upon V79 membrane lipid fluidity, determined by measuring the rotational correlation time (τ_c) of the spin label 2,2-dimethyl-5-dodecyl-5-methyloxazoladine-N-oxide (2N14), varies as the ratios 1:2.8:11:24, respectively. Treatment of V79 cells with 0.07 mM BHT increases membrane lipid fluidity by an amount equivalent to a 6.0°C temperature increase; this same amount of BHT produces no hyperthermic sensitization of V79 cells. Thermotolerance was induced by a 20 min. exposure to 44.5°C. No decrease in lipid fluidity was found 16 hours later, at which time the cells had a 4-fold decrease in heat sensitivity. Thus, in each of these studies, no evidence for a relationship between membrane lipid fluidity and hyperthermic cell killing was found.

T-AM-Po82 Changes In Fluorescence Capping of Tumor Cells Upon Response To A Chemotactic Peptide. John A. Wass, KMK Rao, James Varani, Peter A. Ward. Department of Pathology, University of Michigan Medical School, Ann Arbor, MI. 48109

The percentage of capped Walker 256 Carcinosarcoma cells labelled with fluoroscein isothiocyanate concanavalin-A (FITC-ConA) increased significantly over control values (2%) upon exposure to 10^{-8}M N-formyl-methionyl-leucyl-phenylalanine (f-met-leu-phe), a chemotactic agent (8%), 10^{-5}M colchicine, a microtubule inhibitor (15%), and a combination of the two (25%). Chemotactic factor-stimulated capping events, both with and without colchicine, were blocked by preincubating the cells with 10^{-3}M 2-deoxyglucose. In addition, the capping response of the tumor cells exhibited the typical dose-response curve found in previous studies in a cell-swelling assay, a chemotaxis assay, and a nylon wool adhesion assay. Positive results were found at 10^{-6}M through 10^{-10}M f-met-leu-phe, the same range found to be active in the three other assays. It was further found that Zn^{++}, known to produce an age dependent effect on colchicine-induced ConA capping in human peripheral lymphocytes, produced an enhanced fluorescence (binding) of FITC-ConA to these cells while not significantly affecting the degree of capping. The same experiments were performed with FITC-labelled wheat germ agglutinin (WGA) at concentrations similar to those used with the FITC-ConA (10μg/ml). At the concentrations of the chemotactic peptide used (10^{-6}M - 10^{-12}M) WGA did not exhibit sufficient binding to allow examination of the capping phenomena. We now have solid evidence from several lines of investigation for cell surface involvement in chemotactic peptide binding & activation. This work was supported by NIH grants CA 29550 and CA 29551.

T-AM-Po83 EFFECT OF Mg-ATP ON PROTEIN SPIN-LABELLED HUMAN ERYTHROCYTE GHOSTS. J.G. Mohanty, J.T. Wang, and J.M. Rifkind. Gerontology Research Center, NIA/NIH, Baltimore City Hospitals, Baltimore, MD 21224.

Mg-ATP has been shown to play a role in maintaining the shape of the human erythrocyte [Palek et al., Blood 44, 583 (1974)] via the phosphorylation of band 2 of spectrin [Birchmeier & Singer, J. Cell Biol. 73, 647 (1977)]. We have investigated the effect of Mg-ATP on the electron spin resonance (ESR) spectra of erythrocyte ghosts labelled with 4-Maleimido-2,2,6,6-tetramethylpiperidinoxyl spin-label, which labels the protein sulfhydryl groups. Incubation of ghosts with 2 mM Mg-ATP at 37°C for 30 minutes is found to produce a very significant alteration in the spectrum which suggests a decrease in the ratio of weakly immobilized to strongly immobilized spins. A closer look at the spectral change indicates that there is no increase in the signal from the strongly immobilized spins even though the signal from the weakly immobilized spins decreases.

An analogous variation in the signal intensity of the weakly immobilized spins without any change in the strongly immobilized spins was found when the effect of temperature on these spectra were investigated. A reversible continuously increase in the signal intensity was found as the temperature was raised from 7°C to 48°C with transitions at 20°C and 36°C. Mg-ATP was found to eliminate these transitions and markedly reduce the temperature variation of the ESR spectrum.

These results can best be explained by a fraction of weakly immobilized spin-labels which consist of pairs of labels which are located close enough to each other for their signals to be broadened out due to dipolar interactions and/or spin exchange. The distance between these spins increases with temperature while Mg-ATP maintains these spins in closer proximity even at elevated temperatures.

T-AM-Po84 DECREASED MEMBRANE PERMEABILITY OF DRUG-RESISTANT LEUKEMIA CELLS TO DIFFUSIBLE SOLUTES. Jerald J. Killion, Department of Physiology, Oral Roberts University School of Medicine, Tulsa, Oklahoma, 74171.

Tumor cell populations are heterogeneous with respect to many biological and biochemical parameters. Variants often emerge following a change in the tumor-host relationship imposed by various therapeutic modalities. A classical example is the development of resistance by tumor cells to the cytotoxic effects of chemotherapeutic drugs. Resistance is accompanied by marked changes in cell membrane properties, composition and function; however, membrane alterations are difficult to measure in the intact, viable cell. A study was therefore designed to quantitate changes in cellular permeability to low-molecular weight solutes, as measured by the comparative rates of osmotic lysis of drug-resistant and drug-sensitive L1210 leukemia cells when suspended in iso-osmotic concentrations of diffusible solutes. A subline of L1210, resistant to thioguanine (purine antagonist, NSC-725, mw=168) was established in culture, and this subline was totally refractory to the chemotherapeutic effect of thioguanine, in vivo. The kinetics of cell lysis was quantitated by the decrease in the optical density of the cell suspension (549 nm) as a function of time (seconds). Drug-resistant cells showed from a 4-fold to a 2-fold decrease in the rate of osmotic lysis to a variety of diffusible solutes, such as urea, ethyl alcohol, ethylene glycol and polyethylene glycols, suggesting decreased permeability to these substances across the cell membrane. Hence, this simple method demonstrates changes in the permeability of the intact cell membrane and offers evidence that drug-resistant cells may comprise a small subpopulation of permeability-mutants that preexist in the parental tumor. (supported by ORU Intramural Research)

T-AM-Po85 A Comparison of Photoreactivation and Loss of Photoreversibility in E. Coli B/r with Visible and Near-UV Light. Steve Kristoff and Richard Bockrath, Dept. of Microbiology and Immunology and Biophysics Program, Indiana University School of Medicine, Indianapolis, IN 46223.

Direct enzymatic photoreactivation is known to occur when E. Coli are exposed to light of from 310 nm to 440 nm. Indirect, non-enzymatic, photoreactivation and photoprotection occur when cells are exposed to light of between 300 nm and 380 nm. Our data indicate that direct enzymatic photoreactivation with visible (405 nm) light is inhibited and mutation fixation, indicated by loss of photoreversibility, is blocked by treatment of the cells with chloramphenicol before and after UV irradiation. Indirect, non-enzymatic, photoreactivation by BL bulbs, which emit primarily near UV (366 nm) light, and loss of this indirect photoreactivation are not blocked by chloramphenicol. Our assay system involved UV irradiation of an auxotrophic E. Coli B/r strain grown in the presence of chloramphenicol and subsequent exposure of samples of the culture to photoreactiviting light of either 405 nm or from BL bulbs at various times after UV exposure. These data indicate that protein synthesis is required for full enzymatic photoreactivation, but protein synthesis is not required for non-enzymatic photoreactivation and subsequent mutation fixation.

T-AM-Po86 TOTAL INTERNAL REFLECTION/ FLUORESCENCE CORRELATION SPECTROSCOPY STUDY OF ANTIBODY SURFACE BINDING KINETICS. Nancy L. Thompson and Daniel Axelrod, Biophysics Research Division and Dept. of Physics, University of Michigan, Ann Arbor, Michigan, 48109.

We present a first application of total internal reflection/ fluorescence correlation spectroscopy (TIR/FCS) to study the equilibrium binding kinetics of fluorescent solute molecules at a solid surface. In TIR/FCS, a laser beam totally internally reflects at a solid/liquid interface and the shallow (1000 Å) evanescent field in the liquid excites the fluorescence of surface adsorbed molecules. A fluorescence microscope with a stopped-down image plane diaphragm is used to collect fluorescence from a small (≈5 μm^2) surface area. As individual molecules bind and unbind at random on the surface, the fluorescence fluctuates spontaneously. The photon-counted fluorescence intensity is autocorrelated on-line by a minicomputer; the characteristic decay rate of the autocorrelation function reflects the kinetic rates of surface binding (Thompson, et.al., Biophysical Journal, March, 1981). We have obtained autocorrelation functions from the adsorption/desorption of rhodamine labeled immunoglobulin molecules on uncoated quartz. The binding exhibits multiple desorption rates in equilibrium; the shortest of these has a characteristic time of 7-10 ms. The fluorescence fluctuations can be seen visually through the microscope eyepiece as randomly flashing speckles. We have also investigated the binding of rhodamine labeled anti-DNP to specific DNP antigenic sites attached to the quartz surface. (Supported by PHS NS 14565, and HL 24039; ACS/PRF, and the Research Corporation).

T-AM-Po87 LASER CIDNP STUDIES AT HIGH FIELD (360 MHz) OF THE REACTION BETWEEN PHOTOEXCITED FLAVINS AND TRYPTOPHAN DERIVATIVES. S.G.Boxer* and E.F.McCord*, Dept. of Chemistry, Stanford University, Stanford, Ca 94305

Chemically Induced Dynamic Nuclear Polarization (CIDNP) is generated when Tryptophan (Trp), its derivatives or Trp-containing peptides react with photoexcited flavins in a 360 MHz NMR spectrometer. In contrast to tyrosine (Tyr), we find that the nuclear polarization of Trp originates in an electron transfer reaction. Using a series of Trp derivatives, the unpaired spin density distribution of the Trp radical cation and the ground state NMR spectrum are analyzed in detail. The signs and relative magnitudes of the proton isotropic hyperfine coupling constants for each position around the indole ring in the cation deduced from these measurements are: position 3>>2 4 6>1>>5>7 with positions 1, 2, 3, 4 and 6 positive, 5 negative and 7 essentially zero. This result is inconsistent with most available calculations of the unpaired spin density distribution, but is compatible with the pattern of electrophilic aromatic substitution. Possible mechanistic complications in the reaction leading to CIDNP are discussed. The laser-CIDNP spectra of the Trp rich peptides gramicidins A and B are presented as examples of the resolution enhancement obtained with this technique.

This technique has been extended into the UV using a high-powered excimer laser (KrF, 249 nm). This light source permits direct excitation of amino acids (eg. Trp and Tyr) or reactions with well characterized hydrogen abstractors such as acetophenone or acetone. p-OH-acetophenone is found to produce the most intense polarization for Trp and Tyr. (Supported by NIH GM-277738)

T-AM-Po88 SERUM THEOPHYLLINE DETERMINATION BY FLUORESCENCE POLARIZATION IMMUNOASSAY UTILIZING AN UMBELLIFERONE DERIVATIVE AS A FLUORESCENT LABEL. T. M. Li, J. L. Benovic* and J. F. Burd*, Immunochemistry Laboratory, Ames Division, Miles Laboratories, Inc., Elkhart, IN 46515

We report the development of a non-radioisotopic homogeneous immunoassay to determine serum theophylline concentrations using fluorescence polarization. Theophylline is a therapeutic drug which is used in the treatment of asthma. Monitoring this drug in serum is necessary to ensure effective dosage and to avoid toxicity. The fluorescence polarization immunoassay is based on labeling the analyte with a fluorescent probe and monitoring the changes in the probe's fluorescence polarization occurring in the hapten-antibody reaction. Previous reported fluorescence polarization immunoassays invariably involved the use of fluorescein as a fluorescent label. The existence of polymorphic forms in fluorescein and the presence of contaminants in commercial preparations of fluorescein have led us to use an alternative fluorophore, namely, an umbelliferone derivative, in the polarization immunoassay. This fluorescent probe is characterized by a high quantum yield, a large extinction coefficient, a large Stokes shift and the absence of non-specific interaction with normal human serum. The spectroscopic properties of this label including both the excitation and emission polarization spectra are presented, and the procedure to obtain the optimized fluorescence polarization standard curve is described. Using the polarization immunoassay technique, the theophylline concentrations of 25 clinical serum samples were determined. The values obtained correlated well with values determined by high pressure liquid chromatography (equation of linear regression analysis: $y = 0.97x + 1.33$ and correlation coefficient 0.93).

T-AM-Po89 ACETALDEHYDE-INDUCED CHEMILUMINESCENCE OF XANTHINE OXIDASE. Enrique Cadenas & Britton Chance. Johnson Foundation, University of Pennsylvania, Philadelphia, PA 19104.

The oxygen-dependent oxidation of acetaldehyde by xanthine oxidase is accompanied by low level chemiluminescence. Light emission is linearly related to the concentration of enzyme and shows saturation with its substrate at about 6 mM (Km for acetaldehyde was about 3.6 mM) Both superoxide dismutase and catalase inhibit chemiluminescence, producing half-maximal inhibition at a concentration of 0.45- and 2.75 μg/ml, respectively. The pH dependence of the acetaldehyde-induced light emission of xanthine oxidase is similar to that presented for other parameters, such as O_2^- and H_2O_2 generation, increasing from low to high pH, with maximum at about pH 8.0. The chemiluminescence reaction is not affected by EDTA (in the range 5-100 μM), whereas EDTA-Fe^{2+} complex exerts a dual effect, stimulating light emission at low concentrations [maximal effect (25%) at 5.5 μM] and inhibiting chemiluminescence at higher concentrations [maximal effect (53%) at 100 μM]. The chemiluminescence reaction is strictly dependent on O_2^- and shows an apparent Km for O_2^- of 0.21 mM; the rate of chemiluminescence is also increased at O_2^- concentrations beyond 0.22 mM. Spectral analysis of the photoemissive reaction, carried out with a set of gelatin cut-off filters, shows four bands at 420-450, 460-470, 505-525, and 590-630 nm, with relative intensities of 1.0, 0.79, 0.54, and 0.46, respectively. Unlike the blue band chemiluminescence, which is well-defined and represents the highest contribution to this spectrum, the red bands are broad and not well-defined. The oxidation of acetaldehyde by xanthine oxidase does not yield any fluorescence species; no additional data were found between the fluorescence spectrum of the pure enzyme (excitation 304 nm; emission 405 nm) and that of the enzyme-substrate reaction, but for a small decrease (8-9%) on the 405 nm-fluorescence emission, upon addition of acetaldehyde.

This research was supported by USPHS grant HL-SCOR-15061.

T-AM-Po90 SOLUBILITY OF XENON IN LIQUIDS. Gerald L. Pollack, Department of Physics, Michigan State University, East Lansing, Michigan 48824.

A new technique is described for measuring the solubility of radioactive gases in liquids. The gas and liquid are initially separated from each other in a sealed container, they are brought to equilibrium by vigorous stirring, and the concentration of the radioactive gas is monitored, noninvasively, by measuring the radioactive intensity. The technique has been applied to measuring the Ostwald solubility L(T) of Xe-133 in pure linear hydrocarbons and in sucrose-water solutions with fractions of sucrose by weight ranging from 0 to 0.680. In the sucrose solutions the solubility of Xe-133 is found to be directly proportional to the volume fraction of water in solution over the measured range. Tentative results for hydrocarbons are L(20.0°C)=5.13 for Xe-133 in n-hexane and L(20.0°C)=3.93 for Xe-133 in decane. (This research has been supported by the Office of Naval Research.

T-AM-Po91 HIGH RESOLUTION ELECTROPHORETIC TECHNIQUES FOR THE ANALYSIS OF MEMBRANE PROTEINS UNDER DENATURING AND NON-DENATURING CONDITIONS. R.C. Steinfeld and G.A. Vidaver, (Intr. by F.H. Kirkpatrick) Dept. of Chemistry, University of Nebraska at Lincoln, Lincoln, Nebraska 68588 (USA).

One- and two-dimensional polyacrylamide gel electrophoretic techniques have been developed. Under non-denaturing conditions, pigeon erythrocyte plasma membrane was solubilized at 4-6°C by sonication in the presence of the zwitterionic detergent, Zwittergent 3-14 (Calbiochem). The soluble extract was then treated with an admixture of that detergent, Triton X-100 and dibutyl formamide and then resonicated. Isoelectric focusing in gel rods was performed at 8°C followed by a survey of enzymatic activities using histochemical staining techniques. The presence of ATPase, GTPase, and protease activities were observed. The greater utility of the technique was demonstrated by showing the presence of NADH dehydrogenase activity in an extract of mitochondrial membrane. Combining this focusing procedure with a 2nd dimension electrophoresis modified from the method of Davis (Annals N.Y. Acad. of Science (1964) p. 404-427.) has also been done. The technique has been used to identify detergent binding proteins in the membrane extract. In addition, a 2-dimensional separation method for membrane proteins under denaturing conditions was also developed. The method is a modification of one developed by O'Farrell (J. Biol. Chem. (1975) 250, 4007-4021). It employs a combined pH and acrylamide gradient in the 2nd dimension with the addition of urea and n-butyl urea as denaturing agents. (This work was supported by Research Grant HE-13256 from U.S. Public Health Service, the University of Nebraska-Lincoln Research Council and NIH Biomedical Research Support Grant RR-07055.)

T-AM-Po92 VOLTAMMETRIC IMMUNOASSAY USING DINITROESTRIOL. H. B. Halsall, K. Wehmeyer* and W. R. Heineman,* Department of Chemistry, University of Cincinnati, Cincinnati, OH 45221.

Electrochemical methodology is being developed for the detection and quantitation of physiologically important ligands (Science 204, 865 [1979]). Differential pulse polarography (DPP) showed estriol to be electroinactive in the potential range -0.10 V to -1.00 V vs. Ag/AgCl. At similar concentrations (μM), 2,4-dinitroestriol was electroactive, with a wave centered at -0.550 V vs. Ag/AgCl. The peak current was linear with concentration over the range 0.7 μg/ml to 15 μg/ml. The addition of aliquots of α-estriol IgG reduced the peak current for the reduction of dinitroestriol proportionately, indicating binding of the ligand to specific antibody. Subsequent addition of unlabelled estriol resulted in incremental increases in the peak reduction current indicating competitive and reversible binding of the two ligands for the antibody. No reactions were seen with nonspecific IgG. A plot of the peak current vs. concentration of unlabelled estriol added was linear over the range 1.8 μg/ml to 25 μg/ml. A particular advantage of the method is that quantitative analysis does not require separation of bound from free antigen, since the bound antigen does not give a reduction signal in the potential range used. Supported by NIH grant AI-16753 and gifts of specific antibody from New England Nuclear.

T-AM-Po93 **A RAPID SCANNING GEL CHROMATOGRAPH FOR STUDIES OF MACROMOLECULAR INTERACTION.** E. E. Brumbaugh, B. W. Turner, F. R. Smith, and G. K. Ackers, Dept of Biology, The Johns Hopkins University, Baltimore, Md. 21218, Dept. of Nat. Sci., Univ. of N. Florida, Jacksonville, Fla. 32216.

Direct optical scanning of gel chromatography columns provides a versatile method for studying macromolecular interactions [cf. G. K. Ackers, Methods of Protein Separation 2:1 (1976)]. We have developed a new system for rapid scanning of a stationary column, providing solute concentration profiles as a function of time and distance. A quartz fiber optics bundle delivers a 1mm dia. beam of monochromatic light [650-220 nm] to the front of the column. Light guides mounted in a 60° radial array collect transmitted and scattered light exiting from the back of the column. The light guides are mounted on a moving platform driven by a precision helical screw and stepping motor, controlled by a microprocessor. Collected light is detected by a sensitive cooled end-on photomultiplier. For photometric stability, the spectrophotometer operates in a dual beam mode, with a photodiode as the reference signal source. A microprocessor controls analog to digital conversion of the absorbance values, over a 4 O.D. range with 0.002 O.D. resolution. A single scan, which requires less than 5 seconds, generates 500 absorbance values for a 25 cm column. The entire set of data is passed to a Hewlett Packard 1000 computer system for graphics display and further analysis. Real time interactive programs allow flexible control of all parameters during the course of an experiment. The speed of data acquisition and frequency of scans permit much more detailed analysis of reaction boundary profiles than previously possible. The new system provides greatly enhanced capabilities for all studies of macromolecular interactions, including self-assembly, ligand binding, and active enzyme transport. Supported by USPHS Grant GM 24486.

T-AM-Po94 CHARACTERISTICS OF A VIDICON DETECTOR FOR 3-D SPECTROSCOPIC APPLICATIONS
P.D. Smith, G. W. Liesegang, Electrical and Electronic Engineering Section, Biomedical Engineering and Instrumentation Branch, Division of Research Services, and Laboratory of Technical Development, National Heart, Lung, and Blood Institute, National Institutes of Health, Bethesda, Maryland 20205.

A Princeton Applied Research 1254B vidicon and 1216 controller have been interfaced to a Digital Equipment Corporation MNC-11 mini-computer using the MNCDI and MNCDO modules. The majority of the programming is in Fortran, calling MINC I/O routines, linked to a concise assembly language data acquisition routine. A systematic investigation, in both continuous and pulse modes, of the vidicon output as a function of the various scanning parameters eg, prep frames, channel time, channel height, and frame averages has been performed. The programming is capable of analyzing any given frame or total frame integrations. The influence of these parameters on the efficiency of reading the vidicon surface, and in particular, the technique of switching V_1 (prep) and V_2 (read) voltages to improve linearity, read efficiency, and dynamic range will be discussed. Integration of the vidicon and a Nd-glass picosecond laser system under control of the MNC-11 mini-computer will be presented.

In presenting these results, it is hoped to indicate the importance, interaction, and effect of each parameter on the data obtained which is not readily available in the literature. Further, the ability to interface a general purpose computer allows its use for additional laboratory tasks.

T-AM-Po95 MICROCOMPUTER CONTROL AND PROCESSING OF HIGH RESOLUTION DNA THERMAL DENATURATION EXPERIMENTS.
Allen T. Ansevin and Douglas L. Vizard, Physics Department, University of Texas System Cancer Center, Houston, Texas, 77030.

As performed in our laboratory, high resolution DNA thermal denaturation calls for the recording of 300 to 600 temperature and UV absorbance data pairs for each of 4 samples, where the nominal data precision is 5 decimal digits. If only one wavelength is employed for denaturation analysis, an experiemnt can involve more than 5×10^4 bits of information. Since this is followed by several levels of data processing, the task is well beyond efficient manual techniques. Previously, we have used a combination of electronic and mechanical automation for data recording on punched paper tape and subsequent processing by a very large digital computer. We can now utilize a motorola-based 6800 (OR 6809) SWTP computer with an assembly language program to implement the gathering of more data (5×10^5 bits per experiment) and produce two levels of immediate processing so that the course of experiments can be readily monitored. Furthermore, we have written a basic program that uses an efficient polynomial fitting technique designed to calculate derivatives for high resolution profiles that previously required double precision calculations on a large computer. The significance of this work is that high resolution DNA denaturation can be made a routine research tool for the characterization of restriction fragments, viruses, and more complex genomes. With these programs and a comparatively inexpensive computer, a conventional spectrophotometer can be made to outperform most commerical microprocessor-controled spectrophotometers. Supported by NIH Grant GM-23067.

T-AM-Po96 USE OF DYNAMIC LIGHT SCATTERING IN ANALYSIS OF PROTEIN CRYSTALLIZATION BY INCOMPLETE FACTORIAL EXPERIMENTS.
C.W. Carter, Jr., C. Dooley, and T.J. Mercolino, Biochemistry Dept. 231H University of North Carolina, Chapel Hill, N.C. 27514

We have previously suggested that it is possible to identify cause-and-effect relationships involved in crystallizing proteins by analyzing suitably designed statistical, or incomplete factorial, experiments (Carter and Carter, 1979, JBC, 254, 12219-12223). Further progress in establishing this approach requires measurement of some property related to crystal growth, preferably one which can be measured in solution in a reasonably short time. One such property is the change in the aggregate size distribution of a crystallizing (or precipitating) solution on dilution of the protein concentration. Kam, et al., (1978, J. Mol. Biol. 123, 539-555) have shown from simple thermodynamic considerations that this property should reflect the tendency of a protein solution toward crystallization or precipitation, and have provided a scheme for measuring it by dynamic light scattering. In their method, experimental determinations of the z-average diffusion coefficient, $\langle D \rangle_z$, at different protein concentrations are fitted to one of a family of curves calculated from the theoretical model. The different calculated curves are characterized by a single parameter, the ratio between initial and final equilibrium constants of the aggregating system, K_∞/K_1.

Using an improved factorial design which permits optimally balanced interactions between all ionic species being tested, we are studying the dependence of experimental K_∞/K_1 values on fifteen factors thought to influence protein crystallization, and their first-order interactions. Examples will be given from current application of this method to bacterial exonuclease III(EXOIII)from E. Coli, a protein which has not previously been crystallized.

T-AM-Po97 DETERMINATION OF INITIAL RATES: A LINEAR PLOT USING UP TO 70% OF A REACTION. Elizabeth A. Boeker (introduced by Neal Langerman). Department of Chemistry and Biochemistry, Utah State University, Logan, UT 84322.

Initial rates are ordinarily estimated by fitting either a straight line or a polynomial through the first few points of a plot of product versus time. The first procedure necessarily underestimates the true initial rate. The second is used infrequently, apparently because of a general reluctance to apply complex analysis to data that may be rather poor. Both waste a large part of the information available from a reaction.

Despite the fact that no simple transformation of most integrated rate equations produces a straight line, a plot of the average rate at any time t, $(P-P_o)/(t-t_o)$ or $\Delta P/\Delta t$, versus product formed $(P-P_o)$ approximates a straight line extremely closely for all cases examined so far. The intercept of this plot at zero time $(P=P_o)$ is dP/dt_o, the initial rate.

For a first order reaction, whether reversible or irreversible, the theoretical error in estimating the initial rate by fitting a straight line to a plot of $\Delta P/\Delta t$ versus P is less than 0.7% if 10 points are collected over the first 50% of a reaction, and less than 1.6% for 70% of the reaction. For an irreversible second order reaction, a plot of $\Delta P/\Delta t$ versus P is a straight line. For a reversible enzyme catalyzed reaction with one substrate and one product, the error depends on the values of K_s/K_p and $(K_s/S_o)(1+P_o/K_p)$. The maximum error is less than 1% for data over the first 50% of the reaction and less than 2.1% for 70%. This error occurs when K_s/K_p is between 0 and 0.5 and $(K_s/K_o)(1+P_o/K_p)$ is between 0.5 and 2.0. For the simplest possible enzyme catalyzed reaction with one substrate and two products, and considering all possible values for the concentrations and Michaelis constants of the substrate and products, the maximum error is again less than 1.0 or 2.1% for 50 or 70% reaction, respectively.

T-AM-Po98 A METHOD FOR RESUSPENDING SMALL VESICLES SEPARATED FROM SUSPENSION BY PROTAMINE AGGREGATION. K.K. Gunter, T.E. Gunter, A. Jarkowski, and R.N. Rosier. Dept. of Rad. Biol. and Biophys., Univ. of Rochester, Rochester, N.Y. 14642.

Despite the usefulness of the technique for separating small vesicles from suspension by aggregation with polylysine or protamine (1), followed by either filtration or centrifugation, its application has been restricted to separation of vesicles for analytical measurements. The technique could not be used for preparative work because the aggregates produced could not be easily disaggregated. Recently, it has been found that after aggregation of vesicles by protamine and separation of the vesicles from suspension by low speed centrifugation, the addition of an excess of heparin, followed by vortexing or homogenizing the pellet in fresh medium, satisfactorily disaggregated the vesicles. This process has been tested with vesicles made from red blood cells, sarcoplasmic reticulum, mitochondrial inner membrane, phospholipids, and phospholipids plus cytochrome oxidase, easily producing successful resuspensions in all these cases. Leakage of ^{14}C-sucrose or ^{86}Rb from phospholipid vesicles (found to be the worst case) was not appreciably more rapid from protamine-heparin treated vesicles, than from similar vesicles treated with protamine alone, and was not much larger than leakage from untreated vesicles.

Specifically, after aggregation of 2 mg of cytochrome oxidase vesicles (1 mg/ml) by 180 µg of protamine as in (1) and separation from suspension by spinning at 6K rpm for 1 min in a JA-20 rotor, the vesicles were completely resuspended by addition of 640 µg of heparin and rapid vortexing for 1 to 2 min in a test tube.

Supported by NIH (AM-20359) and DOE (DE-AC02-76EV03490).

(1) R.N. Rosier, T.E. Gunter, D.A. Tucker, and K.K. Gunter. Anal. Biochem. 96 384 (1979).

T-AM-Po99 CHLORIDE ION-SELECTIVE MICROELECTRODES: AN IMPROVED ION-EXCHANGE RESIN. Clive Marc Baumgarten, Dept. of Physiology, Medical College of Virginia, Richmond, VA.

Most intracellular chloride activity (a_{Cl}^i) measurements have been made with Cl ion-selective microelectrodes (ISE) based on Corning 477315 liquid ion-exchange resin. Although use of this Cl-ISE is widespread, fabrication of Cl-ISE remains difficult. Often, the resistance of the Cl-ISE is >100 GΩ. and the response to Cl is less than the expected -58mV/10-fold increase in a_{Cl}^i. Because the high resistance of the Cl-ISE may contribute to its non-ideal behavior, an attempt was made to lower the resistance of the resin. The concentration of the ionophore in the 477315 resin was increased 5-fold (5X resin). Glass blanks (Pyrex 7740) were siliconized with tri-n-butylchlorosilane and filled with either 477315 (n=21) or 5X (n=32) resin. ISE made with 5X resin had a significantly lower resistance (43±14 GΩ vs. 226±88 GΩ) and more ideal slopes (-55±3 vs. -49±7 mV/10-fold increase in a_{Cl}^i) than those made with 477315. All 5X-ISE gave linear responses to <1mM a_{Cl}^i while 8 of 21 477315-ISE had reduced sensitivity at low a_{Cl}^i. The selectivity of the 5X-ISE were similar to that of the 477315-ISE and to published values ($k_{i,j}$: propionate, .25-.58; acetate, .18-.26; methanesulfonate .20 - .27). The apparent a_{Cl}^i of quiescent rabbit papillary muscle was 12.3 mM. This is comparable to my previous results. These data suggest that this modification of the Corning 477315 ion exchange resin is suitable for making a_{Cl}^i measurements. The lower resistance of the 5X-resin results in a higher yield of useful ISE and should permit fabrication of ISE with smaller tip diameters. Increasing the ionophore concentration may produce similar results with resins selective for other ions. (Supported by HL24847 and A.D. Williams Foundation. R.W. Mason of Corning Glass Works supplied the modified resin.)

T-AM-Po100 THE DEVELOPMENT OF PHOTOELECTRON MICROSCOPY FOR THE STUDY OF BIOLOGICAL MEMBRANES. O. Hayes Griffith*, Gertrude F. Rempfer, Karen K. Nadakavukaren, William A. Houle, and Douglas L. Habliston, Institute of Molecular Biology and Department of Chemistry, University of Oregon, Eugene, Oregon 97403.

In order to visualize biological surfaces, photoelectron microscopy utilizes electrons emitted under the action of UV light. The approach is similar to fluorescence microscopy except that the limitations imposed by light optics are replaced by electron optics. The mechanism of contrast is different from transmission and scanning electron microscopy and it is possible to visualize different features. Advantages of photoelectron microscopy include surface selectivity, sensitivity to minute topographical details, and photoelectron quantum yield contrast. Fundamental quantum yield data and preliminary photoelectron micrographs of model systems, cell surfaces, and photosynthetic membranes will be presented.

W.A. Houle, H.M. Brown, and O.H. Griffith, Proc. Nat. Acad. Sci. U.S.A. 76, 4180 (1979); G.F. Rempfer, K.K. Nadakavukaren, and O.H. Griffith, Ultramicroscopy 5, in press.

T-AM-Po101 ANTIBODY DETECTION BY FLOURESCENCE FLUCTUATIONS, O. Adawi and M. B. Weissman, Physics, University of Illinois at Urbana-Champaign, Urbana, IL 61801.

Bead-agglutination immunoassays use the ability of antibodies to cross-link antigen-coated beads to detect antibodies in solution. Several light-scattering methods have been developed to detect low levels of such aggregation in small volumes of solution (1). We have adapted a version of a fluorescence fluctuation molecular weight measuring technique (2) to detect the early stages of this aggregation. The main advantage of the fluorescence method is its relative insensitivity to bubbles and other stray scatterers.

A solution of 0.4 μm fluorescent latex beads (Dow Chem.) is coated with antigen (we used BSA), rinsed and exposed to the suspected antibody. After the aggregation develops for several hours, the solution is diluted and flowed, by syringe pump, past a fluorescence detector with $\sim 10^{-5}$ cm^3 observed volume, containing $\sim$ 1000 beads at a time. Noise at the detector output is dominated by number fluctuations in the 1 Hz to 50 Hz range, so that the aggregation may be determined by the net noise magnitude. Data gathering requires about a minute. Sensitivity in early trials appears to be better than by quasi-elastic light scattering. The method uses labeled beads, not labeled molecules, in contrast to the method of Nicoli et al. (3).

(1) Von Schultess et al., Molec. Immunol. 17, 81 (1980).
(2) Weissman et al., PNAS 73, 2776 (1976).
(3) Nicoli et al., PNAS 77, 4904 (1980).

T-AM-Po102 THEORETICAL INTERPRETATION OF THE KINETICS OF COMPLEX BIOLOGICAL SYSTEMS: SOME USEFUL NUMERICAL APPROXIMATIONS. A. S. Verkman and James A. Dix, Biophysical Laboratory, Harvard Medical School, Boston, MA 02115

Analysis of the kinetics of fast biological reactions in terms of detailed reaction mechanisms presents difficulties because of problems in interpreting kinetic data. Mathematical treatment of cell or vesicle suspensions is made more difficult because the system is heterogeneous. Numerical methods have been developed by which reaction mechanisms and rate constants may be deduced from the concentration dependence of a reaction time course as measured by complementary temperature-jump and stopped-flow techniques. Analytic expressions for temperature-jump relaxation times as a function of reactant concentration are often difficult to obtain for complex mechanisms; an alternate approach is to simulate chemical relaxation by solving differential equations describing the kinetics numerically using initial conditions appropriate for a small perturbation from equilibrium. The simulated trace can then be fitted to the experimental trace or to sums of exponentials to yield rate constants. Stopped-flow experiments, being non-linear perturbations, generally have complex, non-exponential functional forms. Since experimental limitations frequently permit only exponential regression, a method has been developed to compare quasi-exponential data traces with exact numerical solutions to kinetic equations. The effects of unstirred layers on the stopped-flow trace are calculated explicitly by solving a system consisting of a diffusion process in solution coupled to a surface chemical reaction. Examples of the numerical methods and useful experimental approaches to examine mechanisms are given for membrane-probe interactions detected by optical means. Supported by NIH 2 R01 GM 15692.

T-AM-Po103 THE MEMBRANE POTENTIAL OF RAT ERYTHROCYTES INFECTED WITH RODENT MALARIAL PARASITES (P. Chabaudi). R. B. Mikkelsen, K. Tanabe, and D.F.H. Wallach. Department of Therapeutic Radiology, New England Medical Center, Boston, MA 02111.

Invasion of erythrocytes by malarial parasites is accompanied by modification of host cell membrane permeability and involves alteration of the osmotic environment of the parasite. To explore these interrelated factors of parasite growth, we measured the membrane potential (E_m) of P. Chabaudi-infected erythrocytes with ^{3}H-triphenyl methyl phosphonium (TPMP) and with intracellular and extracellular H_2O space determined with ^3H_2O and ^{3}H-polyethylene glycol (MW=4000). The intracellular H_2O space for infected and non-infected erythrocytes were not measurably different (0.4µl/10 cells). Erythrocytes were purified to less than 0.1% white cell contamination and separated on metrizamide gradients into cell fractions enriched in early (ring, early trophozoite), late (late trophozoite, schizont)and gametocyte stages of parasite development. The E_m of non-infected erythrocytes ranged between -8 to -12mV as expected for the erythrocyte Donnan equilibrium. The E_m of erythrocytes infected by early stage parasites ranged between -12 to -20mV whereas schizont-rich fractions were characterized by E_m between -36 to -56mV. The E_m's of both infected and non-infected erythrocytes were insensitive to the antimalarial drugs antabuse (1-100µg/ml) and chloroquine (<0.1mM). The E_m of infected, but not normal, erythrocytes was less negative after incubation with 5µM antimycin A, 1µM carbonylcyanide m-chlorophenyl hydrazone and dicyclohexylcarbodiimide (<0.1mM). At these reagent concentrations, the E_m of schizont-rich, infected cells was reduced to that of non-infected cells. Total mitochondrial volume contribution for infected cells is minimal and thus the measured E_m may result from a proton pump localized in the parasite plasma membrane. Supported by N.I.H. AI 16087.

T-AM-Po104 QUANTITATIVE LATERAL CELL MEMBRANE ANALYSIS BY HIGH-RESOLUTION ELECTRON MICROSCOPY. John H. Frenster, Marilyn A. Masek*, and Diane A. Frenster*. Department of Medicine, Stanford University, Stanford, Calif. 94305, and Institute for Medical Research, Santa Clara Valley Medical Center, San Jose, Calif. 95128.

Cell membranes mediate intercellular signals via binding, passage, and/or release of molecular species in a great variety of interacting cell systems. Interacting cells are often tightly apposed to each other, even involving extensive areas of their cell surfaces laterally from the point of original contact. High-resolution transmission electron microscopy was used to analyze quantitatively the tightness of apposition and the lateral extent of apposition of interacting normal and neoplastic cells within biopsied lymph nodes of newly-diagnosed patients with the nodular sclerosis type of Hodgkin's Disease at original pathologic staging of their disease (J. Natl. Cancer Inst. 63, 331 (1979). Ultrastructural criteria were used to identify neoplastic Hodgkin's cells and Reed-Sternberg cells, and to identify normal lymphocytes, macrophages, monocytes, plasma cells, and fibroblasts. Phagocytosis was scored separately, and was found only within normal cells. DNA helix openings within the nuclei of normal and neoplastic cells were localized, measured, and counted after acridine orange ultrastructural probes of these conformation structures (Nature 248, 334 (1974). Normal lymphocytes apposed to neoplastic cells were found to display the tightest apposition surfaces, while normal macrophages were found to display the greatest lateral extent of cell membranes in contact with other normal macrophages. The lateral extent of such macrophage cell membrane apposition was greatly increased by the process of interdigitation of the two cells' cell membranes. Supported in part by Research Grants CA-10174 and CA-13524 from the National Cancer Institute, USPHS.

T-AM-Po105 AUTOMATED PHASE CONTRAST AND FLUORESCENCE IMAGE ANALYSIS OF CELLULAR VERSUS NUCLEAR MORPHOLOGICAL CHANGES INDUCED IN CHO CELLS BY IONIC CHANGES OF THE MEDIUM

Beltrame,F., Chiabrera,A., Grattarola,M., Parodi,G., Vecchio,D.*, Viviani,R.
SIBE, E.E. Dept., University of Genoa, Viale Causa 13, 16145 Genoa, Italy
*Oncology Dept., University of Genoa, Viale Benedetto XV 10, 16132 Genoa, Italy

CHO cells were grown in a thermostated Bellco microchamber under the microscope objective of the automated image analyzer ACTA developed at SIBE. For fluorescence measurements, Acridine Orange (10^{-8} M) was added to cell suspension. Previous experiments showed that, at the dye and cell concentrations used, the cellular proliferation was not affected.

Different media, which are able to reversibly block the cell cycle, have been obtained by equimolar substitutions of Na^+ and K^+, and have been introduced into the micro chamber. Time lapse imaging of the cells have been performed both in phase contrast and in fluorescence by means of the ISIT camera of ACTA, and the digitalized images were stored on tapes.

The sequence of events are described which, at visible wavelength, characterize the morphology of the nucleus and of the whole cell when the cell cycle is reversibly blocked by the different media.

T-AM-Po106 INFRARED STUDIES OF CARBON MONOXIDE IN MYOGLOBIN J.O.Alben, D.Beece, S.F.Bowne, W.Doster, L.Eisenstein, H.Frauenfelder, D.Good, M.C.Marden, P.P.Moh, L.Reinisch, A.H.Reynolds, E.Shyamsunder and K.T.Yue--Department of Physics, University of Illinois at Urbana-Champaign, Urbana, Illinois 61801, and Department of Physiological Chemistry, Ohio State University, Columbus, Ohio 43210.

We have used Fourier-transform infrared spectroscopy to investigate the ligand of carboxymyoglobin, Mb-CO, and its photodissociated state in the temperature range 12 to 100K. Using ^{13}CO and ^{12}CO we can unambiguously assign absorption peaks to the photodissociated and protein-bound CO. In the bound state of Mb-^{13}CO absorption peaks are observed at 1901, 1883 and 1925 cm^{-1}, in agreement with earlier observations. At the temperatures studied the photodissociated ligand is constrained to the heme pocket. Three peaks in the photodissociated state with wave numbers of 2071, 2082 and 2096 cm^{-1} for ^{13}CO have temperature dependent amplitudes. In one plausible interpretation, the states at 2071 and 2082 cm^{-1} correspond to CO molecules that are weakly bound to the walls of the heme pocket. The state at 2096 cm^{-1} may represent a rotationally constrained, but otherwise free, CO molecule. (Supported in part by the U.S. Department of Health, Education and Welfare under Grants No. GM 18051 and HL-17839, by the National Science Foundation under Grant No. PCM 79-05072, and by the American Heart Association under Grant No. 78-1089.)